THE ACID/BASE PROPERTIES OF PROCAINE, DIBUCAINE, AND DYCLONINE IN AQUEOUS SOLUTION STUDIED BY FOURIER TRANSFORM INFRARED SPECTROMETRY.

by

DARLA GAULT LITTLE

Submitted in Partial Fulfillment of the Requirements

for the Degree of

Master of Science

in the

Chemistry

Program

Carol W. Muncy — March 20, 1989

Major Professor — Date

Sally M. Hotchkiss — March 22, 1989

Dean, Graduate School — Date

YOUNGSTOWN STATE UNIVERSITY

March, 1989

YOUNGSTOWN STATE UNIVERSITY

Graduate School

THESIS

Submitted in Partial Fulfillment of the Requirements

for the Degree of Master of Science in Chemistry

THE ACID/BASE PROPERTIES OF PROCAINE, DIBUCAINE, AND DYCLONINE IN AQUEOUS SOLUTION STUDIED BY FOURIER TRANSFORM INFRARED SPECTROMETRY.

Presented By Darla Gault Little

Accepted By The Department Of Chemistry

Daryl W. Maney — March 20, 1989
Major Professor — Date

Elmer Foldvary — March 20, 1989
Date

Thomas N. Dobbelstein — 3-20-89
Date

Sally M. Hotchkiss — March 23, 1989
Dean, Graduate School — Date

ABSTRACT

THE ACID/BASE PROPERTIES OF PROCAINE, DIBUCAINE, AND DYCLONINE IN AQUEOUS SOLUTION STUDIED BY FOURIER TRANSFORM INFRARED SPECTROMETRY.

Darla Gault Little

Master of Science

The primary effect of local anesthetic agents in producing a nerve conduction block is to decrease the permeability of the nerve membrane to sodium ions.[1] According to the specific receptor hypothesis, the most favored theory today, the anesthetic must first diffuse through the nerve sheath and then bind to a receptor site located in the nerve membrane.[1] It is well known that the pK_a or dissociation constant of a specific local anesthetic is directly related to its nerve blocking action.[2] Fourier transform infrared spectrometry was used to analyze the characteristics of procaine, dibucaine, and dyclonine, all local anesthetics. A pK_a study was performed using aqueous and mixed solvent solutions of varying hydrophobicity to investigate the solvent effect on the pK_a of these local anesthetic agents. By comparing and contrasting the infrared spectra of these anesthetic agents in aqueous, 25%, 50%, and 75% acetonitrile solutions, the effects of varying solvents

and pH could be studied. Procaine, dibucaine, and dyclonine were analyzed in an approximate concentration of 0.04 M at a pH range of 2 - 12. Common absorption bands were observed as the solvents and pH were changed.

From their absorption spectra, the pK_a values of procaine, dibucaine, and dyclonine in water were experimentally determined using two different methods of calculation. These experimental values, listed in Table 3, compare favorably with reported literature values for aqueous solutions. Addition of acetonitrile to prepare aqueous solutions containing 25, 50, and 75 volume percent acetonitrile caused the pK_a values to vary, neither steadily increasing nor steadily decreasing, but remaining in the range of 8 to 9.

ACKNOWLEDGEMENTS

I thank and extend my utmost appreciation to Dr. Daryl Mincey, Dr. Thomas Dobbelstein, Dr. Elmer Foldvary, and Dr. Jim Mike for their help and professional guidance throughout this research project. I also thank my husband Bob, my Mom, Dad and family for their loving support, but most of all I thank my Lord and Saviour Jesus Christ without whom none of this could be possible.

TABLE OF CONTENTS

LIST OF SYMBOLS

SYMBOLS	DEFINITIONS
A	Absorbance
A-	Alkaline Form
Aa	Absorbance of HA
Ab	Absorbance of A-
CFM	Cubic Feet per Minute
cm^{-1}	Reciprocal Centimeter
FTIR	Fourier Transform Infrared
HA	Acid Form
Hz	Cycle per Second
IR	Infrared
Log	Logarithm
M	Moles per Liter
[pH]	Measured pH
pK_a	Negative Logarithm of the Dissociation Constant
psi	Pounds per Square Inch
®	Registered Trademark
[ ]	Molar Concentration
**	Equilibrium Constants Calculated for Mixed Solvents
v	Velocity

LIST OF FIGURES

LIST OF TABLES

CHAPTER I

INTRODUCTION

PROCAINE

Structure and Chemistry

Procaine, $C_{13}H_{20}N_2O_2$, also referred to as 4-amino-benzoic acid 2-(diethylamino) ethyl ester is a tertiary amine and is classified as an ester linked local anesthetic. Its structure is illustrated in Figure 1. Other pertinent chemical and physical data for this compound include: a melting point of 61°C, a molecular weight of 236.30 a.m.u., and its action as an alkaloidal base.[1,3]

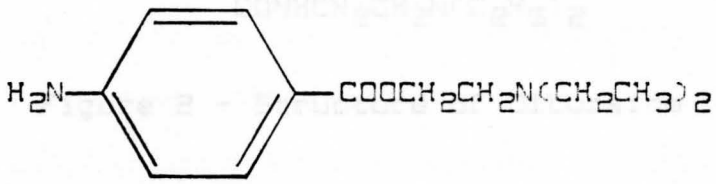

Figure 1 - Structure of Procaine[2]

The hydrochloride form, procaine hydrochloride, occurs as a white crystalline powder that is freely soluble in water.[3] As Novocaine® it is employed as the sole local anesthetic agent for pain control in dentistry.[4]

DIBUCAINE

Structure and Chemistry

Dibucaine, $C_{20}H_{29}N_3O_2$, also known as Percaine®, Cinchocaine®, Nupercaine®, and 2-butoxy-N-[2-(diethylamino)-ethyl]-4-quinolinecarboxamide is a quinoline derivative and is classified as an amide type local anesthetic.[5,6] Its structure is illustrated in Figure 2. Other chemical and physical data for this compound include: a melting point of 64°C, a molecular weight of 343.92 a.m.u. and its action as a lipid soluble base.[5,6]

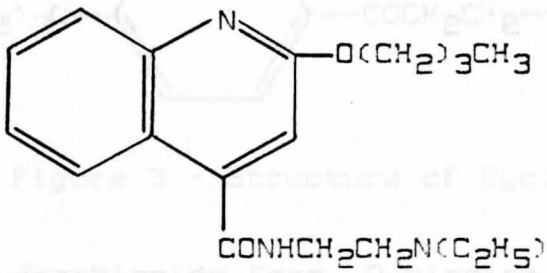

Figure 2 - Structure of Dibucaine

The hydrochloride form, Dibucaine hydrochloride, is a white crystalline compound which is partially soluble in water, but freely soluble in alcohol, acetone, and chloroform.[5] Dibucaine is known to be one of the most potent, most toxic, and longest acting of the commonly employed local anesthetics.[7] It is about fifteen times as potent and as toxic as procaine, and its anesthetic action lasts about three times as long.[7] Dibucaine hydrochloride is infrequently used either topically or by injection.[7]

Dyclonine

Structure and Chemistry

Dyclonine, $C_{18}H_{27}NO_2$ or 1-(4-Butoxyphenyl)-3-(1-piperdinyl)-1-propanone is chemically unique from all other local anesthetics in that it is a ketone.[8] Its structure is illustrated in Figure 3. Other important chemical and physical information include: a melting point of 175-176°C for the hydrochloride, a molecular weight of 289.43 a.m.u. and its action as a topical anesthetic.[8]

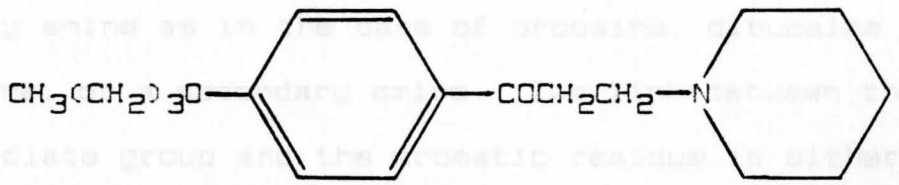

Figure 3 - Structure of Dyclonine

The hydrochloride form, Dyclonine hydrochloride is a white crystalline compound which is slightly soluble in water, but freely soluble in both alcohol and acetone.[8] As Dyclone® hydrochloride it is primarily used as a topical anesthetic and is administered to patients with a known sensitivity to local anesthetics of other chemical groups.[9]

General Properties of Local Anesthetic Drugs

Local anesthetics have many actions in common, and before discussing the pharmacology of the individual members these general properties will be considered.[6]

Chemistry and Structure - Activity Relationship

All useful local anesthetics consist of three parts. There is a water loving or hydrophilic amino group that is connected by an intermediate group to a lipid soluble or lipophilic aromatic residue. The amino group is either a tertiary amine as in the case of procaine, dibucaine and dyclonine, or a secondary amine. The link between the intermediate group and the aromatic residue is either an amide bond, as in dibucaine, or an ester linkage as in procaine.[10] Dyclonine as mentioned previously is chemically unique in that it is a ketone.[8] The nature of this intermediate linkage is important in defining several properties of the local anesthetic, including the basic mode of biotransformation.[1] Amide linked local anesthetics such as dibucaine are relatively resistant to hydrolysis.[1] Changes in any part of the local anesthetic molecule will alter the anesthetic potency and the toxicity of the compound.[6] In the case of procaine, increasing the length of the alcoholic group leads to a greater anesthetic potency.[6] It also leads to an increase in toxicity so that compounds with an ethyl ester, like procaine, exhibit the least toxicity.[6] The length of the two terminal groups on the

tertiary amino nitrogen is also important.[6]

Mode and Site of Action of Local Anesthetics.

The nerve membrane is the site at which local anesthetic agents exert their pharmacological actions.[11] Several theories exist today as to precisely where on the nerve membrane local anesthetics act to produce a conduction blockage.[12] The most favored theory today proposes that local anesthetics act by attaching themselves to specific receptors in the nerve membrane.[1] The action of the drug is direct, not brought on by some change in the general properties of the cell membrane.[1] Both biochemical and electrophysiological studies have shown that a specific receptor site for local anesthetic agents exists in the nerve membrane.[1] The local anesthetic receptor is most likely located at or near the sodium channel in the nerve membrane, either on its external surface or on the internal axoplasmic surface.[1]

The mechanism or mode of action of local anesthetics can be described as follows. The local anesthetic agent will block nerve conduction by interfering with the process essential to the generation of the nerve action potential, namely the large transient increase in the permeability of the membrane to sodium ions that is produced by a slight depolarization of the nerve membrane.[6] Thus the primary effect of local anesthetic agents in producing a conduction block is to decrease the permeability of the nerve membrane to sodium ions.[1] As stated previously, the local anesthetic

receptor is most likely located at or near the sodium channel in the nerve membrane. Therefore, there is strong evidence that when a local anesthetic molecule diffuses through the nerve sheath and binds to a receptor site located in the nerve membrane it acts as an antagonist to block sodium ion permeability and the final result is a conduction blockade.

Effects of pH and pK_a on Local Anesthetic Activity.

As prepared in the laboratory, a local anesthetic amine or base is only slightly soluble in water and quite unstable on exposure to air.[2] This form of the drug has little or no clinical value. Weakly basic it combines readily with acids to form local anesthetic salts. These local anesthetic salts are quite soluble in water and comparitively stable. Thus, local anesthetics used for injection are dispensed as salts, most commonly the hydrochloride salt dissolved in either water or saline solution.[2]

It is a well known fact that the pH of the local anesthetic solution and the characteristic pK_a of the local anesthetic have a direct effect on its nerve blocking action.[13] Acidification of tissue will decrease local anesthetic activity. For example, if a local anesthetic is injected into an inflamed area anesthetic activity will decrease because the inflammatory process produces acidic products. The pH of normal tissue is 7.4, the pH of an inflamed area is 5 to 6. On the other hand, alkalinization of a local anesthetic solution speeds the onset of action or

the time it takes for the local anesthetic to begin working.[13] This is especially true when anesthetics are applied to isolated nerve trunks or to the cornea, where the buffering capacity of the tissue fluids is limited.[14] It has been predicted therefore that previous alkalinization of an anesthetic solution will increase its clinical effectiveness.[14] However objective tests have failed to substantiate this point, and most alkaline preparations have the disadvantage of being relatively unstable.[14]

As previously stated, local anesthetics are available as salts.[2] In aqueous solution the anesthetic salt exists in two forms simultaneously, the uncharged basic form and the charged cationic form.[2] The relative proportion of each form present in solution depends on both the pH of the solution or the surrounding tissue and also the pK_a, or dissociation constant, of the specific agent.[13] The two factors involved in the anesthetic action of a local anesthetic are diffusion of the agent through the nerve sheath and binding at the receptor site in the cell membrane.[15] The uncharged, lipid soluble, free base form is responsible for diffusion of the local anesthetic through the nerve sheath whereas the charged cationic form is necessary for binding at the receptor site.[2]

A local anesthetic with a high pK_a has very few molecules available in the free base form at a normal tissue pH of 7.4.[16] Anesthetic action of this agent would be poor because too few base molecules would diffuse through the nerve membrane. On the other hand a local anesthetic with a

low pK_a has a very large number of base molecules which are able to diffuse through the nerve sheath. However, anesthetic action of this agent would also prove inadequate because at a normal intracellular pH only a very small number of base molecules would associate back to the cationic form necessary for binding at the receptor site.[16]

In clinical situations the pH of the extracellular fluid determines the ease with which a local anesthetic moves from the site of administration into the cell membrane.[17] The intracellular pH remains quite stable and independent of the extracellular pH.[17] This is because the hydrogen ion like the local anesthetic cation does not diffuse through tissues.[17] The pH of extracellular fluid may therefore differ from that of the nerve membrane.[17] The ratio of anesthetic cation to base may therefore also vary at these sites.[17]

The pK_a of a local anesthetic not only gives us some idea of the relative proportion of uncharged and charged molecules in solution but also is directly related to the rate of onset of clinical action of a specific local anesthetic.[18] As in the case of procaine, the onset of action is quite high due to the fact that its pK_a value is also high.[19] It can be concluded that the relative onset of action of a local anesthetic is directly proportional to its respective pK_a.[19]

These concepts are the main goals of this research project which are to study the acid/base properties of local anesthetics in aqueous acetonitrile solutions using Fourier

Transform Infrared Spectrometry. These pK_a studies are performed with aqueous and mixed solvent solutions of varying hydrophobicity to investigate potential changes in pK_a upon nerve membrane interaction of these local anesthetic agents.

Pharmacological Actions

Local anesthetics not only block conduction in nerve axons in the peripheral nervous system but also interfere with the function of all organs in which conduction or transmission of impulses occurs.[20] Therefore, they have important effects on the central nervous system, the autonomic ganglia, the neuromuscular junction, and all types of muscle fiber.[20]

All nitrogenous local anesthetics, including procaine, dibucaine, and dyclonine, may cause stimulation of the central nervous system or CNS.[20] This action produces restlessness and tremor which may lead to clonic convulsions.[20] Typically, the more potent the anesthetic the more readily convulsions may be produced.[20] Alterations of CNS activity are thus predictable from the local anesthetic agent in question and the blood concentration level.[20]

A study done by Frank and Sanders in 1963 suggested that the apparent stimulation and the subsequent depression produced by applying local anesthetics to the CNS were both, in fact, due solely to depression of the neuronal activity. The evidence for this theory is that, when a local anesthetic, in this case procaine, is applied to the cortical

neurons in isolated slabs of cerebral cortex, only depression of the directly evoked electrical responses is obtained.[6]

Depression of activity is also the only effect that anesthetics like procaine produce in monosynaptic and polysynaptic spinal reflexes, according to a study done by Taverner in the 1960's.[20] Unlike cocaine, a natural anesthetic, synthetic anesthetics such as procaine, dibucaine and dyclonine are less stimulating to the higher cerebral centers and do not cause addiction.[10,21]

Local anesthetics also affect transmission of the neuromuscular junction.[22] Harvey in 1939 observed that the close intra-arterial injection of as little as 0.2 milligram of a particular local anesthetic into the cat's tibialis anterior muscle reduced twitches and tetanic responses evoked by maximal motor-nerve volleys, and the response of the muscle to injected acetylcholine.[22] The muscle, however, responded normally to direct electrical stimulation. A local anesthetic will not only affect the neuromuscular junction but it also have a marked affect on the synaptic endings of the ganglion cells. When procaine was added to the fluid perfusing a ganglion, preganglionic stimulation failed to elicit postganglionic discharges and the ganglion cells became insensitive to stimulation by acetylcholine.[22]

Following systematic absorption, local anesthetics act on the cardiovascular system.[22] The primary site of action is the myocardium, where decreases in electrical excitability, conduction rate, and force of contraction

occur.[22] Studies on isolated atrial and ventricular muscle revealed that procaine increased the effective refractory period, raised the threshold for stimulation, and prolonged conduction time.[22] These cardiac actions of this local anesthetic would be of therapeutic interest were it not for the rapid metabolic destruction of the compound and the propensity of local anesthetics to cause central stimulation.[22]

Finally, local anesthetics have been known to depress contractions in strips of isolated intestine and in the intact bowel. This spasmolytic action seems to be caused by local anesthetic depression of the smooth muscle. This study was done by Zipt and Dittmann in 1971.[22]

Chapter II

HISTORY

General Description of Infrared Spectrometry

When electromagnetic radiation passes through molecules it is transmitted, scattered and absorbed. The absorption phenomenon helps resolve relationships between the wavelength of absorbed radiation and molecular structure. For the infrared region of absorption which pertains to wavenumbers within the range of 12,800 to 10 cm^{-1}, molecules can be treated as masses (atoms) connected by springs (bonds). It is a property of mechanical systems that they have characteristic vibrational frequencies or resonances that absorb energy from applied oscillatory forces. Small masses or shift springs give rise to high vibrational frequencies and it is a consequence of the tightness of bonds that molecular vibrations occur in the infrared region. The probability of absorption per molecule depends on the change of dipole moment during vibration. A large change in dipole moment accompanies intense absorption.[23]

Even for simple molecules the number of vibrational frequencies is large. However, not all of these vibrations will appear in the spectrum because many are highly symmetrical vibrations that produce small changes in dipole moment. A further complication is that overtones and

combination bands occur with moderate intensity. Fortunately, certain functional groups and structural units have characteristic absorption frequencies that change very little from molecule to molecule. For many structural units, the frequency shifts that do occur can be related to variations in the neighboring structure.[23]

Principles of Fourier Transform Infrared Spectrometry

Introduction

Since radiant energy consists of trains of electromagnetic waves, generally of many frequencies superimposed, the instantaneous electrical and magnetic fields at any point will be the resultant of those due to the individual frequencies. Therefore it should be possible, in principle, to retrieve all the information carried by a beam simply by letting it fall on a radiation detector and plotting the response as a function of time. Before the invention of the Michelson interferometer there was difficulty with such an approach in that alternating fields, with frequencies of the order of 1014 Hz, were many orders of magnitude too fast to follow with any known detector.[24]

The Michelson Interferometer

This speed difficulty was overcome through the use of the Michelson interferometer which is diagrammed in figure 4.

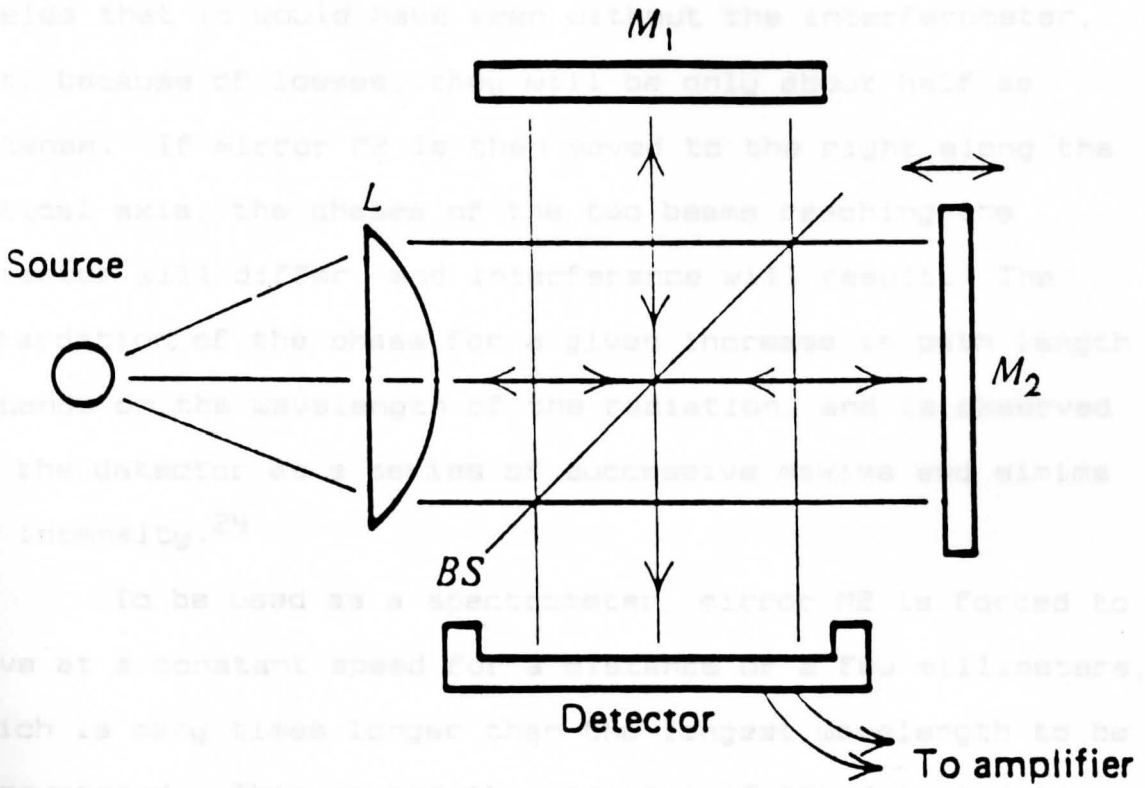

Figure 4. Schematic Diagram of Michelson Interferometer[24]

Radiation from the source is collimated by lens L and then divided into two equal parts by the beam splitter BS. The beams are reflected back by plane mirrors M1 and M2. Portions of both beams are finally incident on the detector. If the two mirrors are an equal distance from BS, the detector will see the same time-varying electromagnetic fields that it would have seen without the interferometer, but, because of losses, they will be only about half as intense. If mirror M2 is then moved to the right along the optical axis, the phases of the two beams reaching the detector will differ, and interference will result. The retardation of the phase for a given increase in path length depends on the wavelength of the radiation, and is observed by the detector as a series of successive maxima and minima of intensity.[24]

To be used as a spectrometer, mirror M2 is forced to move at a constant speed for a distance of a few millimeters, which is many times longer than the longest wavelength to be encountered. This causes the response of the detector to fluctuate at a rate dependent on the speed of motion and the wavelength of the radiation. The action of the interferometer can be thought of as equivalent to chopping the radiation at a frequency given by $2\upsilon\tilde{\nu}$ where υ is the velocity of the moving mirror in centimeters per second, and $\tilde{\nu}$ is the wavenumber of radiation in cm^{-1}. In a typical instrument, this is equivalent to chopping simultaneously at a frequency continuously variable from about 1250 Hz at the high

wavenumber end of the spectrum to 125 Hz at the low end. These frequencies are easily followed by a thermal detector which responds to the time derivative of the temperature rather than the temperature itself. This detector is known as a pyroelectric detector.[25]

This combination of frequencies with corresponding amplitudes will produce a unique interferogram. The pulsating beam leaving the interferometer is directed through the sample cell and focused on the detector.[25] See Figure 5.

FTIR Detectors

Interferograms are not readily interpreted without a digital computer. From a mathematical standpoint the interferogram is the Fourier transform of the spectrum. Therefore, the job of the computer is to apply the inverse Fourier transform.[26]

Fourier transform infrared spectrometers employ infrared detectors of two types. The first type is known as a thermal detector which operates by sensing the change of temperature of an absorbing material with output obtained from a pyroelectric detector, bolometer, thermistor bolometer, pneumatic detector, or Golery detector.[27] The second type of detector is a quantum detector which senses infrared radiation based on the interaction of radiation with the electrons in a solid which cause electrons to be excited to a higher energy state.[27]

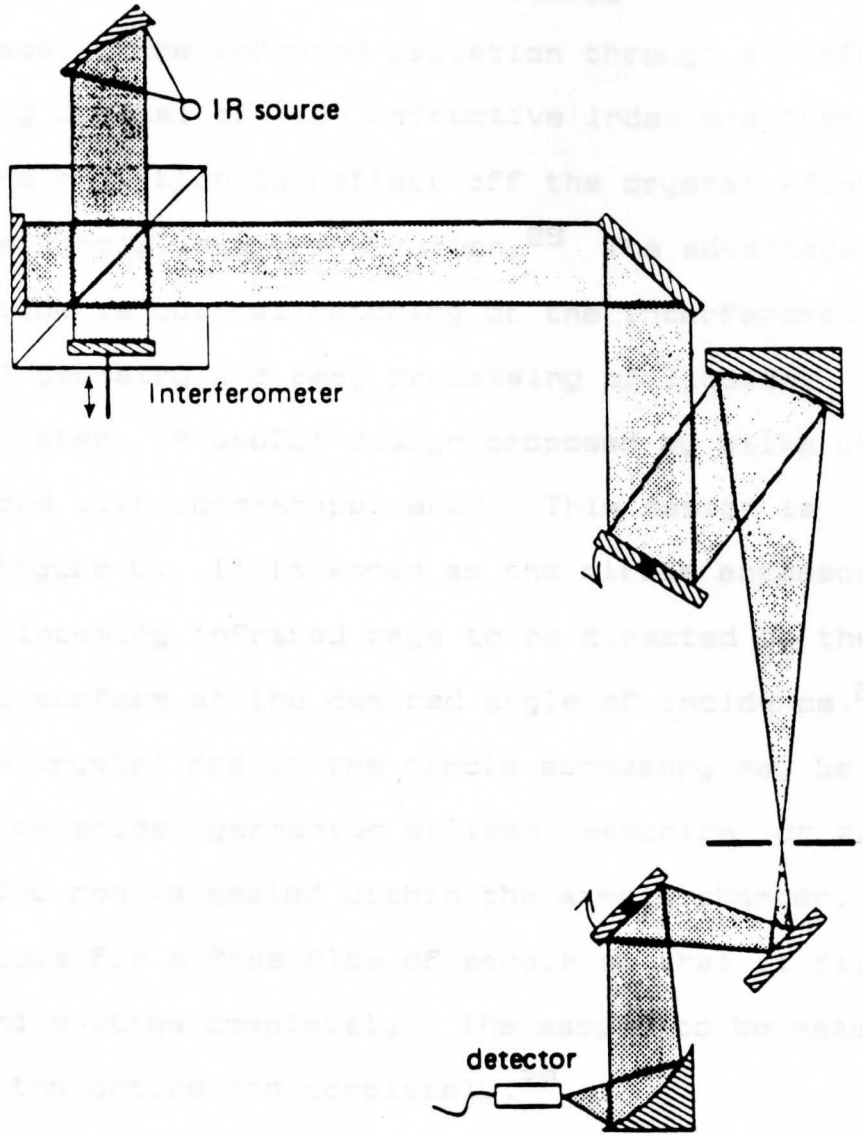

Figure 5. Optical Diagram of FTIR Spectophotometer[28]

Cylindrical Internal Reflection - Sampling Techniques

Sample analysis may be performed by using a technique known as internal reflectance spectroscopy. This technique involves passing the infrared radiation through an infrared transmitting crystal of high refractive index and then allowing the radiation to reflect off the crystal after extending slightly into the solution.[29] The advantage of this technique is optical matching of the interferometer beam and crystal geometry and easy processing of liquids, especially water. A useful design proposed by Wilks utilizes a crystal rod with cone-shaped ends. This design is illustrated in Figure 6. It is known as the circle accessory and allows the incoming infrared rays to be directed to the cylindrical surface at the desired angle of incidence.[29]

The crystal rod in the circle accessory may be made up of zinc selenide, germanium silicon, sapphire, or zinc sulfide. The rod is sealed within the sample chamber. This chamber allows for a free flow of sample so that it fills smoothly and empties completely. The sample to be measured must cover the entire rod completely.[29]

This circle cell is useful for the fourier transform infrared analysis of strongly absorbing liquids, solutions, and mixtures. Normally, when water is used as a solvent it is difficult to perform FTIR determinations because water's highly absorbing bands, especially the OH stretch in the region of 3000 cm^{-1} tend to obscure the weaker more

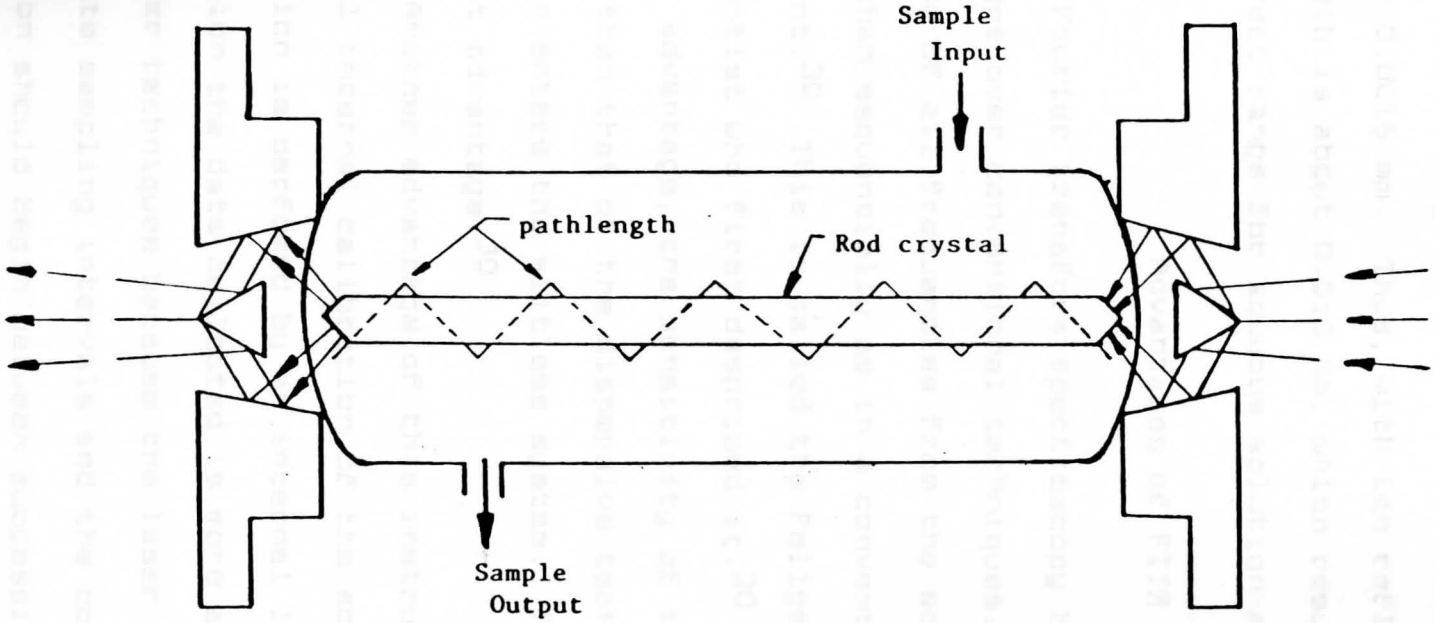

Figure 6. Optical Diagram of a Flow Thru Circle Accessory[29]

important bands. This problem is overcome by internal reflection spectroscopy because the beam penetration into the sample is extremely small. The effective path per reflection is about 0.0015 mm. Thus, with ten reflections the effective pathlength is about 0.015 mm, which results in absorbances in the correct range for aqueous solution measurements.[29]

Advantages of FTIR

Fourier transform spectroscopy has two great advantages over conventional techniques.[30] First of all it makes use of all frequencies from the source simultaneously, rather than sequentially as in a conventional scanning instrument.[30] This is called the Fellgett advantage, after the scientist who first described it.[30] In addition to the Fellgett advantage, the sensitivity of the FTIR method is greater than that of the dispersive technique because more radiation enters the slitless system. This is known as the Jacquinat advantage.[30]

Another advantage of this instrumental technique is continual internal calibration of the scanning mirror. This calibration is perfomed by an internal laser. Due to this calibration the data collected is more accurate and precise than other techniques because the laser signal is used to coordinate sampling intervals and the point at which data collection should begin between successive scans.[31]

Lastly, the use of microcomputers and automation make this technique more useful and less time consuming. Before

the 1970's the interferogram had to be analyzed using an audio-frequency wave analyzer and an XY plotter.[27] Micro-computers have allowed for more rapid spectra generation from interferograms due to the rapid performance of mathematical computations. Also, data manipulation such as baseline correction, smoothing, and subtractions can be performed now due to increased computer power and storage capability.[32]

Disadvantages

Although there are many advantages in using FTIR spectroscopy there are also its share of disadvantages. These disadvantages include the sensitivity of the instrument to temperature and vibration, alignment of the instrument's components, and a decrease in accuracy due to approximations used in computer calculations.[32,33]

A disadvantage which must also be pointed out when cylindrical internal reflection techniques are used is that this is a low light throughput technique. For this reason, the intensity of infrared radiation reaching the detector is decreased and high resolution may not be obtained.[34]

The cell's pathlength utilized in cylindrical internal reflection accessories also presents a problem. This pathlength limits detection of substances in very small concentrations.[33] A concentration of 0.5% is usually the lower limit of detection. However, this lower level of detection can be decreased by using a Quantum detector.[35]

Fourier Transform Infrared Spectrometers Instrumental Design

All FTIR spectrometers consist of four basic systems. These systems include the interferometer and detector system, the data acquisition and optics control system, a general purpose computer, and the operator interface.[32] These have all been discussed previously to some extent.

Background of FTIR Spectrometry of Aqueous Solutions

Due to the invention of the cylindrical internal reflectance technique, the infrared spectra of aqueous solutions can now be studied both qualitatively and quantitatively.[32]

Quantitative studies were performed by Wang and Rein and by Mathias. Wang and Rein measured the spectra of solutions of varying concentration of beta lactams in aqueous solutions.[35] Mathias studied various concentrations of glycine in water solutions. Both groups found that there was an excellent Beer's Law relationship.[29,35] Other studies include the analysis of shampoo formulations by Sabo, Gross, and Rosenburg and the analysis of fermentation broths containing methanol, ethanol and acetone by Kuehl and Crocombe. Goulden analyzed cows milk and Baca studied the effects of varying solvent and pH of 1-adamantanamine, an anti-viral agent.[32]

Qualitative studies include an evaluation of aqueous antibiotic solutions by Wang and Rein.[35] Another study by Mathias involved the determination of the spectra of water-soluble polymers such as polyacetamide-acrylic acid.[29]

CHAPTER III

APPARATUS AND MATERIALS

BioRad FTS-40 FTIR Spectrometer

The FTS-40 is a high performance research grade Fourier Transform Infrared Spectrometer manufactured by BioRad Laboratories, Inc., Digilab Division. The FTS-40 consists of two major components, an optical bench and a model 3240 Data system.[36] See Figure 7.

The optical bench houses the infrared power source, the single mode helium-neon laser, the fast scanning 60 degree Michelson interferometer, the sample compartment, and the pyroelectric bolometer.[37]

The 3240 Data system controls the optics bench and performs all the mathematical functions. It includes a central processing unit, a twelve-inch, high resolution color monitor, a full upper and lower case keyboard and joystick, a data storage unit, a 6-color, single-page, digital plotter, and a 120 character per second dot matrix printer.[37] The optics bench requires dry air or nitrogen at a minimum of 12 psi, at approximately 0.2 CFM for proper operation of the air bearing. In addition, it is highly recommended that an oil/water trap and micron filter be used to prefilter the bearing air.[37] The ceramic IR source requires a supply of non-corrosive cooling water. A minimum water flow of one liter

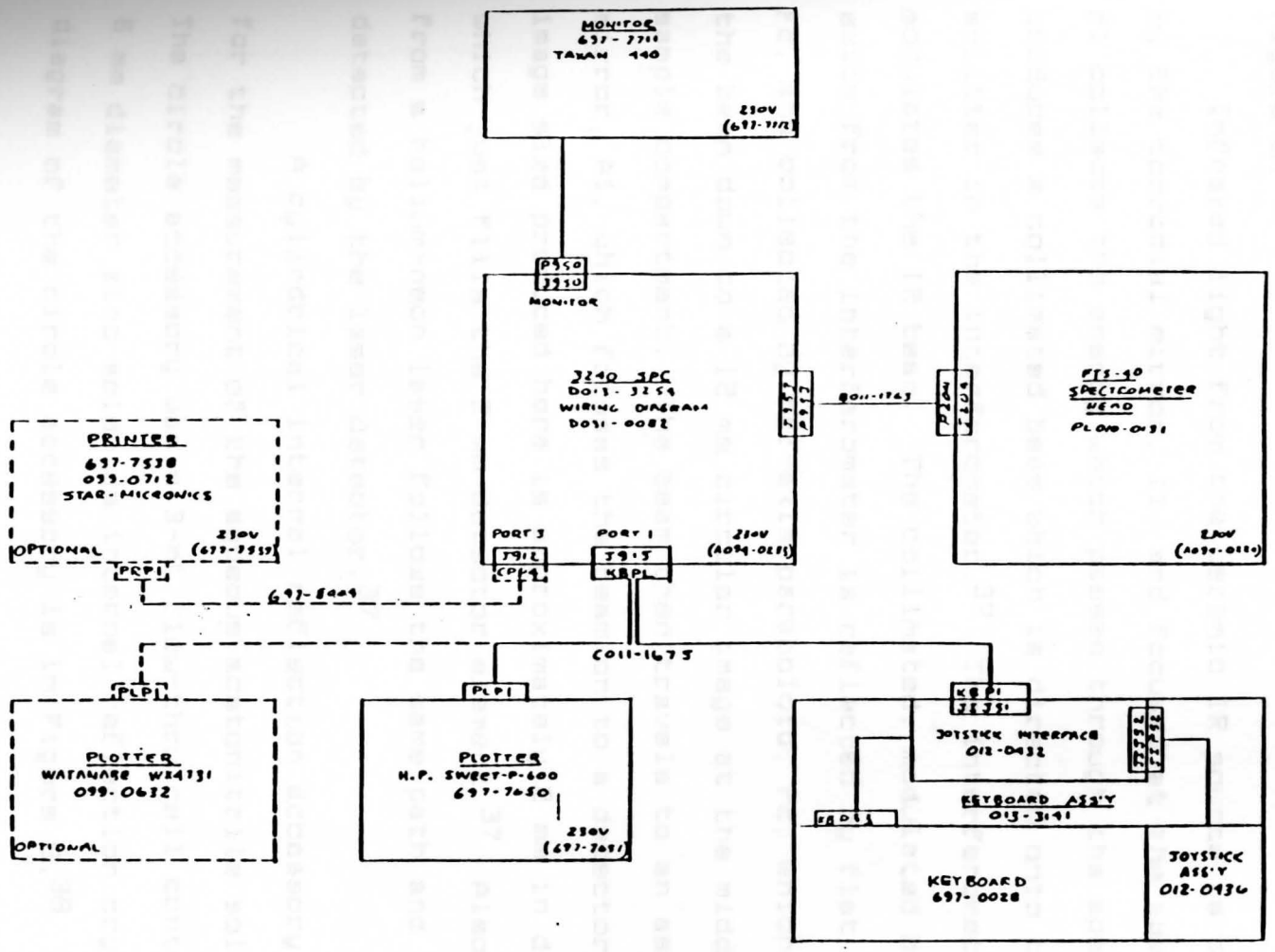

Figure 7. FTS-40 Block Diagram[37]

per minute at not more than 28 C is necessary.[37] A schematic diagram of the optics bench of the FTS-40 is illustrated in Figure 8.[37]

Infrared light from the ceramic IR source is collected by the torrodial mirror, T1, and focused at the aperature. P1 collects the energy which passes through the aperature and produces a collimated beam which is directed onto the beam splitter in the interferometer.[37] The interferometer then modulates the IR beam. The collimated, modulated beam that exits from the interferometer is reflected by flat mirror, F2, and collected by off-axis paraboloid, P2, which focuses the beam down to a 12 mm circular image at the middle of the sample compartment. The beam then travels to an aspheric mirror, A1, which focuses the beam on to a detector, D1. The image size produced here is approximately 2 mm in diameter which just fills the 2 mm detector element.[37] Also light from a helium-neon laser follows the same path and is detected by the laser detector.[37]

A cylindrical internal reflection accessory was used for the measurement of the aqueous acetonitrile solutions. The circle accessory was a 3-mL flow-thru cell containing a 6 mm diameter zinc selenide internal reflection crystal. A diagram of the circle accessory is in Figure 9.[38]

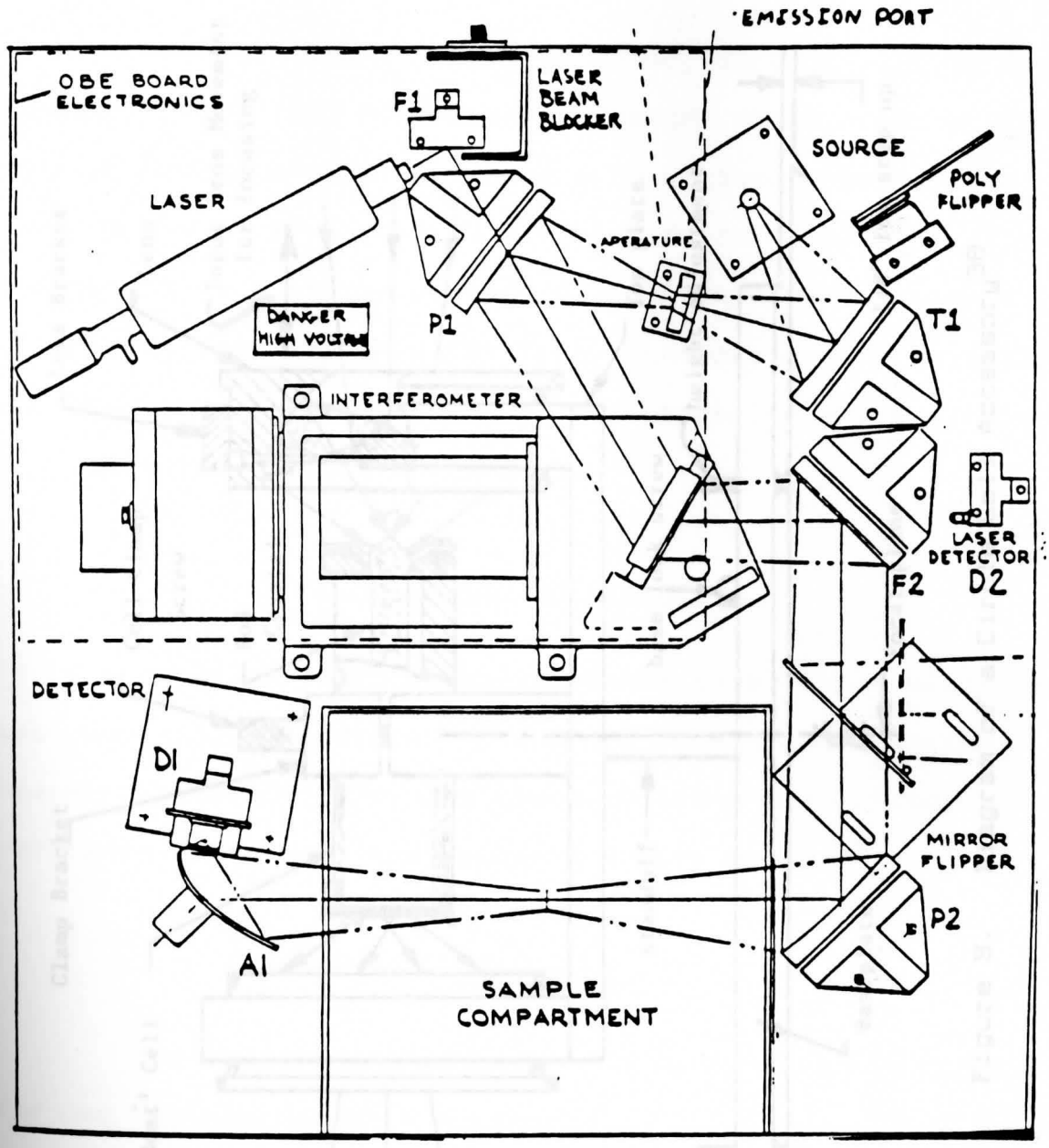

Figure 8. FTS-40 Optical Schematic[37]

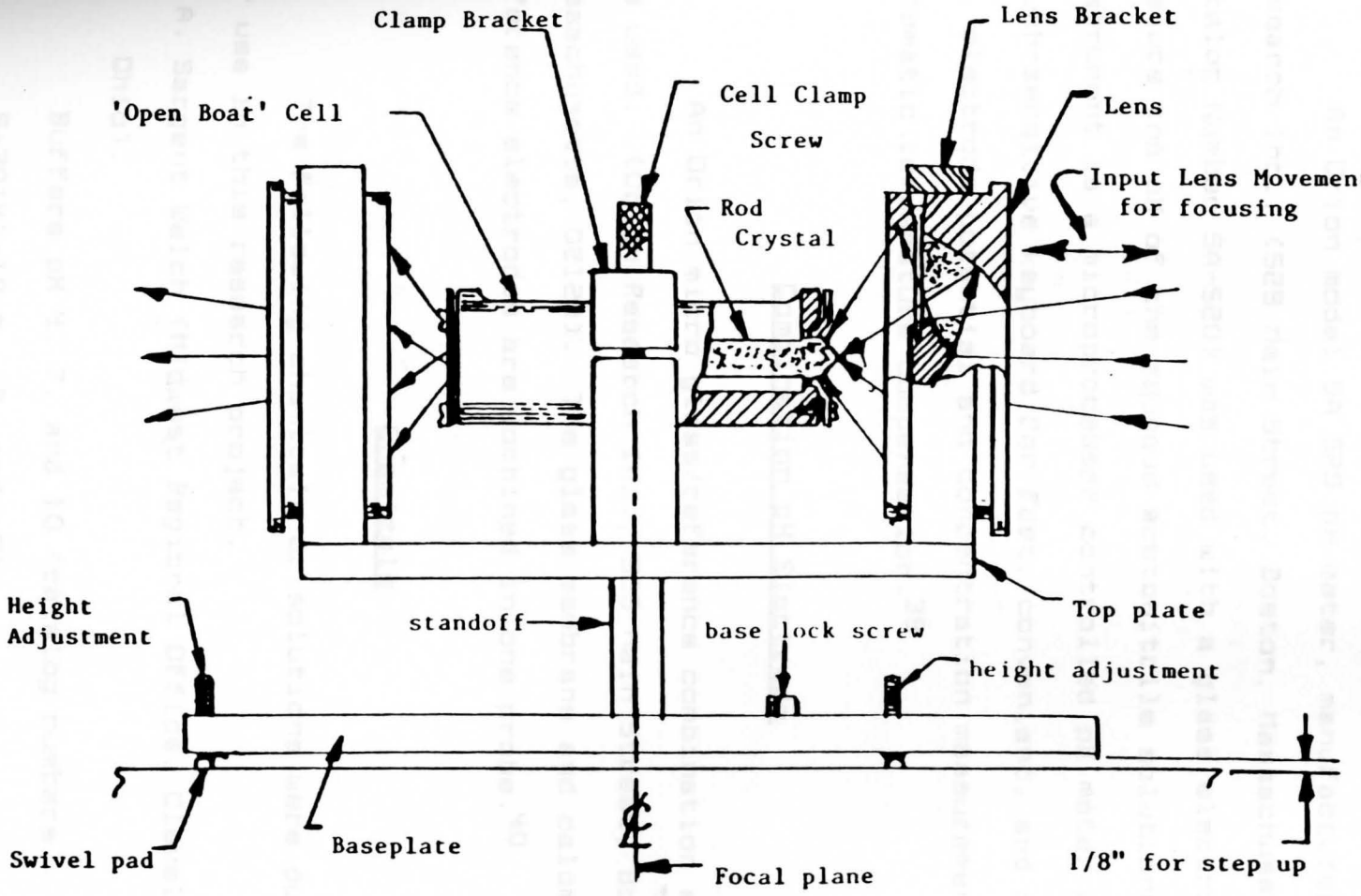

Figure 9. Diagram of a Circle Cell Accessory[38]

pH Meter

An Orion model SA 520 pH meter, manufactured by Orion Research Inc., (529 Main Street, Boston, Massachusetts 02129, Catalog Number SA-520) was used with a glass electrode to measure the pH of the aqueous acetonitrile solutions. This instrument is a microprocessor controlled pH meter with a touch-sensitive keyboard for fast, convenient, and reliable pH, electrode potential and concentration measurements with automatic temperature compensation.[39]

Combination pH Electrode

An Orion micro glass/reference combination electrode was used. (Orion Research Inc., 529 Main Street, Boston, Massachusetts, 02129). The glass membrane and calomel reference electrodes are combined in one probe.[40]

Chemicals

The following chemicals or solutions were purchased for use in this research project.

A. Sargent Welch (Midwest Regional Office, Cleveland, Ohio).

Buffers pH 4, 7, and 10 (catalog numbers S-30141-10-A, -B, and -C).

B. GFS Chemicals (Columbus, Ohio).

6M Double-distilled Hydrochloric Acid from Vycon. (Catalog number 660).

C. Fisher Scientific Company (Chemical Manufacturing Division, Fairlawn, New Jersey).

Acetonitrile (Catalog number 700 196).

D. Matheson, Coleman and Bell Manufacturing Chemists (Norwood, Ohio).

Acetonitrile (Catalog number AX149 2726).

E. Sigma Chemical Company. (P.O. Box 14508, St. Louis, Missouri) provided:[41]

1. Procaine Hydrochloride Anhydrous Salt. (Catalog number 37F-0644).
2. Dibucaine Hydrochloride Anhydrous Salt. (Catalog number 45F-0769).
3. Dyclonine Hydrochloride Anhydrous Salt. (Catalog number 15F-0489).

F. Malinckrodt Inc. (Paris, Kentucky).

Potassium hydroxide pellets.

CHAPTER IV

EXPERIMENTAL METHODS

Introduction

The experiment in this research project deals with the determination of the infrared spectra of both aqueous and aqueous/acetonitrile solutions of procaine, dibucaine, and dyclonine to observe the structural changes which occur in these compounds as a function of pH and solvent composition. Once these spectra are determined, they are manipulated by using the cursor motion key to determine the baseline and to select important peaks. Then the absorption bands or peaks attributed to anesthetics in all solutions are used to determine the pK_a of these drugs in aqueous and mixed solvents.

Part A: Preparation of Reagents

This experiment involved the preparation of the following solutions:

1. 5 M solution of potassium hydroxide.
2. 25% acetonitrile solution in water.
3. 50% acetonitrile solution in water.
4. 75% acetonitrile solution in water.
5. 0.04 M solutions of procaine in water, 25%

acetonitrile, 50% acetonitrile, and 75% acetonitrile.

6. 0.03 M solutions of dibucaine in water, 25% acetonitrile, 50% acetonitrile, and 75% acetonitrile.
7. 0.03 M solutions of dyclonine in water, 25% acetonitrile, 50% acetonitrile, and 75% acetonitrile.

Part B: Flow-thru Cell and Pump Set-up

A circulating pump attached to a flow-thru circle cell is utilized in this experiment. The circle cell is placed into the FTIR chamber compartment. The input hose to this cell originates in the reaction beaker containing the sample solution. The output hose from this cell leads to the same reaction beaker. This beaker also contains the combination pH electrode. In Figure 10 the set-up of this apparatus is shown.[32] This set-up allows the various solutions to be pumped through the circle accessory continuously as the pH is adjusted. When the pH stabilizes at the desired value, the pump is shut off and the spectrum of the solution is measured.

Part C: FTIR Measurement of Samples

Standard operating procedure of the FTS-40.

After the system is turned on the user must log into a directory by typing in a predefined directory name.[36] Now the user is ready to begin working with the menu software by pressing the top menu key.[36] The displayed selections allow

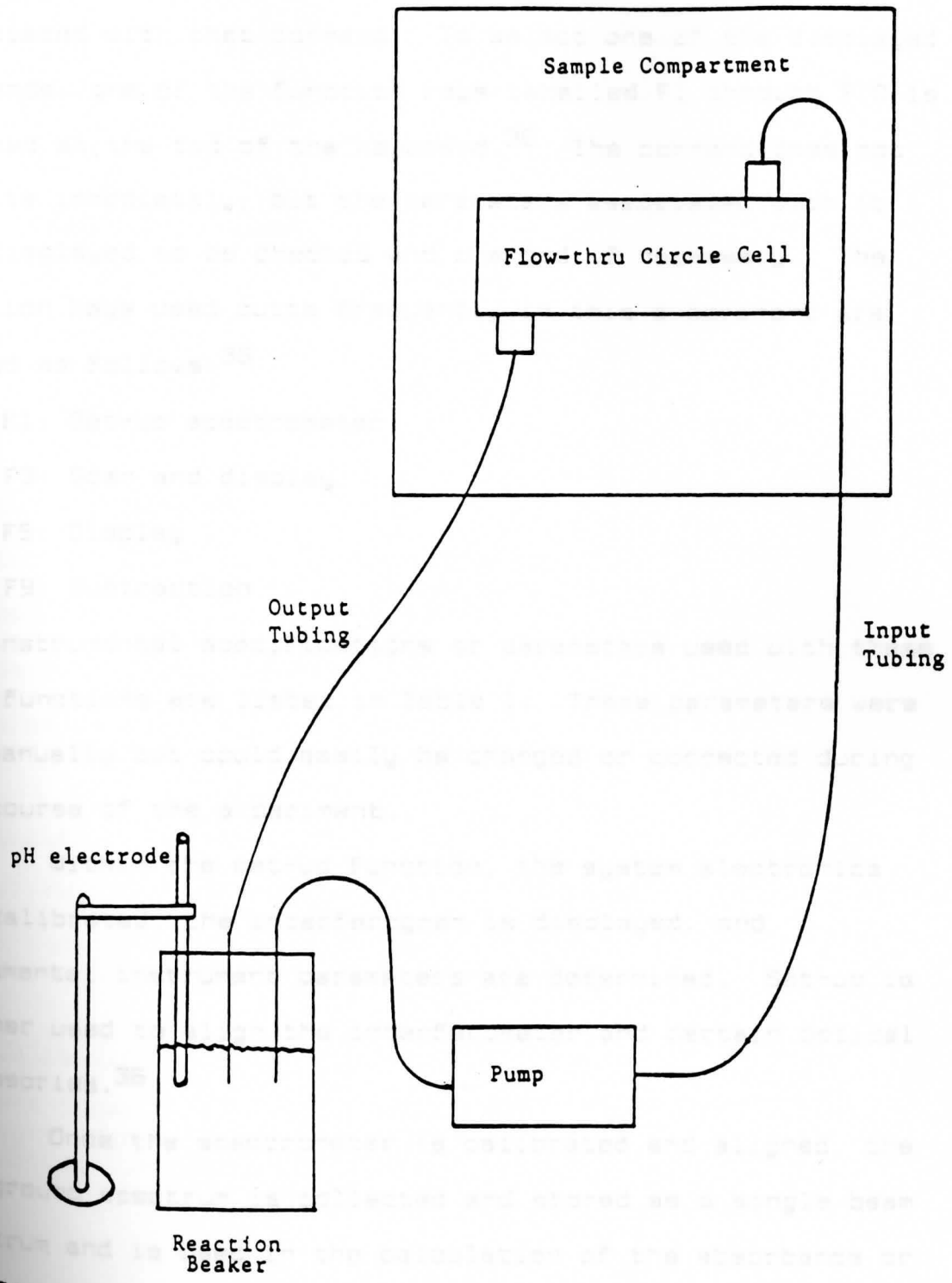

Figure 10. Diagram of the Flow Thru Cell and Pump Set-up[32]

the user to choose a command and bring up the parameter page associated with that command. To select one of the displayed commands, one of the function keys labelled F1 through F10 is pressed at the top of the keyboard.[36] The command does not execute immediately, but the parameters associated with it are displayed to be checked and changed if necessary. The function keys used quite frequently in this experiment are listed as follows:[36]

F1: Set-up spectrometer

F3: Scan and display

F5: Display

F9: Subtraction

The instrumental specifications or parameters used with these four functions are listed in Table 1. These parameters were set manually but could easily be changed or corrected during the course of the experiment.

Within the set-up function, the system electronics are calibrated, the interferogram is displayed, and fundamental instrument parameters are determined. Set-up is further used to align the interferometer and certain optical accessories.[36]

Once the spectrometer is calibrated and aligned, the background spectrum is collected and stored as a single beam spectrum and is used in the calculation of the absorbance or transmittance spectrum of the test sample.[36] A transmittance spectrum is the ratio of the sample single beam spectrum to

Table 1

Instrumental Specifications Used

Spectrometer Set-up

Detector:	Internal
Scan-speed:	20 kHz
Delay:	5.0 seconds
Aperture:	0.5 cm^{-1}
Low Pass Filter:	4.5 kHz
Collect Sensitivity:	1

Scan and Display

Spectrum Type:	Absorbance Background
Resolution:	4 cm^{-1}
Number of Scans:	256
Spectral Region Start:	3000 cm^{-1}
Spectral Region End:	900 cm^{-1}
Noise Level:	0.05
Apodization:	Triangular

Display

Horizontal Axis Start Point:	3000 cm^{-1}
Horizontal Axis End Point:	900 cm^{-1}
Vertical Axis Maximum Value:	0.08
Vertical Axis Minimum Value:	-0.04

Subtraction

Left Edge:	3500.5 cm^{-1}
Right Edge:	3100.0 cm^{-1}
Subtraction Factor:	10

the background spectrum. The absorbance spectrum is produced by computing the logarithm to the base 10 of the reciprocal of the transmittance spectrum.[36] Both the background and sample spectrum can be determined by using the scan and display function, which can be accessed by pressing key F3. First, the background spectrum name is entered and the return key is pressed. To execute the scan and display function, the execute key is utilized. Once the background is stored, the absorbance spectrum may be taken by entering its spectrum name first and then executing the function using the execute key. The sample spectrum is displayed and is saved in its own file by pressing key F8 and the execute key. The spectrum may be recalled at any time by using the display function.[36]

The last parameter page to be used is the subtraction function. The subtraction command produces a plot which is the difference between the sample's absorption spectrum and the reference absorption spectrum.[36] The spectra are not overwritten during a subtraction but instead the original data is retained, and the difference between the two spectra is stored under a new spectrum name. The subtraction function was very useful in this experiment in observing how the spectra of sample solutions at high pH compared to those at a low pH. The peaks that changed drastically in absorbance over the specified pH range were easily spotted and their respective wavenumbers were determined using the cursor motion function.

Part D: Experimental Procedure Using the 3200 Data System

1. Reference spectra of procaine, dibucaine, and dyclonine are collected in aqueous 25% acetonitrile, 50% acetonitrile, and 75% acetonitrile solutions at acidic condition, pH 2.

2. Once an acceptable reference is established, the pH is adjusted to the next interval by the addition of KOH. A pump is used to carry this solution through the circle cell until a stable pH is displayed on the pH meter. The pump is then turned off. Intervals to be tested include pH 4, 5, 6, 7, 8, 9, 10, and 11.

3. The sample spectrum of each aliquot can be determined by using the scan and display command described earlier. All spectra are saved and may be recalled using the display function.

4. Once the sample and reference spectra have been collected, an average baseline is determined for a given peak. The baseline absorbance is subtracted from the maximum for each peak to give a net absorbance value which in turn is used to calculate the pK_a of the drugs in the various solutions.

CHAPTER V

EXPERIMENTAL RESULTS AND DISCUSSION

Introduction

The acid/base properties of procaine, dibucaine, and dyclonine in varying solvents and pH were studied by using Fourier Transform Infrared Spectrometry. The effect of solvent and pH on these compounds in water, 25, 50, and 75 percent acetonitrile were studied by noting the net absorbance of the infrared absorption bands common to all spectra as the pH was adjusted from acidic conditions to alkaline conditions. By using pH 2 solutions as the background, any absorption band changes which occurred as the pH became more basic could be noted.

One major absorption band, peak X, appeared consistently in all the local anesthetics solutions as the pH increased. In the case of procaine peak X occurred in the 1632-1600 cm^{-1} range for all solutions tested. Peak X occurred in the 1579-1334 cm^{-1} range for both aqueous and acetonitrile solutions of dibucaine. Lastly peak X for dyclonine occurred in the 1726-1182 cm^{-1} range for all solutions monitored. The individual wavenumbers for peak X for all solutions tested are listed in Tables 2 and 3. Figures 11 to 22 illustrate the characteristic infrared spectra of procaine, dibucaine, and dyclonine in water and

25, 50, and 75 percent acetonitrile solutions under alkaline conditions.

A correlation chart was used to interpret the characteristics of these infrared spectra. The region from 4000-1400 cm^{-1} is useful for the indentification of various functional groups. The range of infrared wavelengths used in this experiment was approximately 3000-900 cm^{-1}. This region shows absorption bands arising from scissoring, stretching, and bending vibrations. Using this chart, peak X may be attributed to both the NH_2 scissoring vibration and the NH_3 bending vibration mode for procaine, the secondary amide bend and the NH_3 bending vibrational mode for dibucaine, and, lastly, the C-N and C=O stretch vibrational modes for dyclonine.[42]

Determination of pK_a values

The pK_a values of the anesthetics were calculated using the net absorbance value changes of peak X in varying solvents and pH. These values are listed in Tables 4 to 15.

The absorbance values of these peaks were plotted against pH to obtain an S-shaped curve. In Figure 23 is shown the type of curve obtained.[43] A curve fitting program was utilized to give a polynomial fit of the corresponding data. In Figures 24 to 35 are illustrated the curves obtained for the local anesthetic solutions studied. The regression order used for each peak measured is also listed

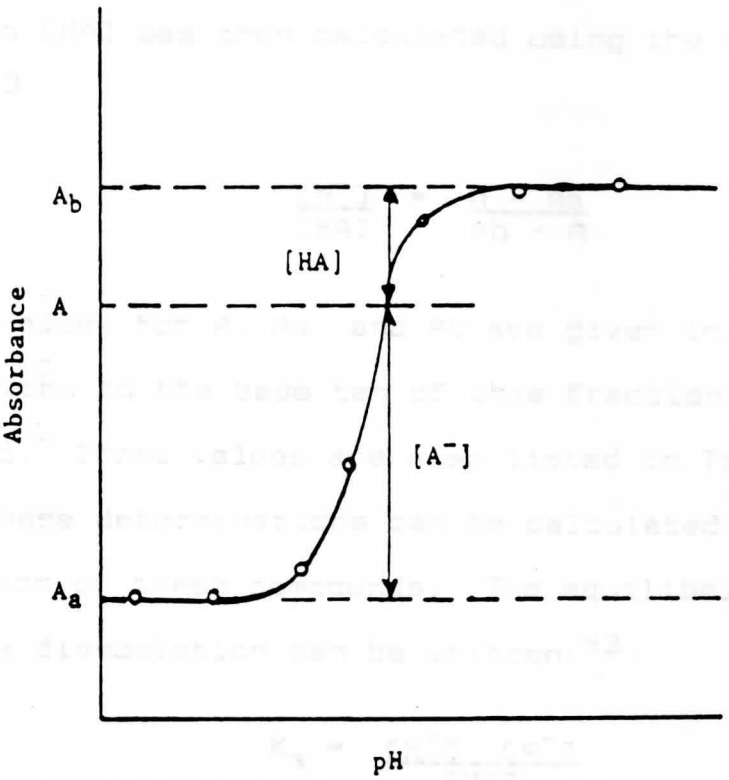

Figure 23. Standard Plot of Absorbance vs pH for a Weak Acid, HA[43]

in Tables 2 to 13. Using these curves the pK_a of procaine, dibucaine, and dyclonine could be determined by two methods.

The first method involved using the S-shaped curves to obtain the relative values for $[A^-]$ and [HA]. The ratio of $[A^-]$ to [HA] was then calculated using the following formula:[43]

$$\frac{[A^-]}{[HA]} = \frac{A - Aa}{Ab - A} \qquad (1)$$

Standard values for A, Aa, and Ab are given in Figure 16. The logarithm to the base ten of this fraction was then calculated. These values are also listed in Tables 2 to 13.

These determinations can be calculated due to the dissociation of these compounds. The equilibrium expression for such a dissociation can be written:[43]

$$K_a = \frac{[H^+]\ [A^-]}{[HA]} \qquad (2)$$

Taking the negative log of both sides of this equation gives:

$$pK_a = pH - \log \frac{[A^-]}{[HA]} \qquad (3)$$

The slope intercept form of the equation which gives a straight line is as follows:[43]

$$\log \frac{[A^-]}{[HA]} = pH - pK_a \qquad (4)$$

Comparing equation 4 to the equation for a straight line, $y = mx + b$, the measured pK_a values can be determined where $y = \log [A^-]/[HA]$, the slope is equal to 1, and the intercept equals the negative pK_a. Thus, when the log term is plotted vs pH, the slope is 1, the intercept is negative pK_a, and the line crosses the pH axis at $pH = pK_a$. At this point $[A^-]$ equals [HA], therefore, the log of the ratio of these terms is zero, making $pH = pK_a$.[43]

Using the above form of the equation the logarithm values of the ratios are obtained and plotted against the measured pH. The best line fit is calculated using linear regression and the measured pK_a is determined by obtaining the pH at which the line crosses the x axis. These graphs are illustrated in Figures 36 to 47.

The second method for determining pK_a involved using a computer program known as Hyperplot. Hyperplot is an easy to use program for data analysis and plotting for the IBM PC/XT/AT computers.[44] Single keystroke commands allow access to 150 Hyperplot functions.[44] Data may be input in one- or two-dimensional form from a disk file, the keyboard, or with a graphics cursor, and output is to a dot matrix printer or a plotter.[44] Once the data is read in, a wide variety of mathematical and graphics functions may be performed.

The Hyperplot function used in this project was differentiation of the plotted data. Namely absorbance versus pH for the local anesthetic solutions. Taking the derivative of y (absorbance) with respect to x (pH) a spike-

shaped curve is obtained. The maximum of the curve is the corresponding pK_a value which can be displayed by using the cursor motion key. The Hyperplot functions for each anesthetic solution are shown in Figures 48 to 59.

The pK_a values obtained by both methods, namely Hyperplot and linear regression are listed in Table 14. These pK_a values must be adjusted due to the fact that the hydrogen ion activity measured by the pH meter must be corrected. The reason for this is that the electrode response is affected by solutions containing nonaqueous solvents.[32] This correction can be done by using a formula proposed by McBryde and Mui. The formula is as follows:

$$** = 10^{-pH} / [H^+] \qquad (5)$$

The symbol ** represents equilibrium constants established for mixed solvents.[45] These constants are 0.97 for 25% acetonitrile solutions, 1.22 for 50% acetonitrile solutions, and 2.42 for 75% acetonitrile solutions.[46] Once the $[H^+]$ is determined using equation 5, the adjusted pH can be calculated. As mentioned earlier, the pH equals pK_a at the pH intercept when the log $[A^-]/[HA]$ is plotted versus pH, thus the values obtained are the adjusted pK_a values. These values are listed in Table 15.

Table 2

Local Anesthetic	Medium	Peak X (cm^{-1})	Hyperplot (pK_a)	Regression Formula (pK_a)
Procaine in	water	1606	9.1	9.0
	25% acetonitrile	1606	8.4	8.6
	50% acetonitrile	1606	8.0	8.2
	75% acetonitrile	1632	9.3	8.7
Dibucaine in	water	1579	8.4	8.2
	25% acetonitrile	1334	8.0	7.8
	50% acetonitrile	1334	8.3	8.5
	75% acetonitrile	1334	8.7	8.7
Dyclonine in	water	1182	8.5	8.3
	25% acetonitrile	1600	8.8	8.6
	50% acetonitrile	1600	8.4	8.4
	75% acetonitrile	1726	8.3	8.3

Table 3

Adjusted pK_a Values

Local Anesthetic	Medium	Peak X (cm^{-1})	Hyperplot (pK_a)	Regression Formula (pK_a)
Procaine in	water	1606	9.1	9.0
	25% acetonitrile	1606	8.3	8.6
	50% acetonitrile	1606	8.1	8.3
	75% acetonitrile	1632	9.7	9.1
Dibucaine in	water	1579	8.4	8.2
	25% acetonitrile	1334	7.9	7.8
	50% acetonitrile	1334	8.4	8.6
	75% acetonitrile	1334	9.1	9.1
Dyclonine in	water	1182	8.5	8.3
	25% acetonitrile	1600	8.8	8.5
	50% acetonitrile	1600	8.5	8.5
	75% acetonitrile	1726	8.7	8.7

Table 4

Experimental Data Obtained From Peak X For Procaine In Water.

Net Absorbance		Log [A-] / [HA]	
pH	Peak X	pH	Peak X
6.49	0.013	6.7	-1.68
7.62	0.016	6.9	-1.37
8.21	0.019	7.1	-1.27
8.43	0.020	7.3	-1.18
8.66	0.023	7.5	-1.08
8.85	0.025	7.7	-0.96
9.01	0.027	7.9	-0.86
9.23	0.030	8.1	-0.73
9.65	0.037	8.3	-0.59
9.88	0.040	8.5	-0.47
10.22	0.043	8.7	-0.31
		8.9	-0.16
		9.1	0.00
		9.3	0.19
		9.5	0.36
		9.7	0.58
		9.9	0.84

Regression order = 5

Table 5

Experimental Data Obtained From Peak X For Procaine In 25% Acetonitrile.

Net Absorbance		Log [A-] / [HA]	
pH	Peak X	pH	Peak X
5.66	0.011	6.75	-1.72
7.68	0.013	7.0	-1.18
8.26	0.014	7.25	-0.95
8.46	0.015	7.5	-0.69
8.74	0.017	7.75	-0.46
8.96	0.019	8.0	-0.29
9.32	0.020	8.25	-0.15
9.53	0.021	8.5	-0.002
9.71	0.021	8.75	0.02
9.96	0.022	9.0	0.29
10.23	0.022	9.25	0.42
10.60	0.023	9.5	0.55
11.30	0.023	9.75	0.75
12.43	0.024	10.0	0.95
13.01	0.024	10.25	1.15
		10.5	1.41
		10.75	1.61

Regression order = 5.

Table 6

Experimental Data Obtained From Peak X For Procaine In 50% Acetonitrile.

Net Absorbance		Log [A-] / [HA]	
pH	Peak X	pH	Peak X
5.81	0.00580	6.75	-1.42
6.94	0.00665	7.0	-1.03
7.87	0.00870	7.25	-0.75
8.12	0.011	7.5	-0.52
8.29	0.011	7.75	-0.42
8.55	0.013	8.0	-0.15
8.73	0.014	8.25	0.04
8.92	0.014	8.5	0.18
9.33	0.016	8.75	0.39
10.49	0.016	9.0	0.60
		9.25	0.82
		9.5	1.14
		9.75	1.57
		10.0	1.90

Regression order = 3.

Table 7

Experimental Data Obtained From Peak X For Procaine In 75% Acetonitrile.

Net Absorbance		Log [A-] / [HA]	
pH	Peak X	pH	Peak X
4.89	0.00805	5.6	-1.87
6.19	0.00845	6.0	-1.56
7.27	0.00910	6.4	-1.25
8.05	0.01	6.8	-1.11
8.57	0.011	7.2	-0.99
9.03	0.013	7.6	-0.81
9.66	0.016	8.0	-0.59
10.41	0.018	8.4	-0.38
10.83	0.018	8.8	-0.18
		9.2	0.08
		9.6	0.40
		10.0	0.86
		10.4	1.56

Regression order = 5.

Table 8

Experimental Data Obtained From Peak X For Dibucaine In Water.

Net Absorbance		Log [A-] / [HA]	
pH	Peak X	pH	Peak X
3.55	0.00110	6.5	-1.68
4.72	0.00115	6.75	-1.27
5.32	0.00310	7.0	-1.0
6.12	0.00415	7.25	-0.76
6.89	0.00580	7.5	-0.57
7.78	0.00685	7.75	-0.34
7.93	0.010	8.0	-0.18
8.15	0.011	8.25	-0.007
8.3	0.014	8.5	0.17
8.48	0.020	8.75	0.40
8.72	0.020	9.0	0.57
8.92	0.024	9.25	0.88
9.10	0.026	9.5	1.27
9.30	0.027	9.75	1.68
10.00	0.028		

Regression order = 4.

Table 9

Experimental Data Obtained From Peak X For Dibucaine In 25% Acetonitrile.

Net Absorbance		Log [A-] / [HA]	
pH	Peak X	pH	Peak X
4.39	0.00045	6.75	-2.24
5.75	0.00140	7.0	-1.21
6.29	0.00205	7.25	-0.99
7.18	0.00560	7.5	-0.41
7.37	0.00760	7.75	-0.13
7.88	0.026	8.0	0.21
8.03	0.053	8.25	0.55
8.15	0.084	8.5	1.06
8.27	0.082	8.75	1.98
8.5	0.090		
9.0	0.095		

Regression order = 4.

Table 10

Experimental Data Obtained From Peak X For Dibucaine In 50% Acetonitrile.

Net Absorbance		Log [A-] / [HA]	
pH	Peak X	pH	Peak X
6.14	0.00425	7.50	-1.86
7.08	0.00720	7.75	-1.05
7.93	0.016	8.0	-0.82
8.10	0.027	8.25	-0.32
8.25	0.057	8.5	0.008
8.38	0.084	8.75	0.36
9.00	0.124	9.0	0.78
9.62	0.148	9.25	1.45

Regression order = 4.

Table 11

Experimental Data Obtained From Peak X For Dibucaine In 75% Acetonitrile.

Net Absorbance		Log [A-] / [HA]	
pH	Peak X	pH	Peak X
5.84	0.00495	7.35	-1.98
6.86	0.00565	7.60	-1.38
7.84	0.00755	7.85	-0.99
8.19	0.00945	8.10	-0.67
8.33	0.010	8.35	-0.41
8.60	0.014	8.6	-0.16
8.89	0.018	8.85	0.07
9.05	0.020	9.0	0.34
9.25	0.020	9.35	0.68
10.37	0.025	9.6	1.05
		9.85	1.75

Regression order = 4.

Table 12

Experimental Data Obtained From Peak X For Dyclonine In Water.

Net Absorbance		Log [A-] / [HA]	
pH	Peak X	pH	Peak X
2.59	0.00565	6.75	-2.46
2.61	0.00560	7.0	-1.63
3.94	0.00535	7.25	-1.13
4.92	0.00415	7.5	-0.76
5.52	0.00240	7.75	-0.53
6.00	0.00750	8.0	-0.28
6.77	0.00915	8.25	-0.05
8.24	0.018	8.5	0.17
8.31	0.019	8.75	0.48
8.52	0.036	9.0	0.79
8.60	0.046	9.25	1.32
8.75	0.056		
9.76	0.058		

Regression order = 5.

Table 13

Experimental Data Obtained From Peak X For Dyclonine In 25% Acetonitrile.

Net Absorbance		Log [A-] / [HA]	
pH	Peak X	pH	Peak X
3.56	0.00175	7.0	-1.86
5.78	0.010	7.25	-1.32
6.37	0.013	7.5	-0.96
7.32	0.020	7.75	-0.71
7.52	0.024	8.0	-0.47
7.90	0.035	8.25	-0.26
8.28	0.055	8.5	-0.035
8.61	0.085	8.75	0.18
8.81	0.124	9.0	0.40
8.96	0.154	9.25	0.64
9.17	0.181	9.5	0.73
10.0	0.198	9.75	1.20
		10.0	1.64

Regression order = 4.

Table 14

Experimental Data Obtained From Peak X For Dyclonine In 50% Acetonitrile.

Net Absorbance		Log [A-] / [HA]	
pH	Peak X	pH	Peak X
4.40	0.00200	7.0	2.32
6.08	0.00595	7.25	1.52
6.78	0.00960	7.5	0.97
7.12	0.014	7.75	0.66
7.37	0.018	8.0	0.40
7.65	0.026	8.25	0.15
7.85	0.039	8.5	-0.12
8.09	0.066	8.75	-0.36
8.20	0.083	9.0	-0.67
8.42	0.194	9.25	-0.86
8.85	0.278	9.5	-1.72
9.00	0.300		
9.50	0.320		

Regression order = 4.

Table 15

Experimental Data Obtained From Peak X For Dyclonine In 75% Acetonitrile.

Net Absorbance		Log [A-] / [HA]	
pH	Peak X	pH	Peak X
4.39	0.00110	7.0	-2.39
6.10	0.00130	7.25	-1.43
6.80	0.00140	7.5	-0.94
7.10	0.00300	7.75	-0.60
7.40	0.00560	8.0	-0.36
7.60	0.00910	8.25	-0.09
7.85	0.015	8.5	0.20
8.10	0.027	8.75	0.44
8.19	0.035	9.0	0.76
8.40	0.068	9.25	1.27
8.70	0.090	9.5	2.03
9.00	0.099		
9.90	0.105		

Regression order = 4.

CHAPTER VI

CONCLUSION

The pK_a values of procaine, dibucaine, and dyclonine in aqueous solutions were determined experimentally using Fourier Transform Infrared Spectrometry. This method proved reliable for obtaining reproducible dissociation constants. The literature values for the pK_a of procaine and dibucaine in water are 9.1 and 8.3 respectively.[47,48] A literature value for the pK_a of dyclonine could not be found. Experimental pK_a values as determined using FTIR are 9.1, 8.4, and 8.5 for procaine, dibucaine, and dyclonine respectively. These values are in good agreement suggesting FTIR spectrometry is a reliable method for determining the pK_a of these local anesthetic agents. Knowing this fact, solutions containing increasing concentrations of the solvent acetonitrile were measured to observe changes, if any, in their respective pK_a values. As increasing concentrations of acetonitrile are used, the hydrophobicity of the solvent environment increases. This rise in hydrophobicity has been known to affect the pK_a of many compounds including amino acids and anti-viral agents.[32,45] Due to this prior work, it was felt that this pK_a study of mixed solvent solutions of varying hydrophobicity could be used to observe potential changes in pK_a upon membrane interaction of procaine,

dibucaine, and dyclonine, all local anesthetics.

Referring to Table 3, it can be shown that increases in acetonitrile caused the pK_a values to fluctuate, neither steadily increasing or steadily decreasing from the pK_a value in water. Initially, procaine and dibucaine both followed the same pattern. In 25% acetonitrile, the adjusted pK_a values were determined to be 8.3 and 7.9 for procaine and dibucaine respectively. On the other hand, the adjusted pK_a value of dyclonine increased slightly to 8.8 with an increase in acetonitrile to 25% of its total volume. In 50% acetonitrile the adjusted pK_a values of procaine decreased to a value of 8.1. Similarly, the pK_a of dyclonine dropped to 8.5. Dibucaine showed a slight increase in pK_a to 8.4. Finally, the addition of 75% acetonitrile caused an increase in pK_a for all three anesthetics to 9.7, 9.1, and 8.7 for procaine, dibucaine, and dyclonine respectively. One could conclude that at this concentration of acetonitrile, namely 75%, the pK_a will increase or become greater. However, solutions which were less hydrophobic gave varying pK_a values, showing no particular pattern for all three drugs. The pK_a values did remain in the range of 8 to 9 under increasing hydrophobic conditions. The pK_a of any typical local anesthetic in use lies between 8.0 and 9.0.[21]

As was mentioned previously, a local anesthetic whose pK_a is too high has very few molecules available in the free base form at a normal tissue pH of 7.4. Anesthetic action

would be poor because too few molecules would diffuse through the nerve membrane. On the other hand, a local anesthetic whose pK_a is quite low has a very large number of base molecules which are able to diffuse through the nerve sheath. However, anesthetic action of this agent would prove inadequate because only a very small number of base molecules would associate back to the cationic form necessary for binding to the receptor site. Procaine, dibucaine, and dyclonine in aqueous solution have pK_a values that are in the favorable range for local anesthetics, namely 8 to 9. As the environment becomes more hydrophobic, which was shown experimentally by adding acetonitrile, the pK_a values of procaine, dibucaine, and dyclonine fluctuated slightly but not enough to greatly affect the performance of these anesthetics on the nerve membrane.

The development of a cylindrical internal reflection cell allowed us to measure the absorbance of aqueous solutions using Fourier Transform Infrared Spectrometry. However, it did have its disadvantages. As mentioned before, the circle cell has a low light throughput. In other words, only 10 to 20 percent of the beam passes through the cell without a sample present. This disadvantage may have caused some experimental error. Another source of error was the low solubility of the anesthetics used in aqueous solutions. The acetonitrile helped to dissolve the anesthetics, but the solutions were easily saturated. Only small molar

concentrations could be made, thus, limiting the detection of these drugs using FTIR spectrometry.

In order to better understand the effects of varying pH and solvent hydrophobicity on local anesthetic agents, further studies should be done and further experimentation should be performed using FTIR spectrometry. This analytical method has been used to study polymers deposited directly upon the internal surface of the reflectance apparatus.[29] This same procedure could be repeated but instead of polymers a synthetic membrane could be coated onto the inner surface of the circle cell. In the case of local anesthetics, this membrane would seem to be a more favorable match to that of the actual nerve membrane and, in turn, should give a more accurate determination of the pK_a of these agents upon membrane interaction.

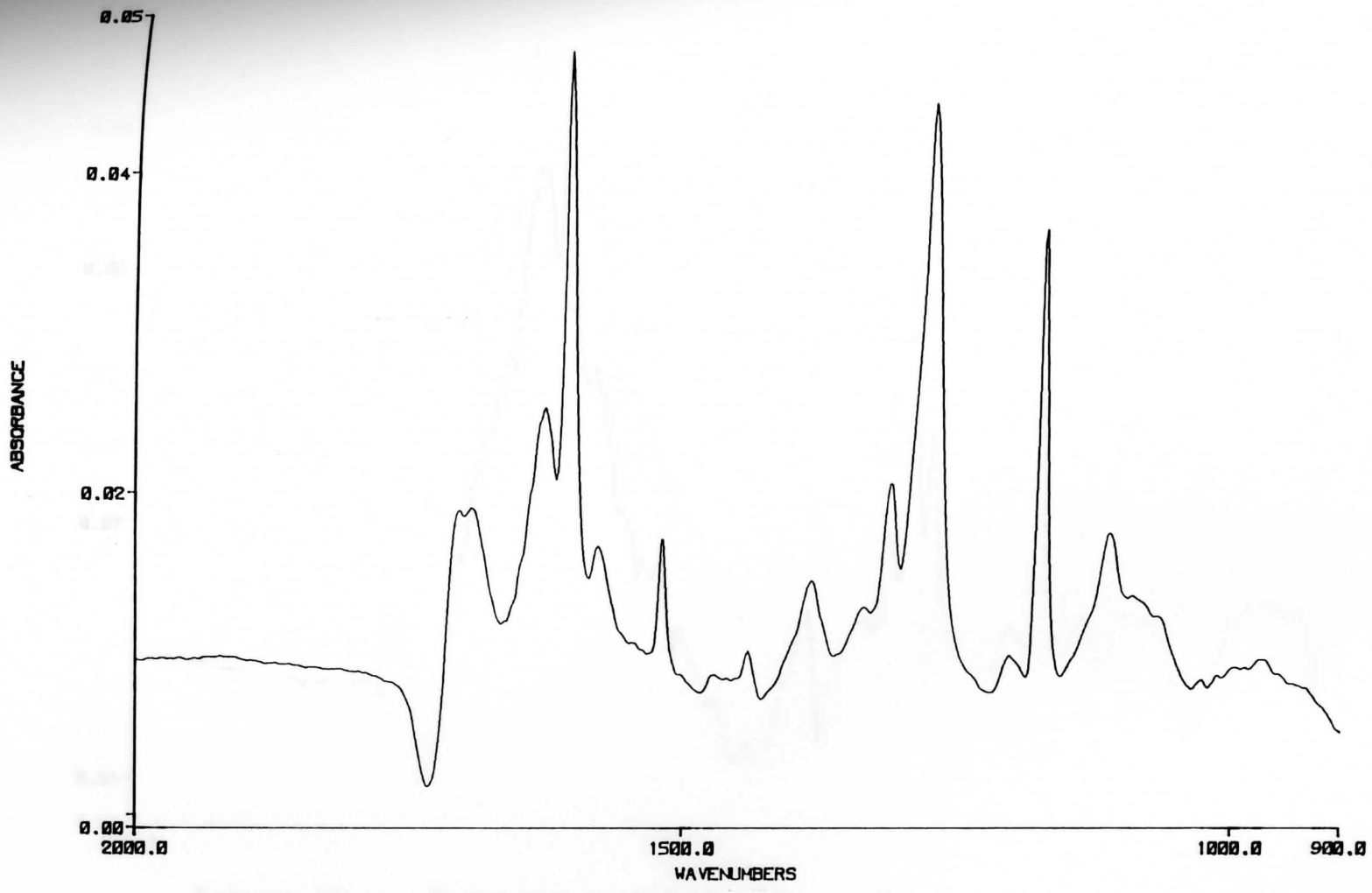

Figure 11. IR Spectrum of Procaine in Water at pH 11

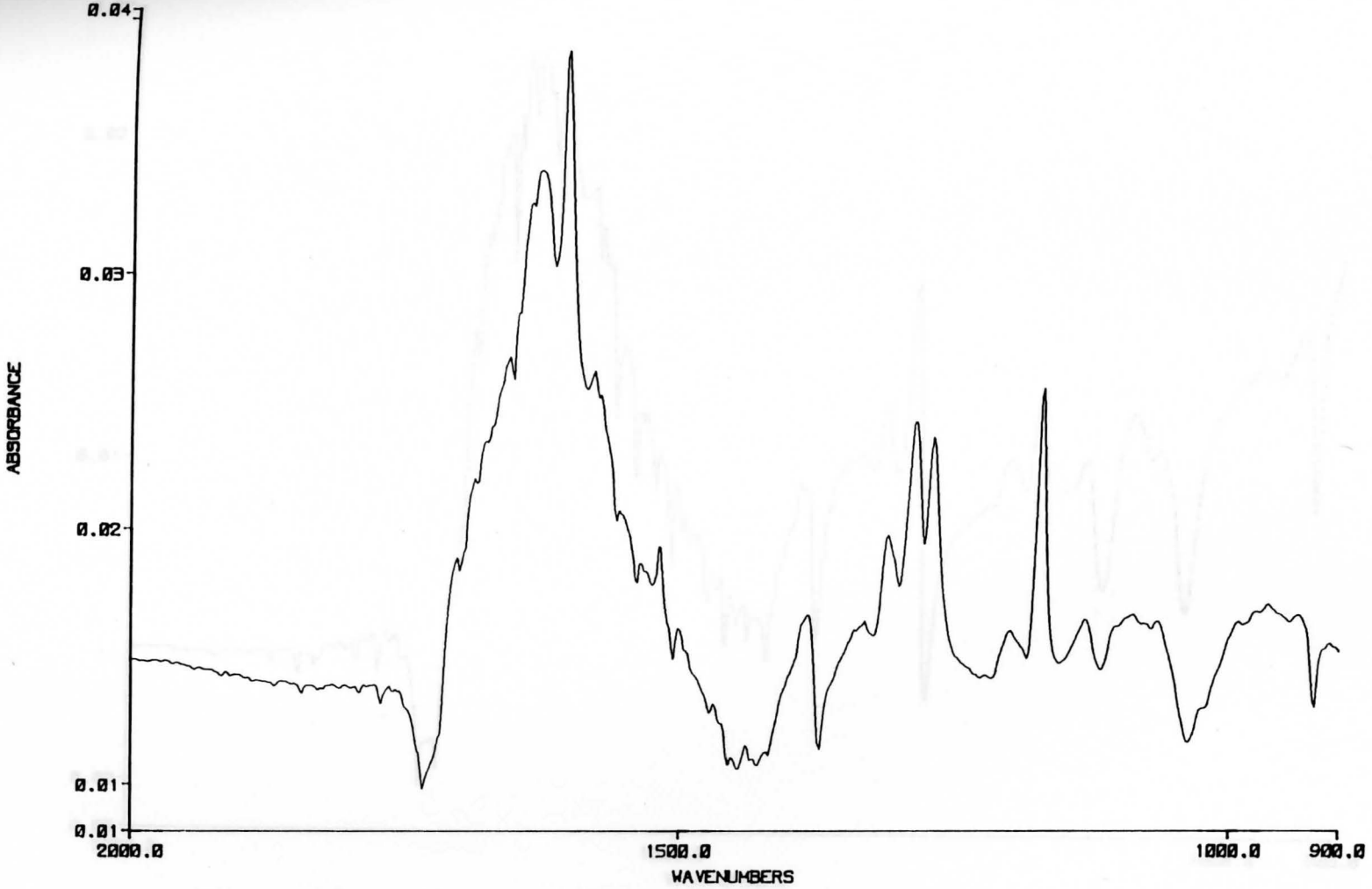

Figure 12. IR Spectrum of Procaine in 25% Acetonitrile at pH 11

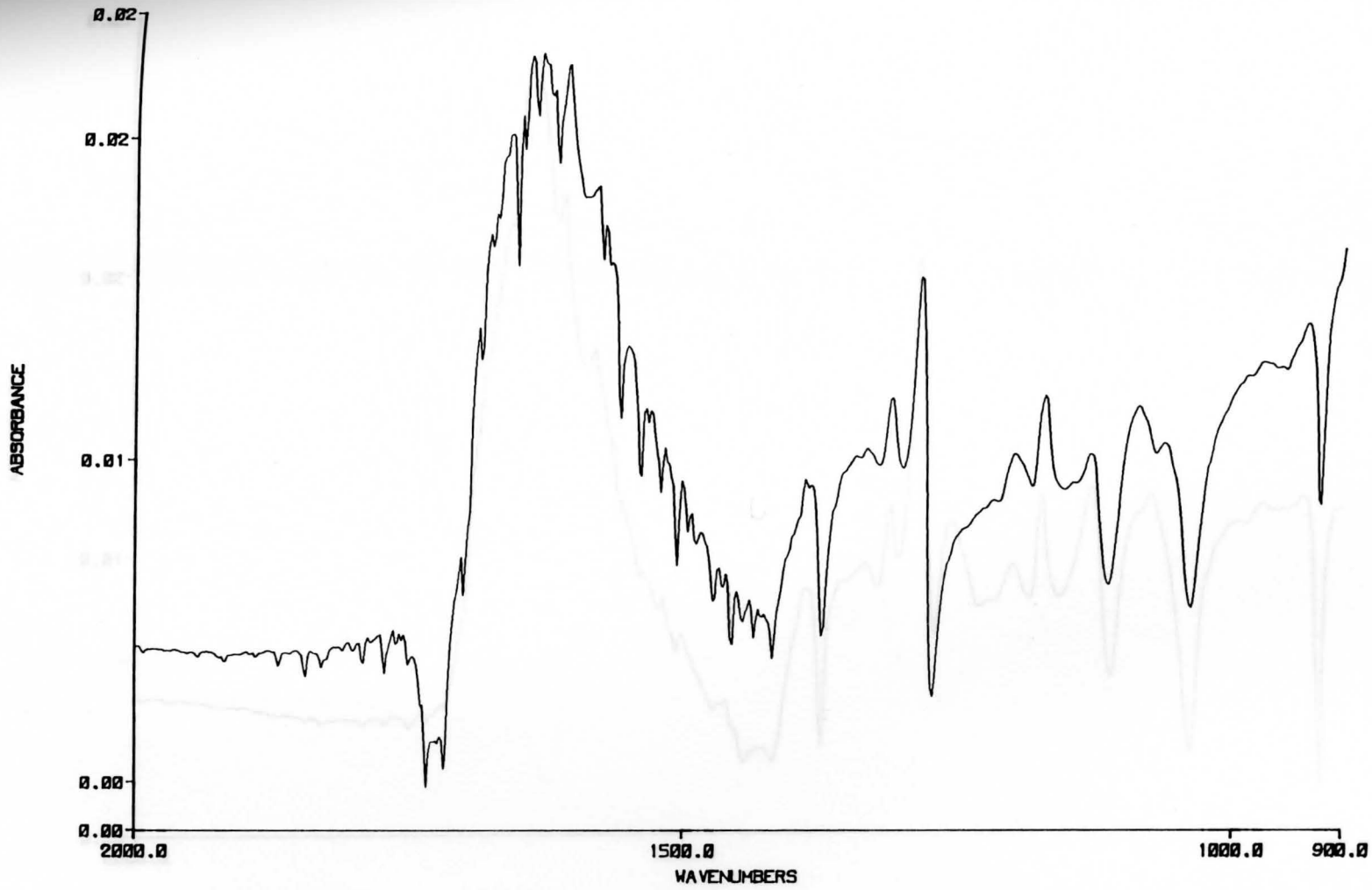

Figure 13. IR Spectrum of Procaine in 50% Acetonitrile at pH 11

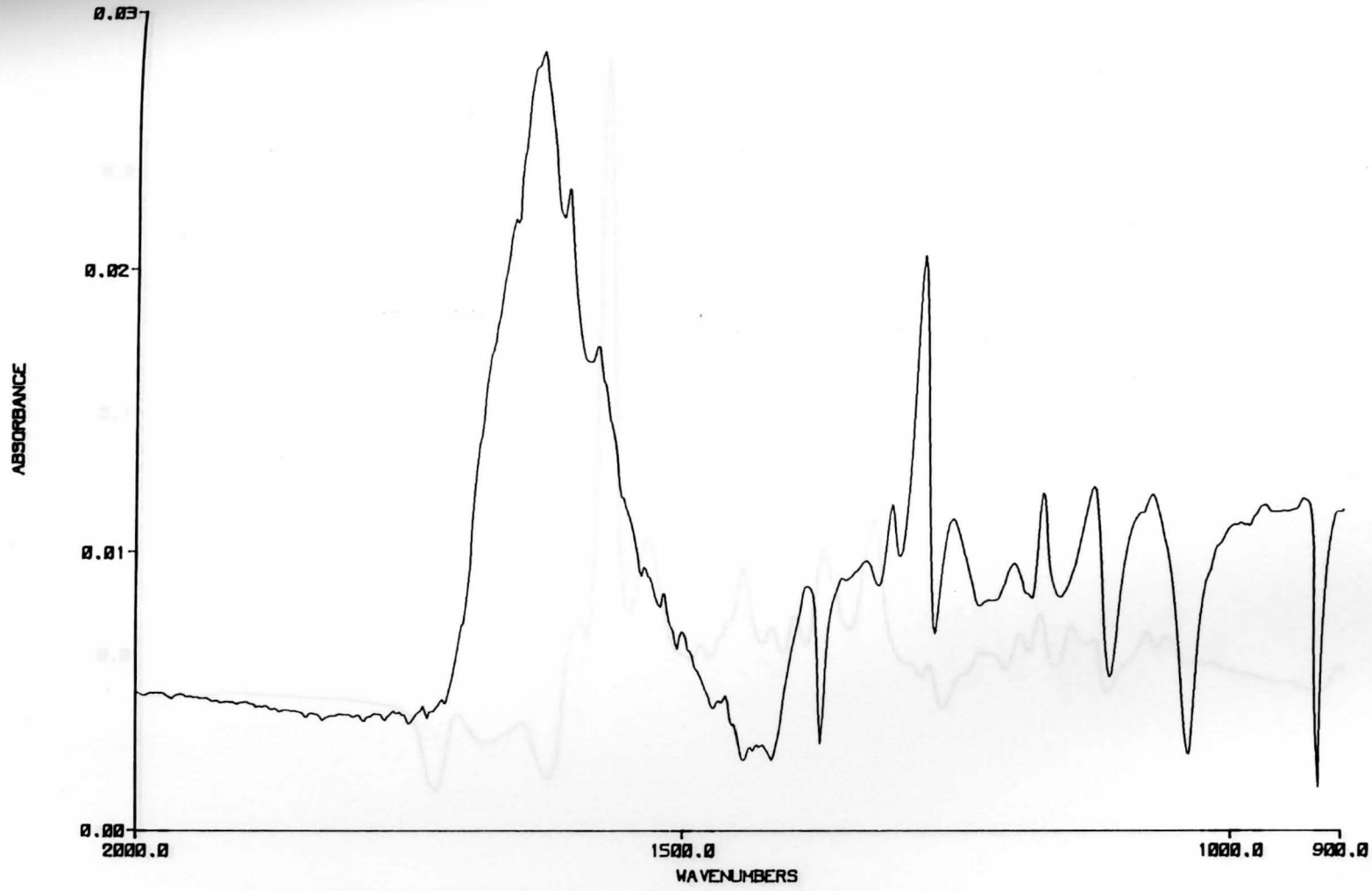

Figure 14. IR Spectrum of Procaine in 75% Acetonitrile at pH 11

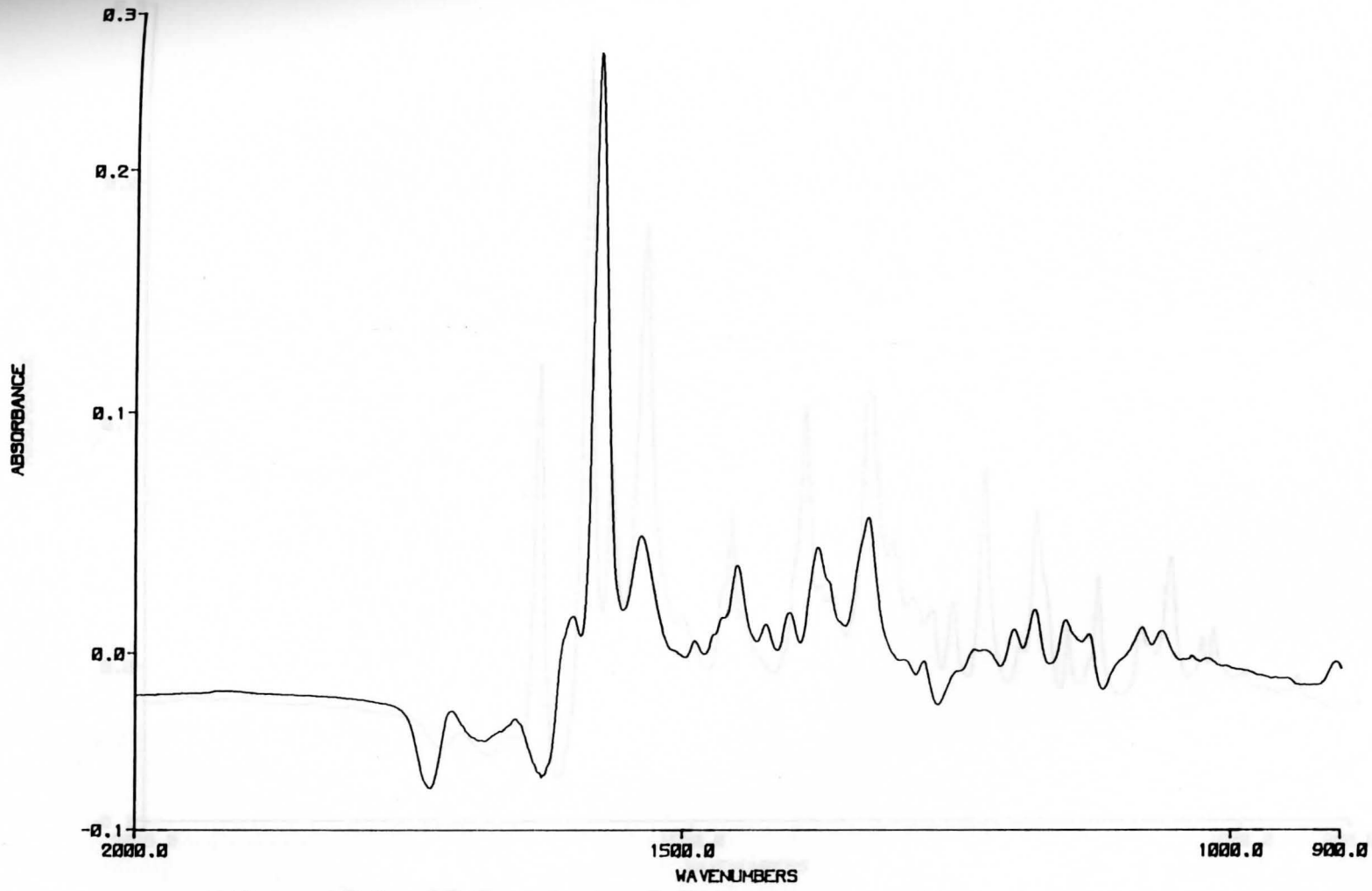

Figure 15. IR Spectrum of Dibucaine in Water at pH 9

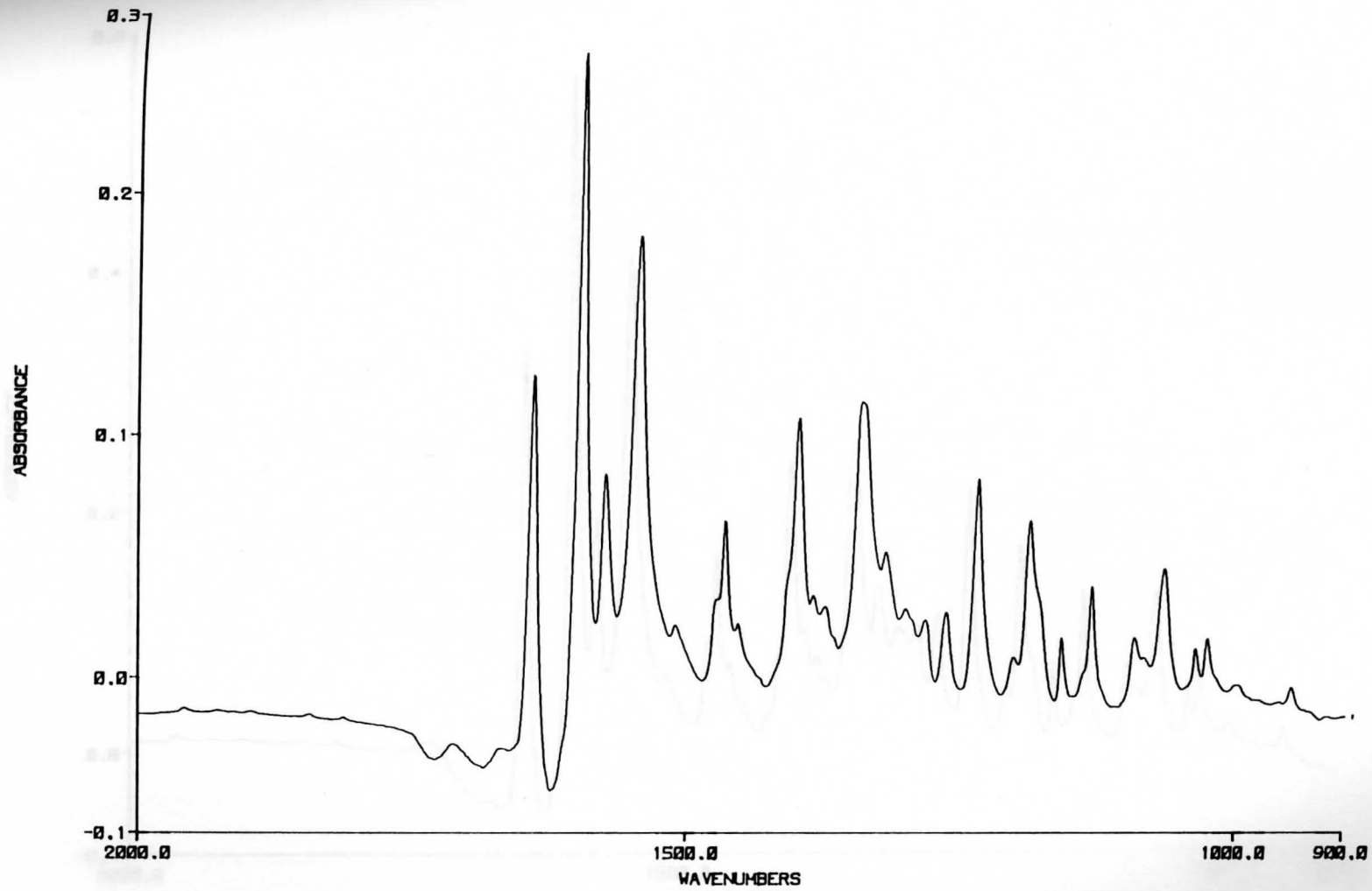

Figure 16. IR Spectrum of Dibucaine in 25% Acetonitrile at pH 9

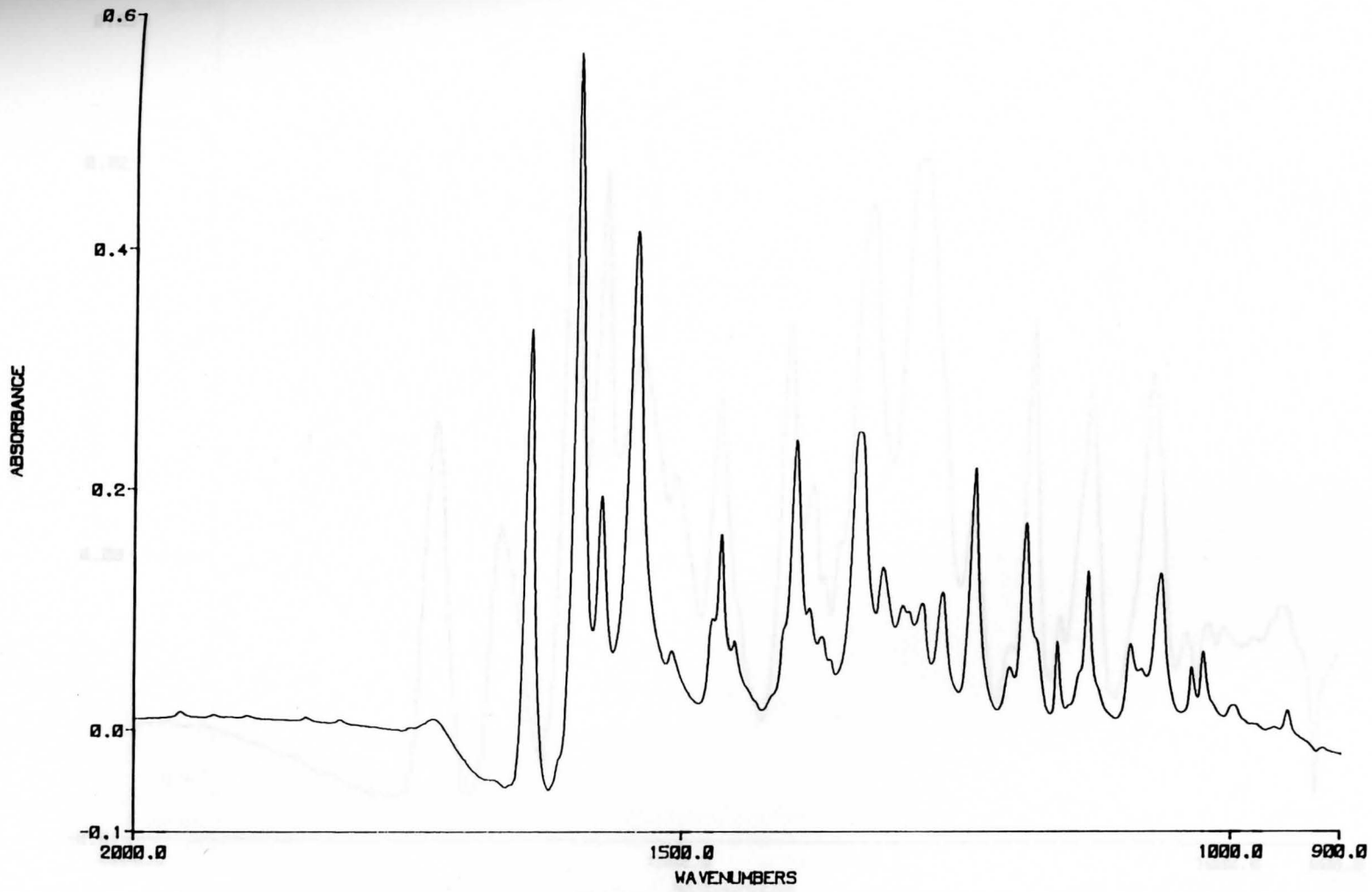

Figure 17. IR Spectrum of Dibucaine in 50% Acetonitrile at pH 9

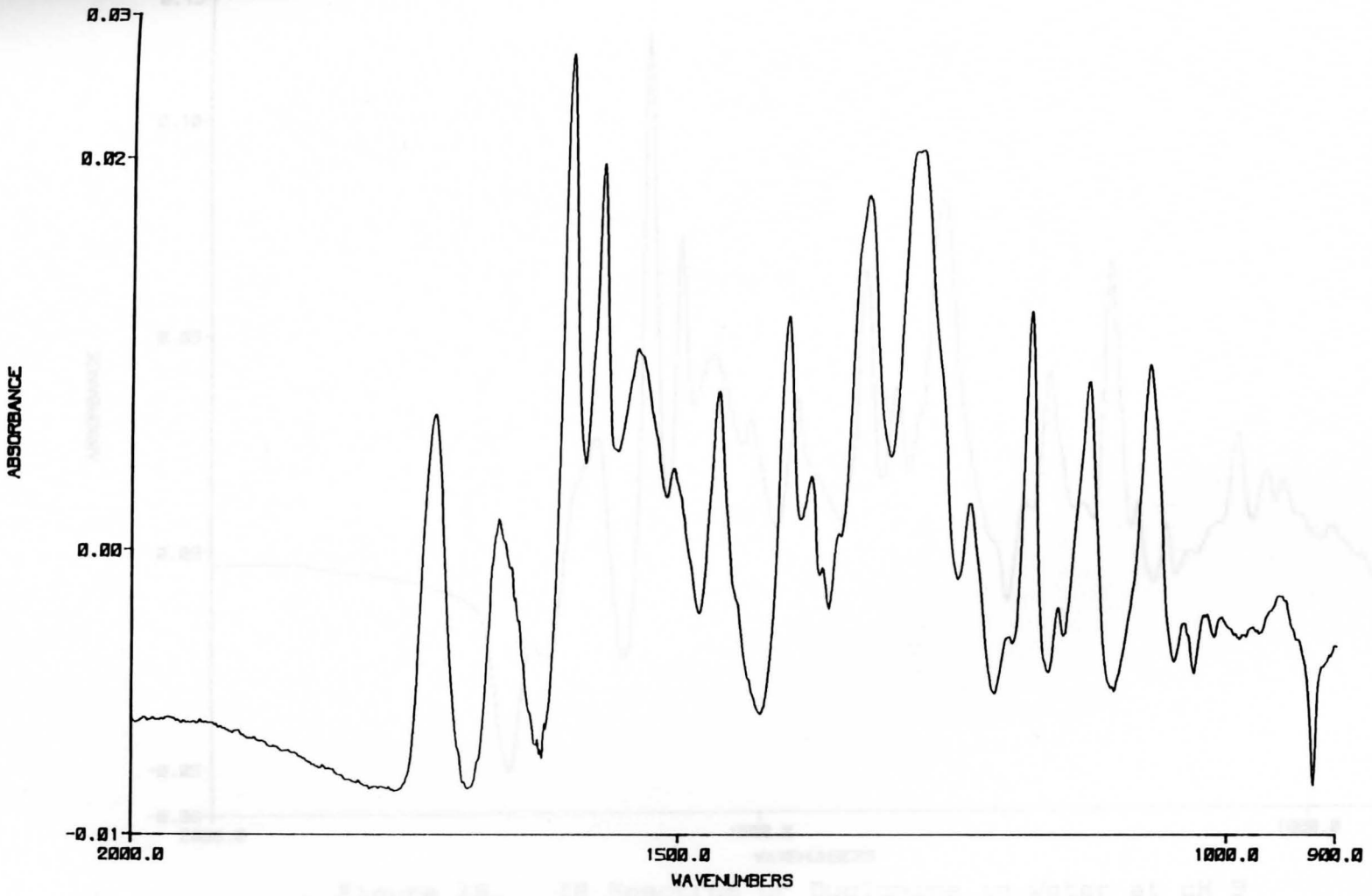

Figure 18. IR Spectrum of Dibucaine in 75% Acetonitrile at pH 9

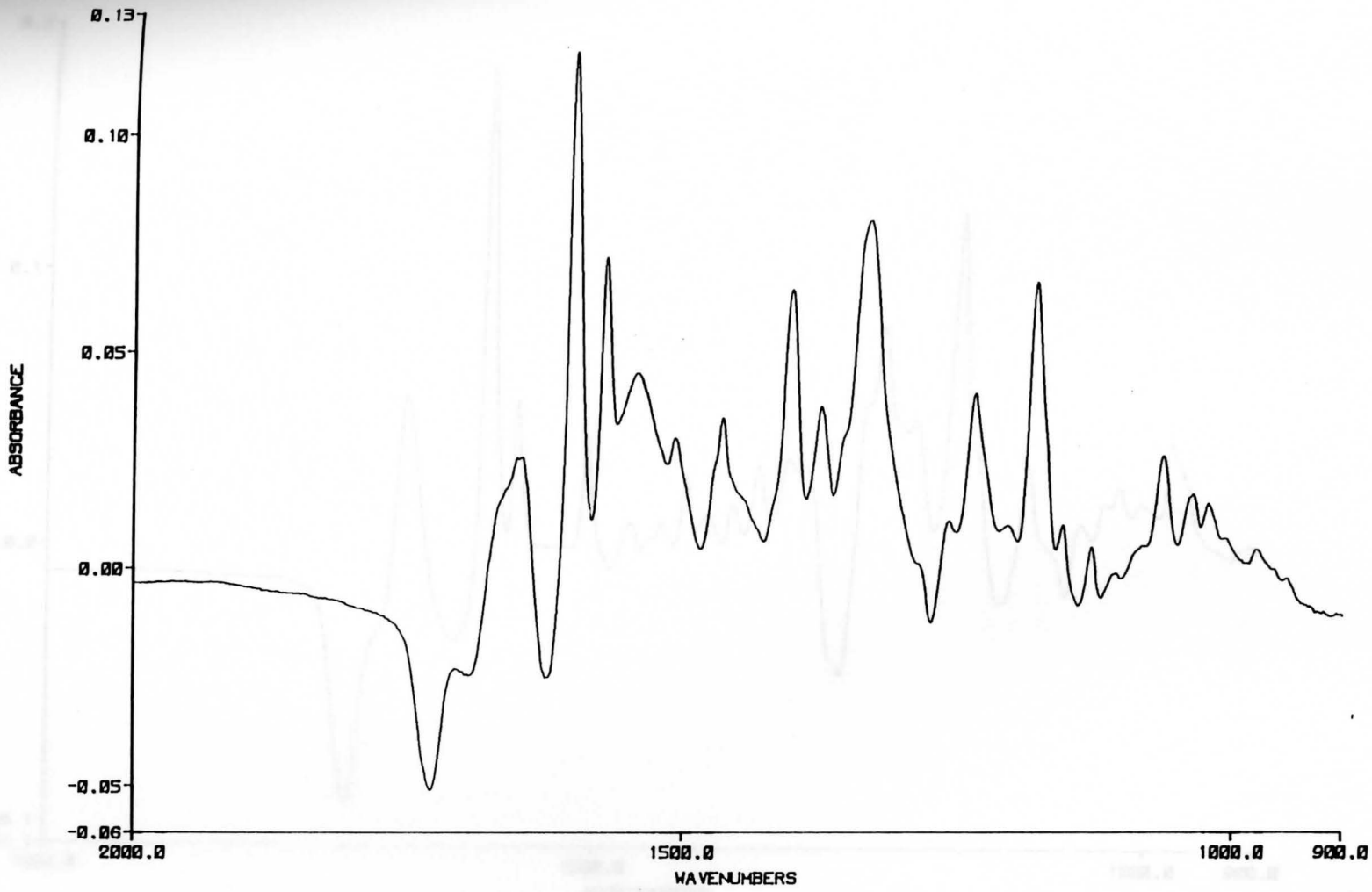

Figure 19. IR Spectrum of Dyclonine in Water at pH 9

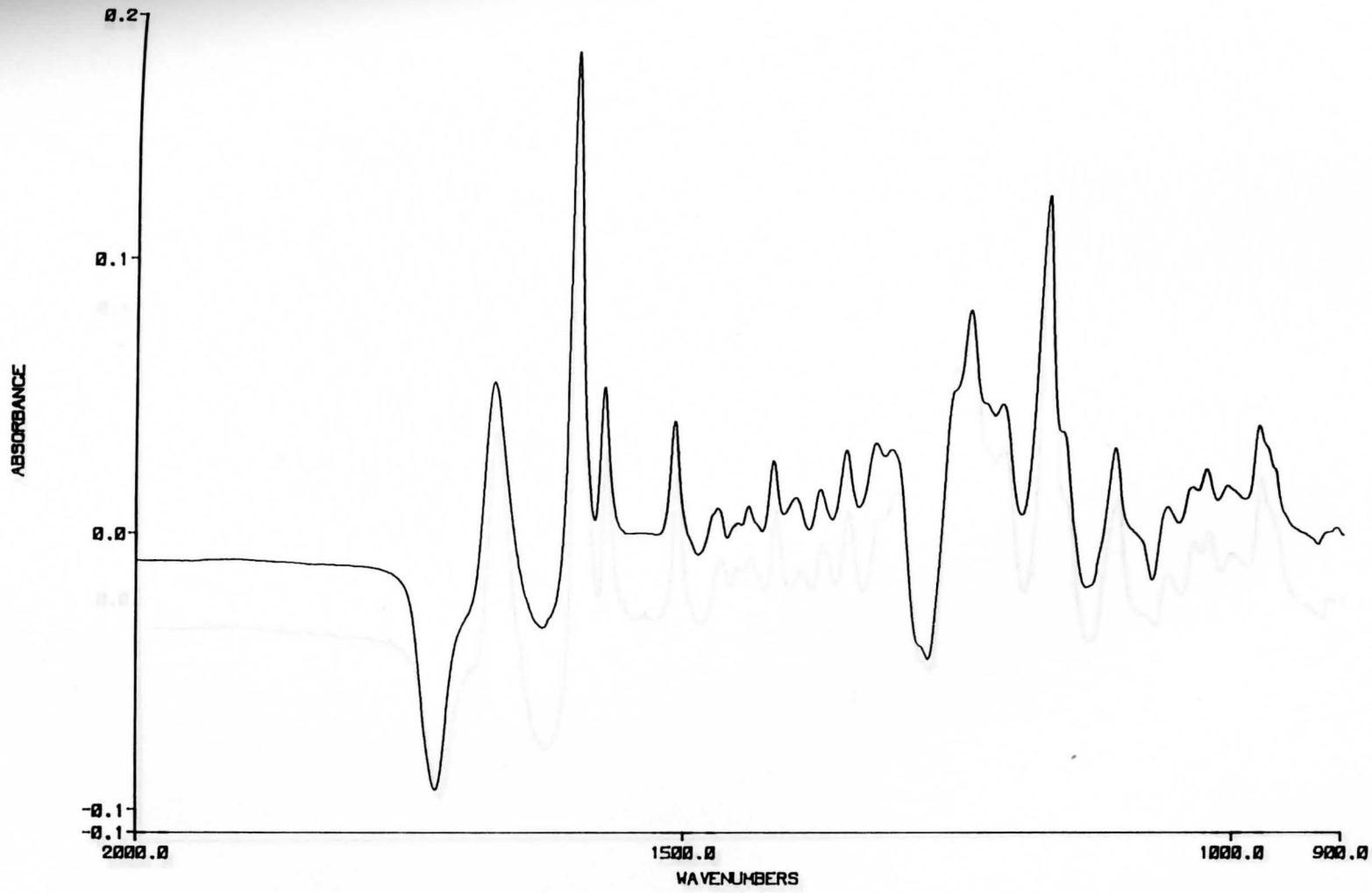

Figure 20. IR Spectrum of Dyclonine in 25% Acetonitrile at pH 9

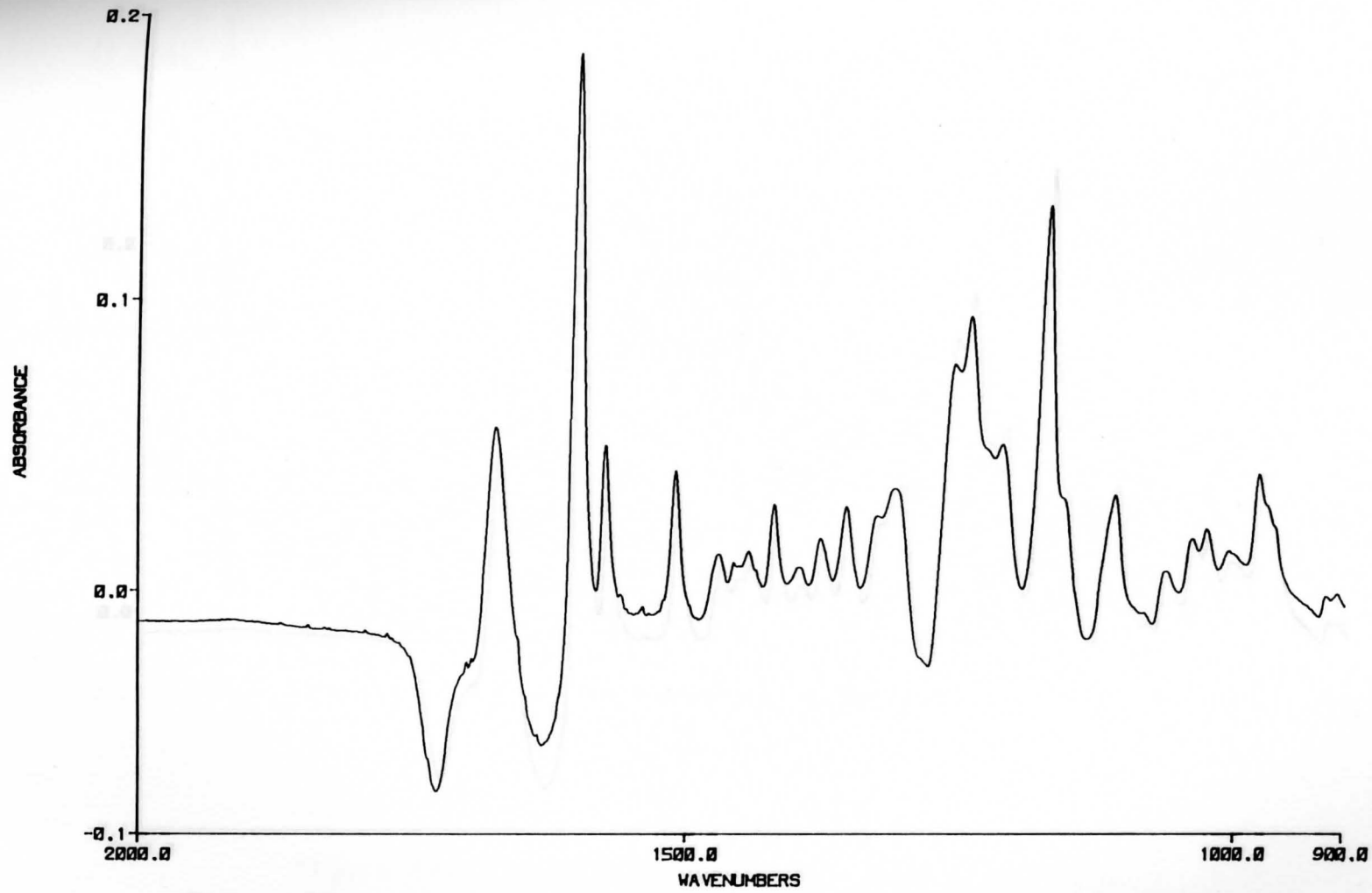

Figure 21. IR Spectrum of Dyclonine in 50% Acetonitrile at pH 9

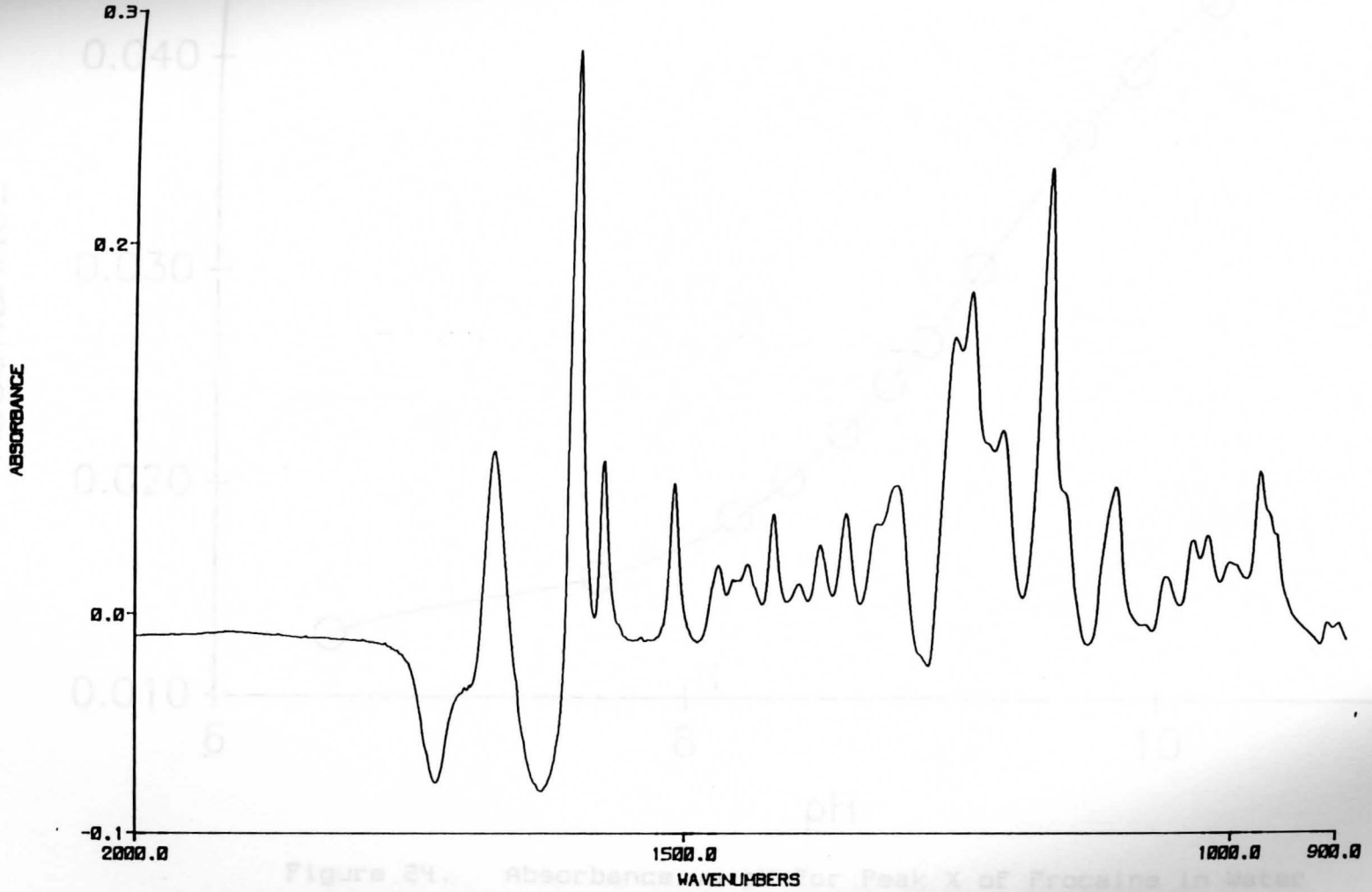

Figure 22. IR Spectrum of Dyclonine in 75% Acetonitrile at pH 9

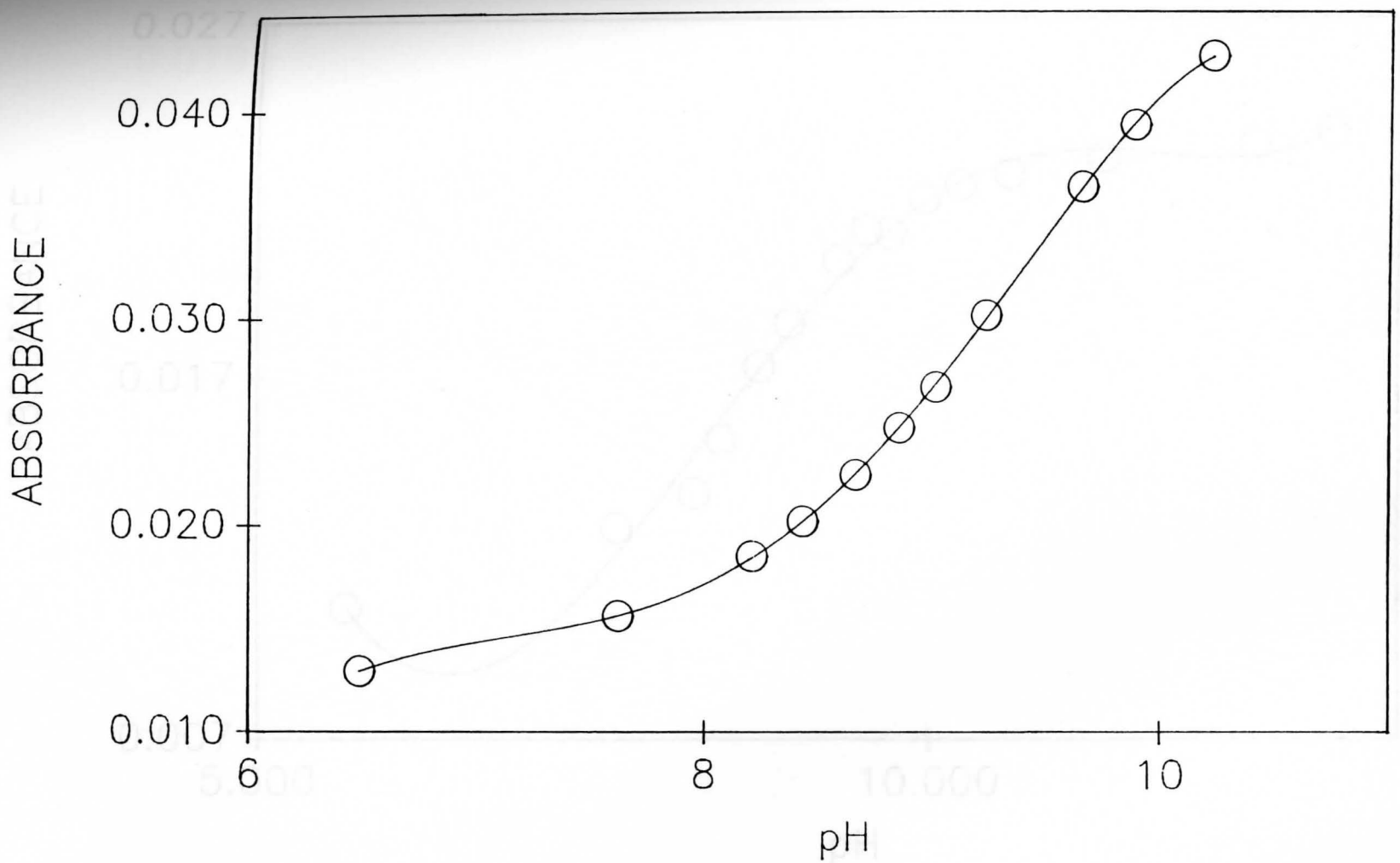

Figure 24. Absorbance vs pH for Peak X of Procaine in Water

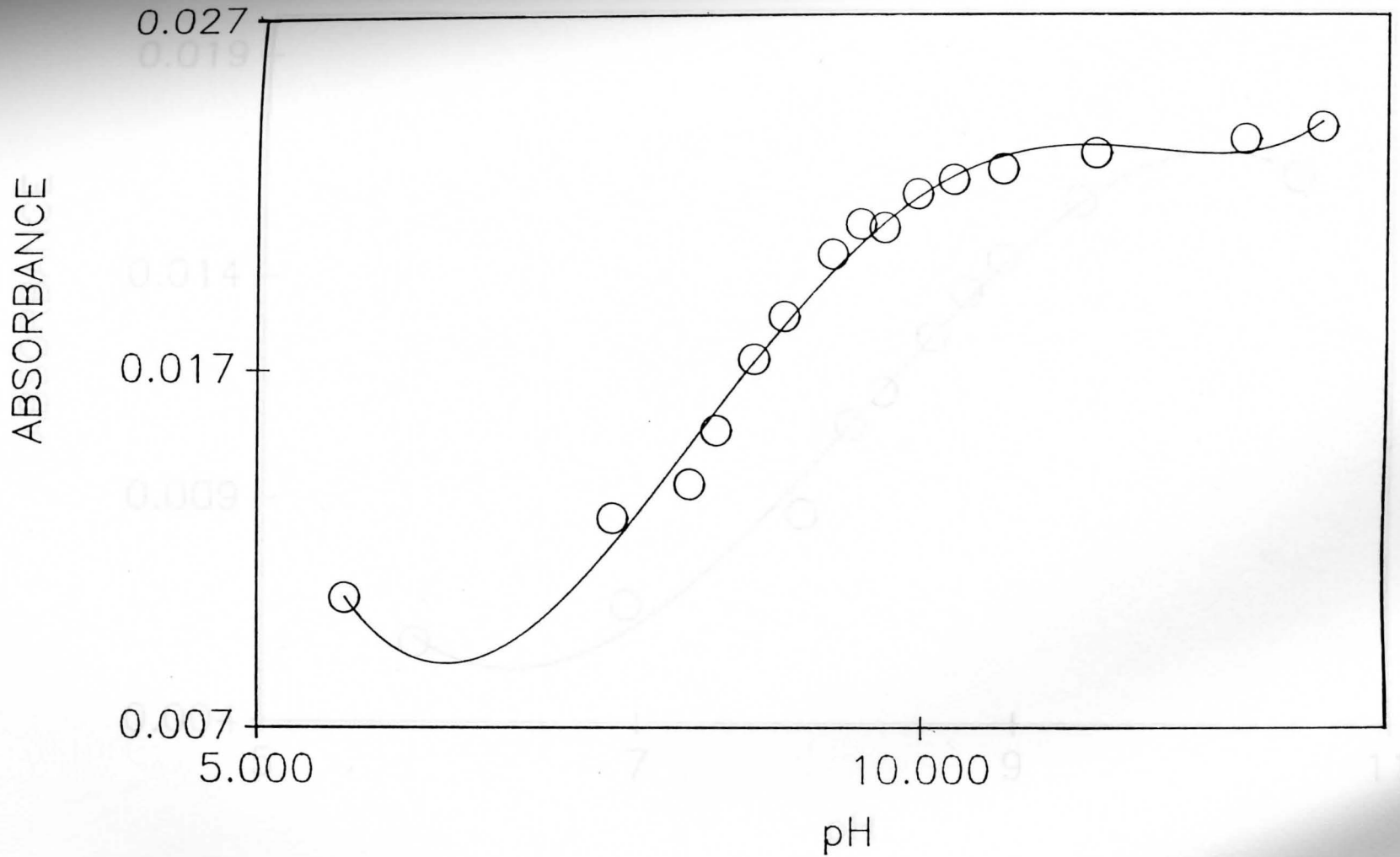

Figure 25. Absorbance vs pH for Peak X of Procaine in 25% Acetonitrile

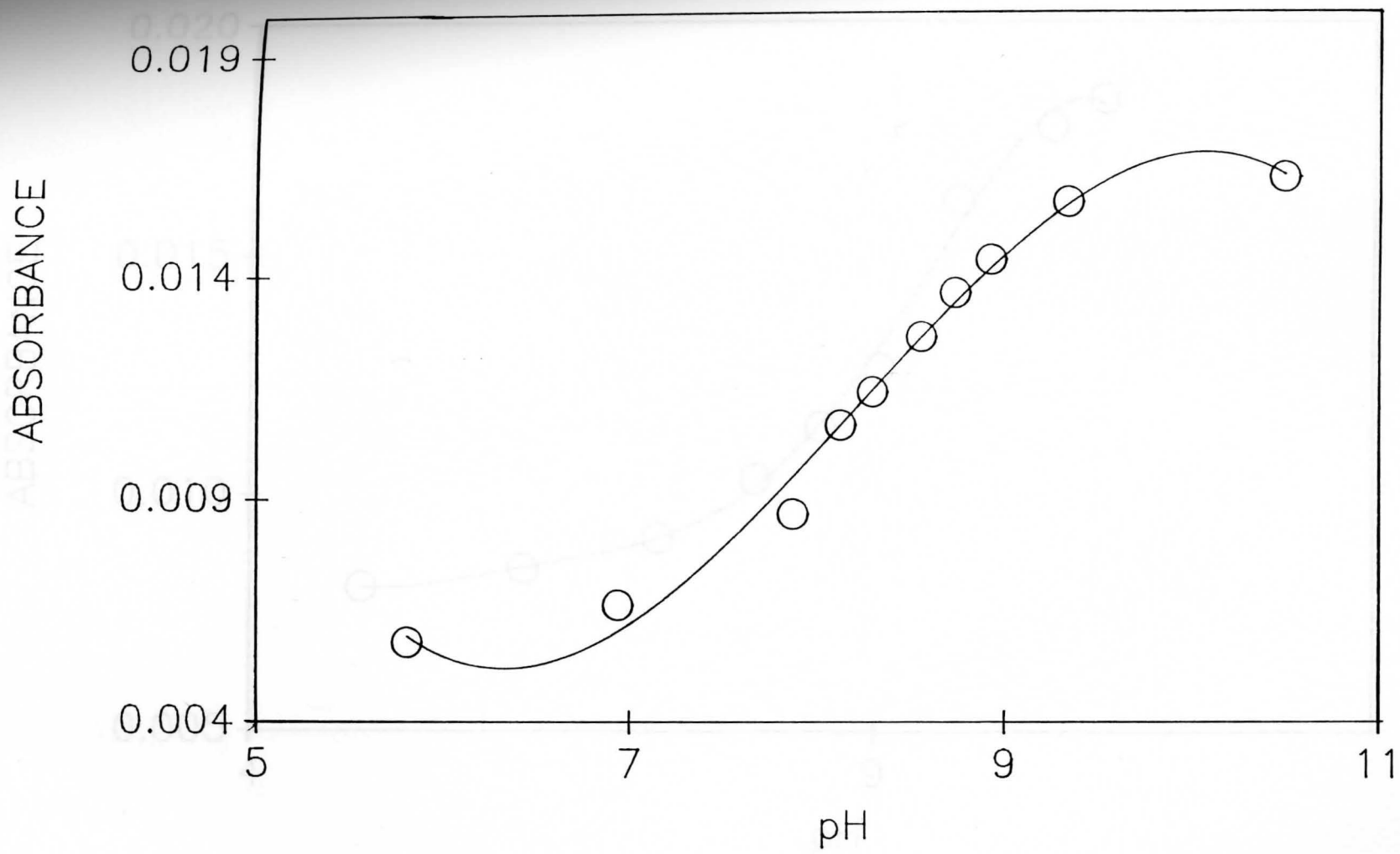

Figure 26. Absorbance vs pH for Peak X of Procaine in 50% Acetonitrile

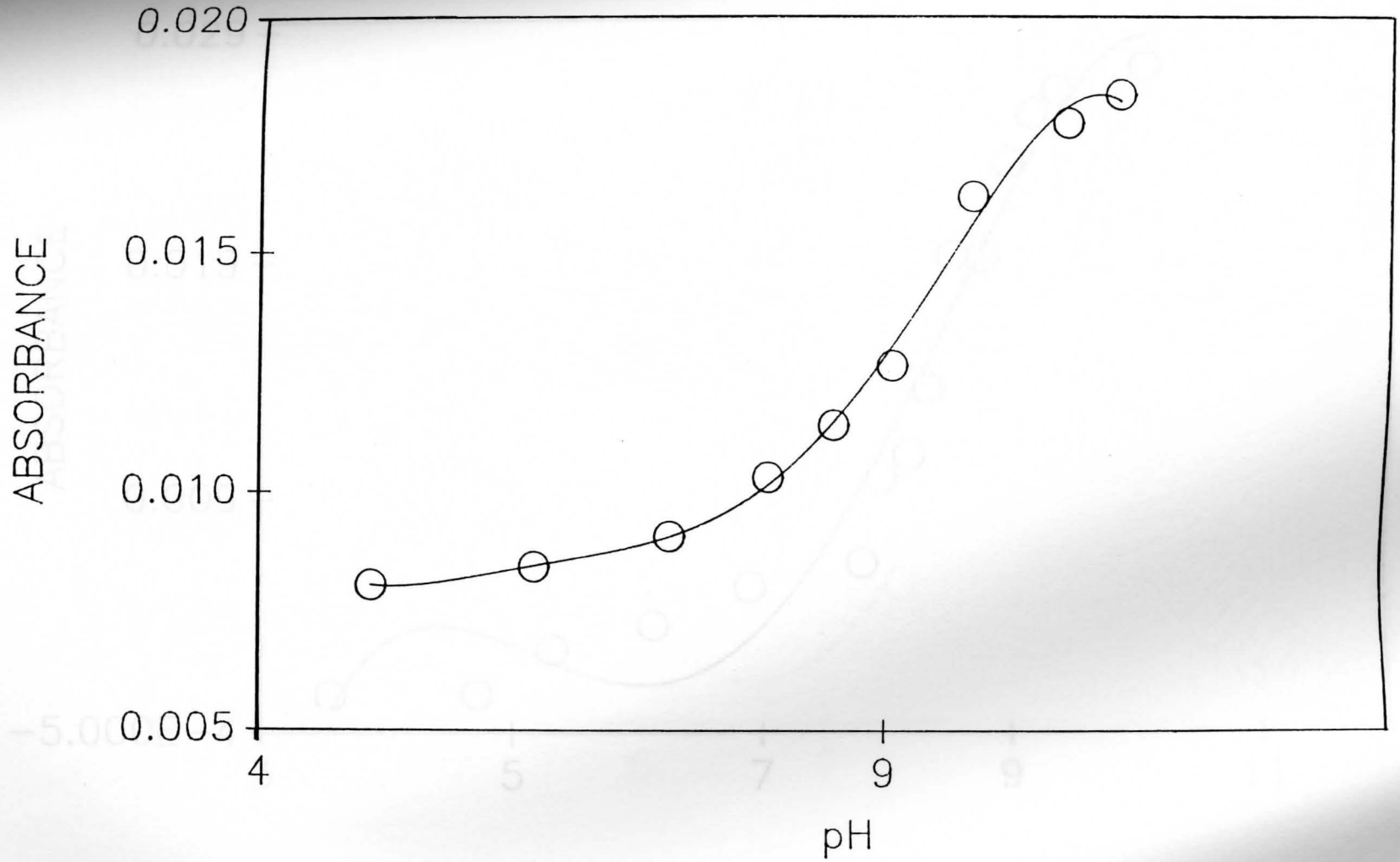

Figure 27. Absorbance vs pH for Peak X of Procaine in 75% Acetonitrile

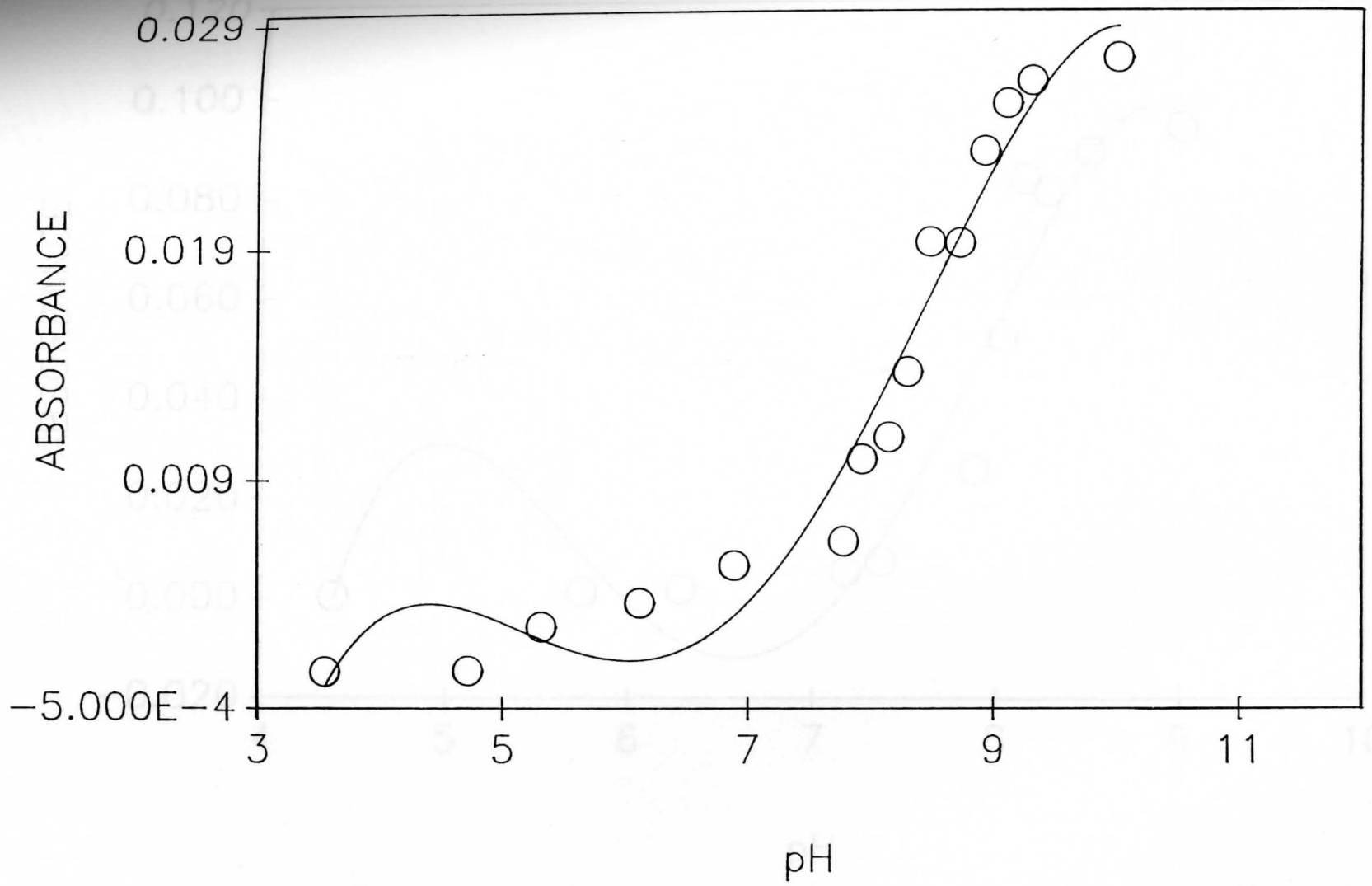

Figure 28. Absorbance vs pH for Peak X of Dibucaine in Water

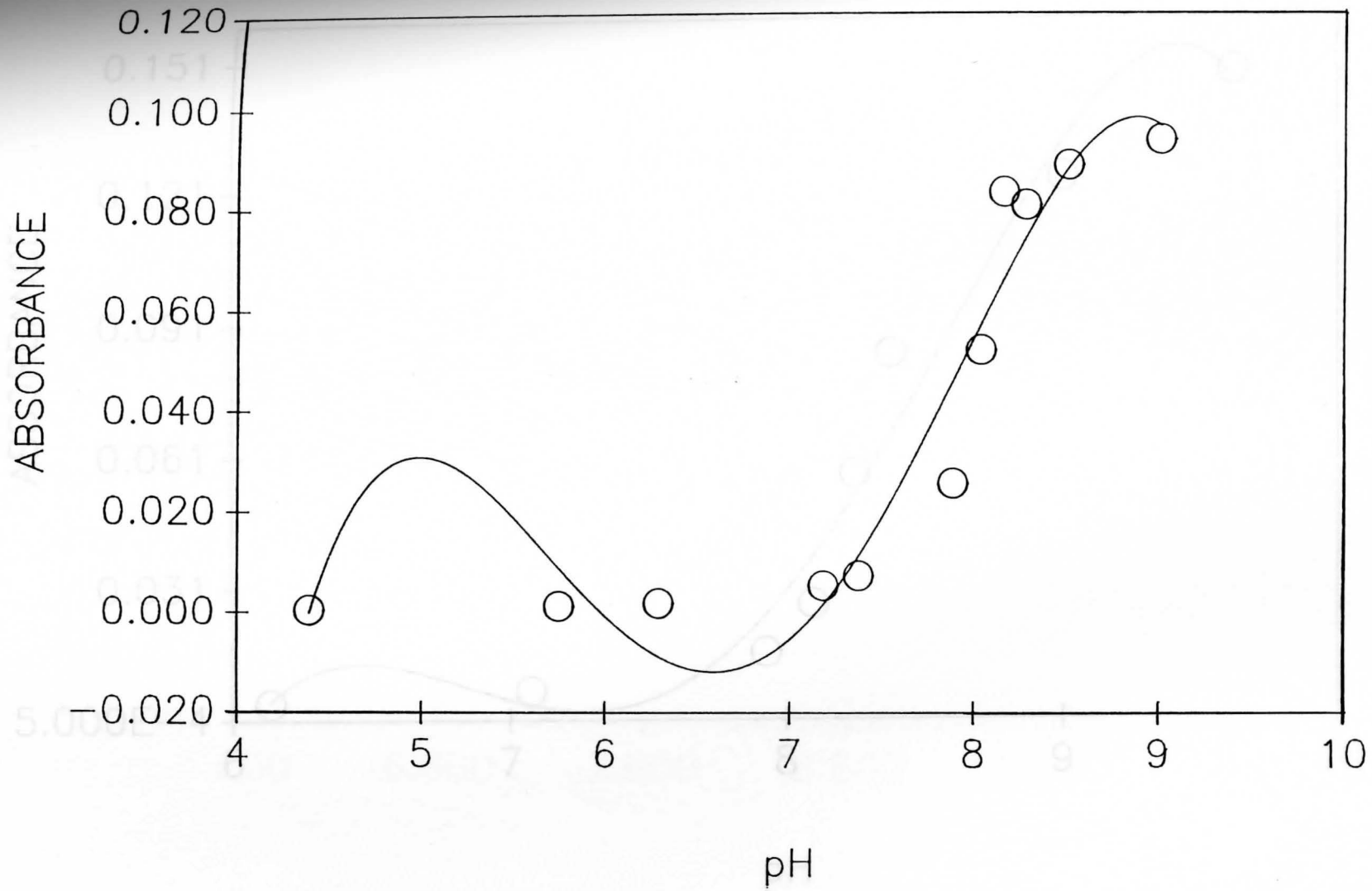

Figure 29. Absorbance vs pH for Peak X of Dibucaine in 25% Acetonitrile

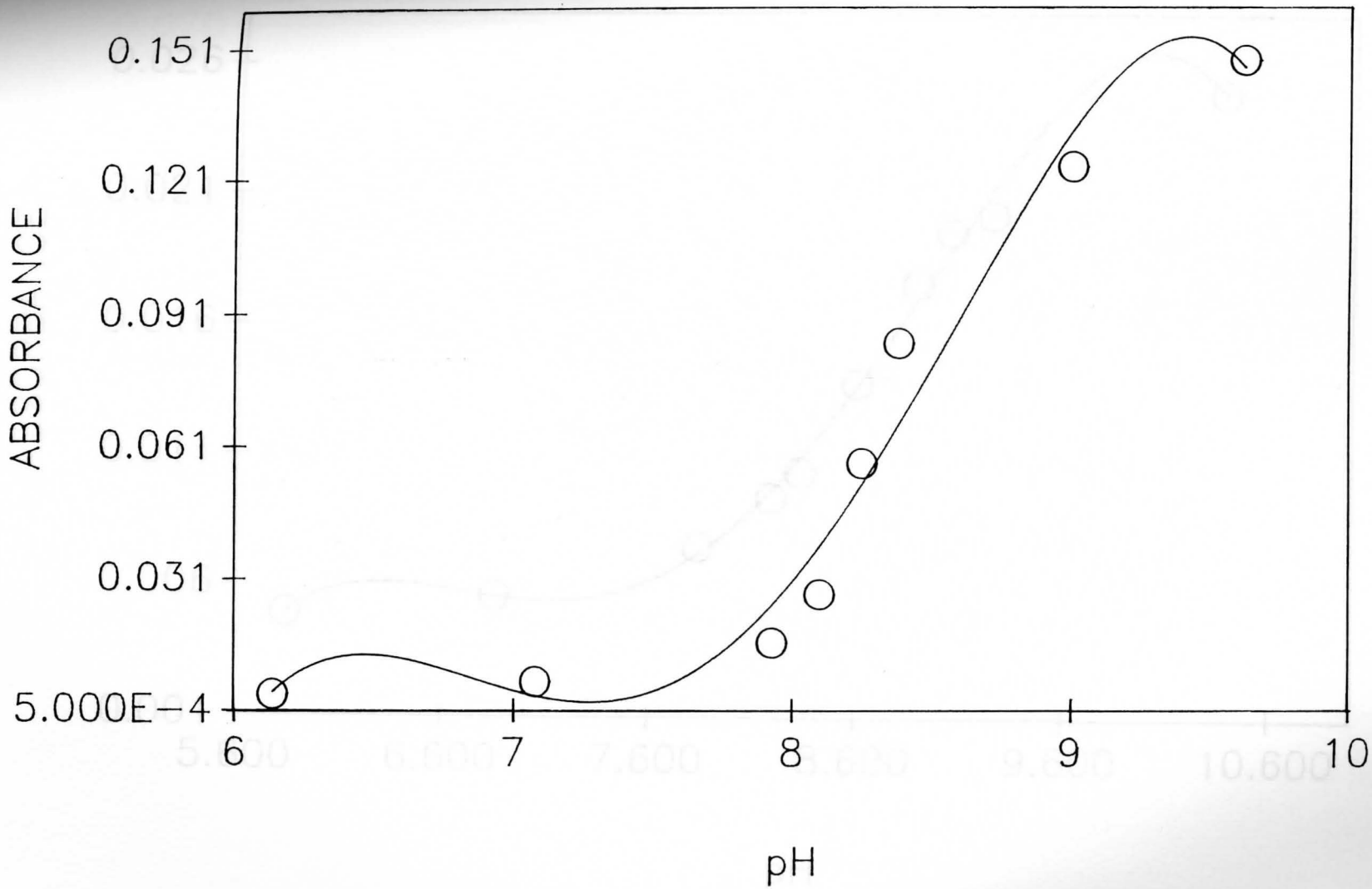

Figure 30. Absorbance vs pH for Peak X of Dibucaine in 50% Acetonitrile

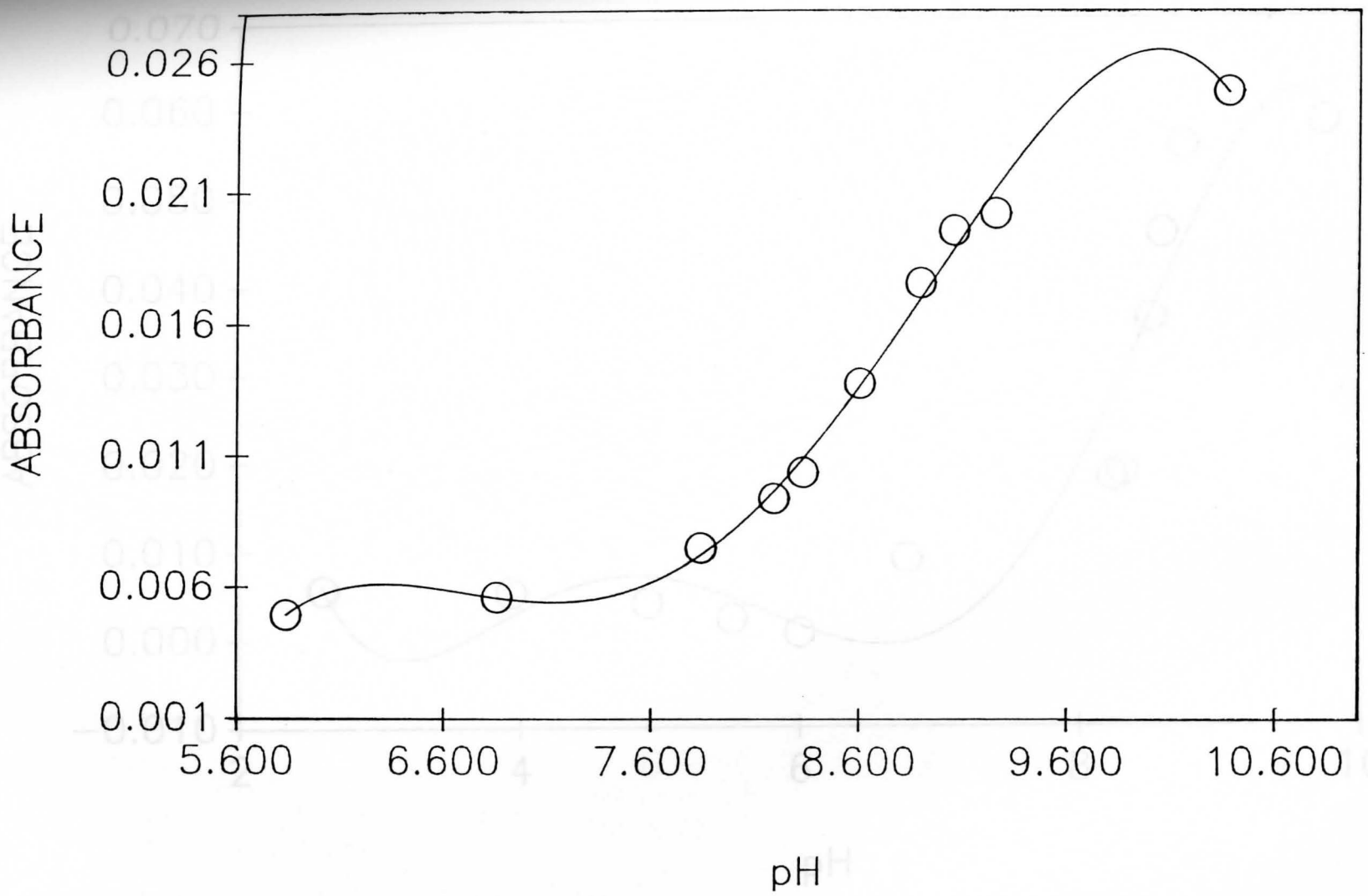

Figure 31. Absorbance vs pH for Peak X of Dibucaine in 75% Acetonitrile

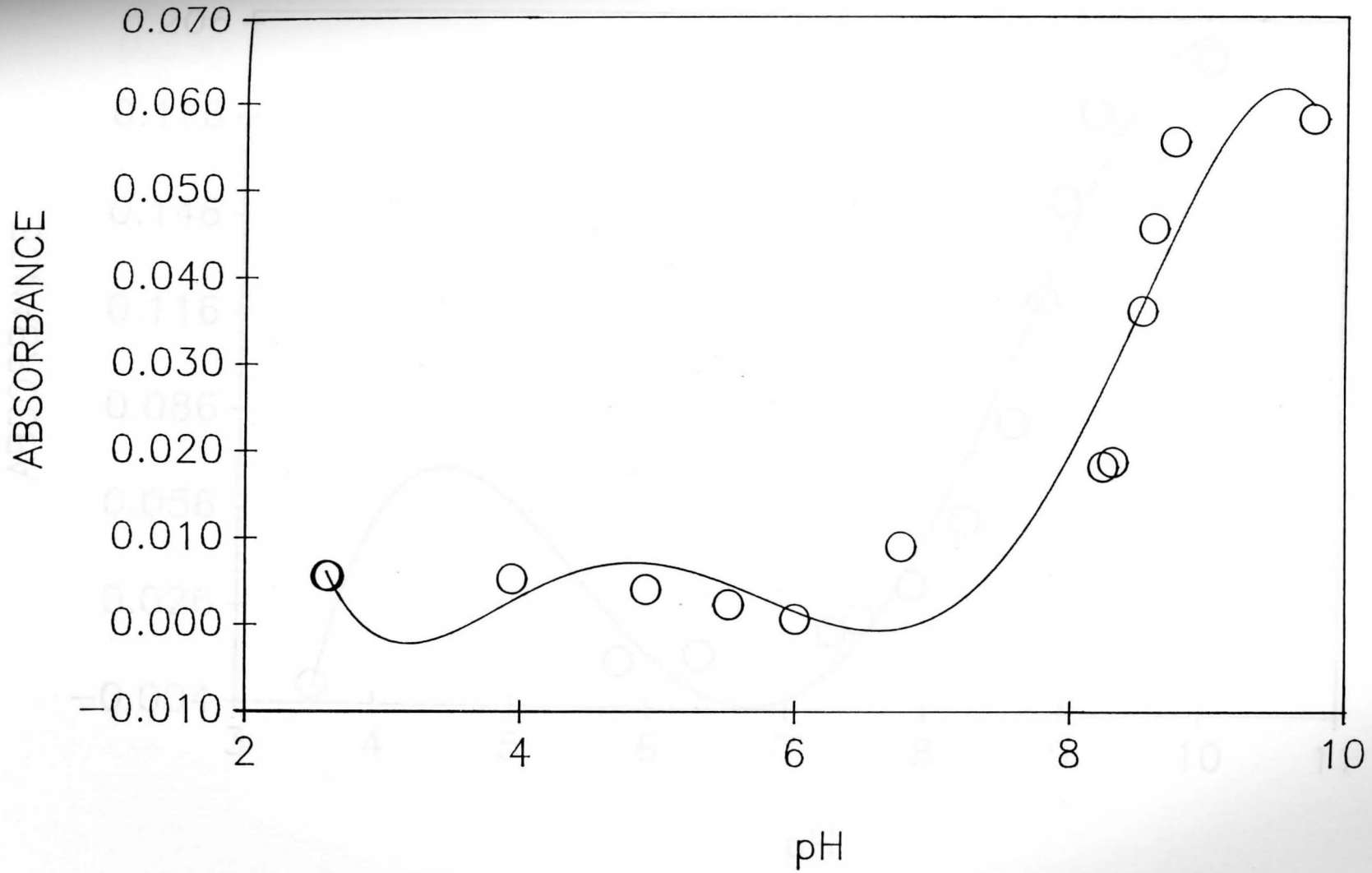

Figure 32. Absorbance vs pH for Peak X of Dyclonine in Water

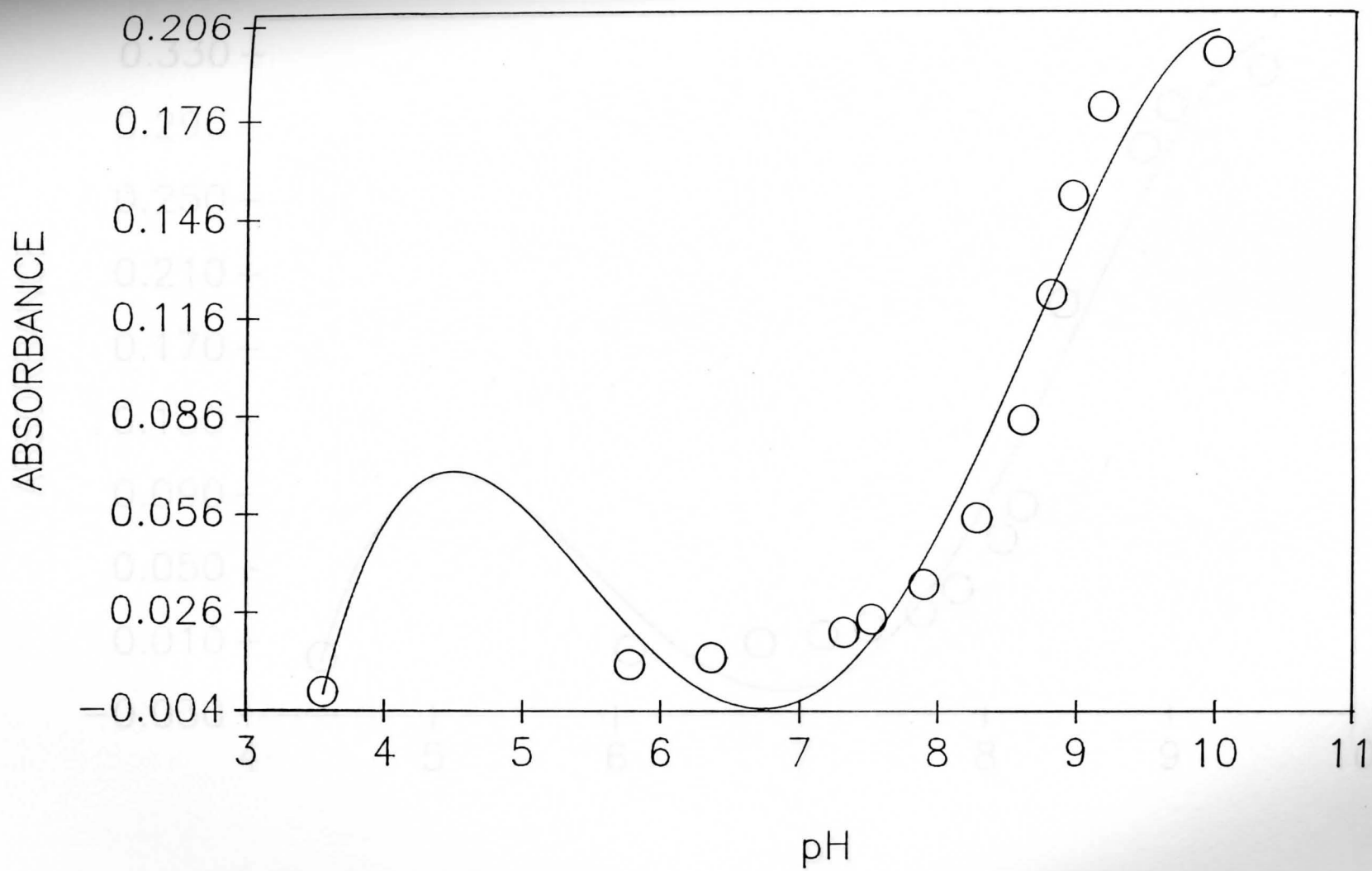

Figure 33. Absorbance vs pH for Peak X of Dyclonine in 25% Acetonitrile

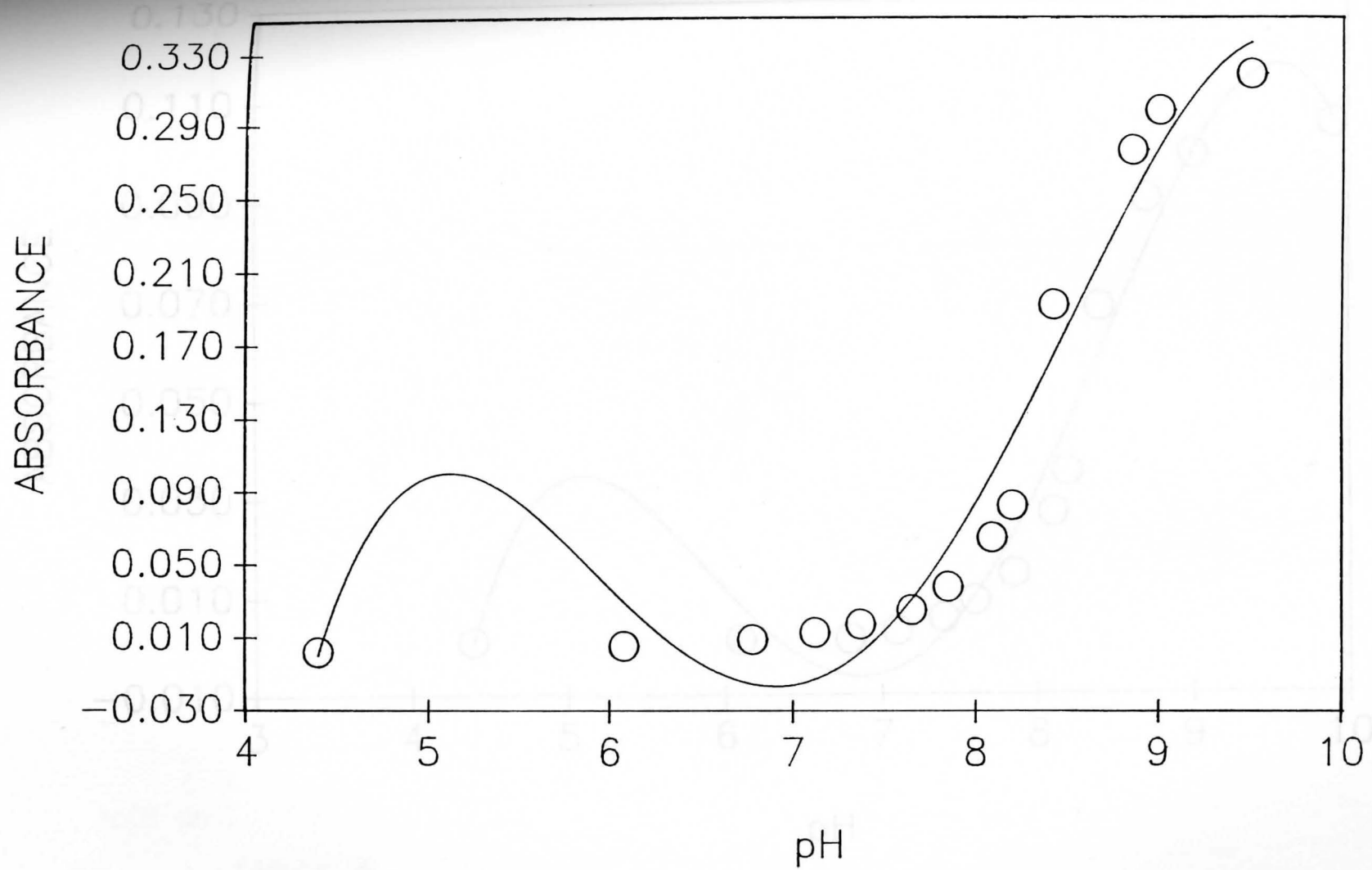

Figure 34. Absorbance vs pH for Peak X of Dyclonine in 50% Acetonitrile

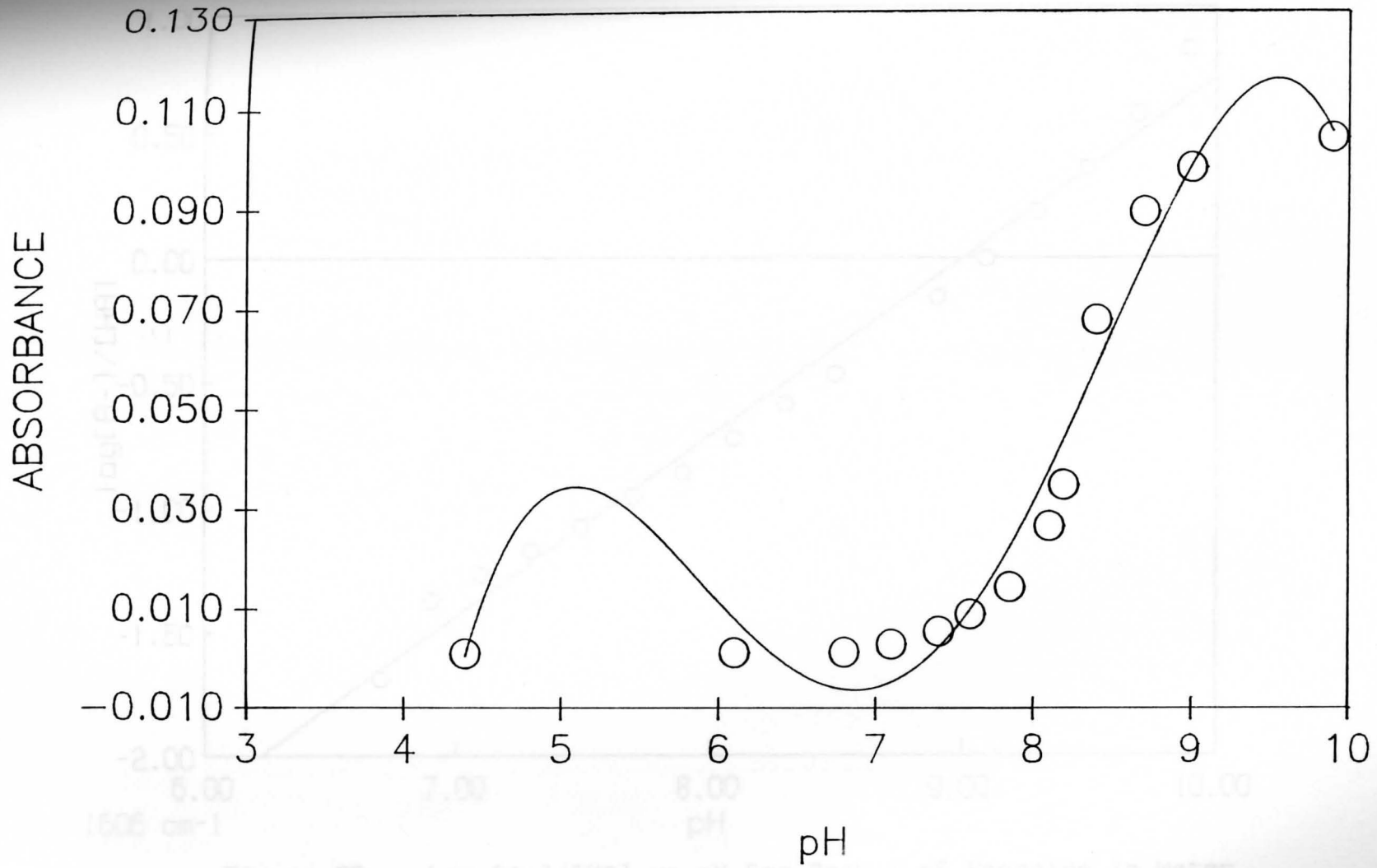

Figure 35. Absorbance vs pH for Peak X of Dyclonine in 75% Acetonitrile

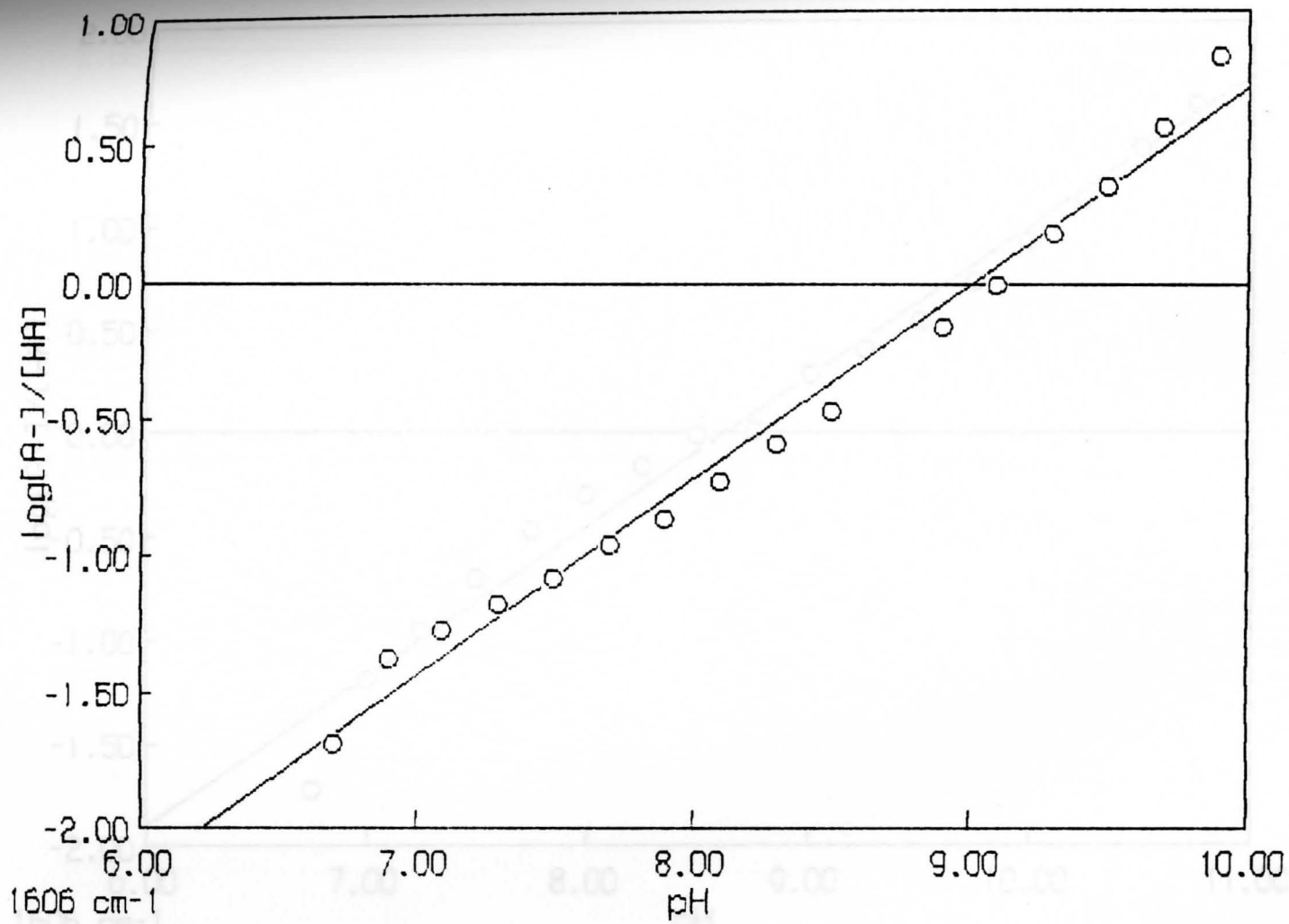

Figure 36. Log [A-]/[HA] vs pH for Peak X of Procaine in Water

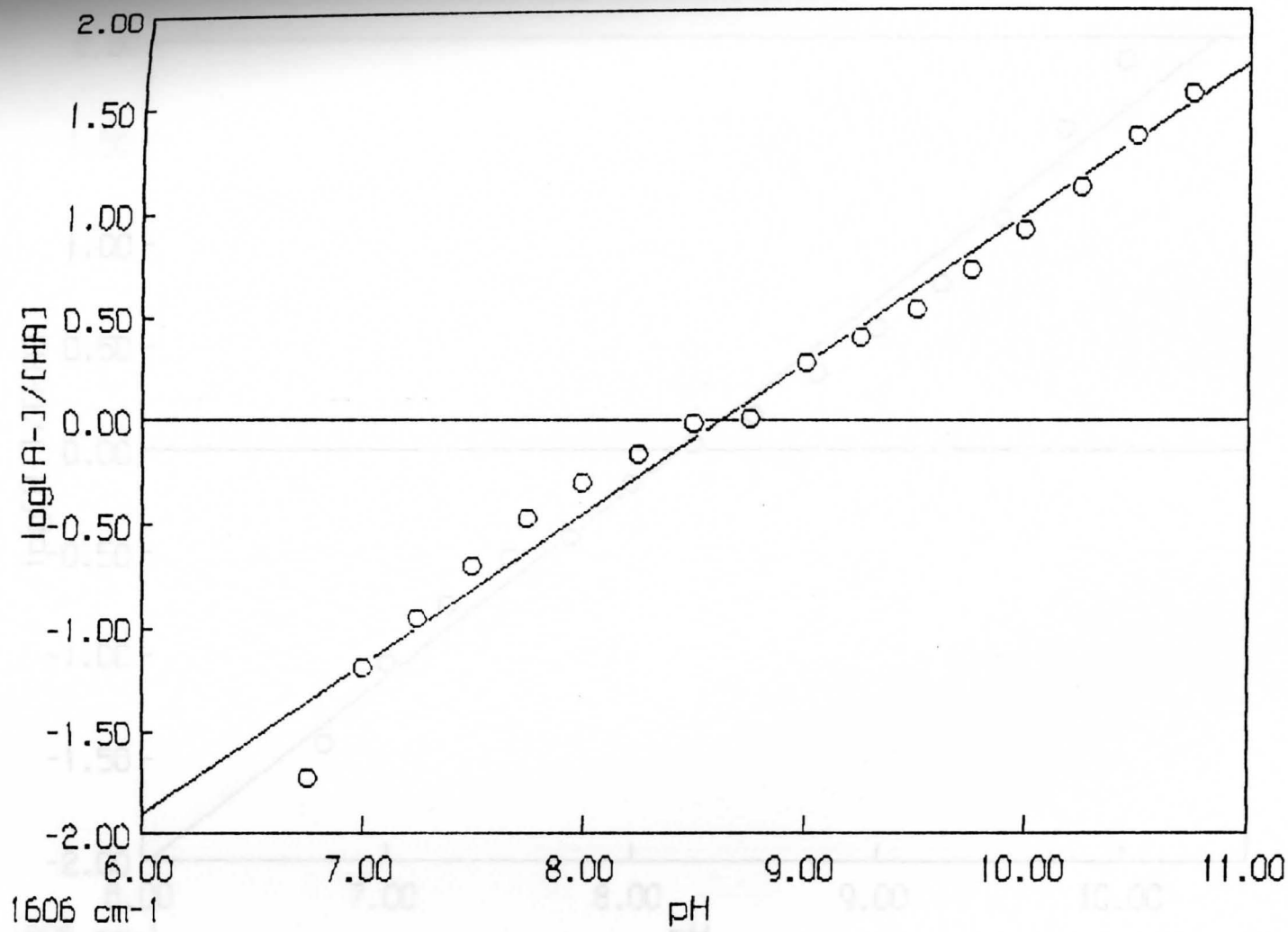

Figure 37. Log [A-]/[HA] vs pH for Peak X of Procaine in 25% Acetonitrile

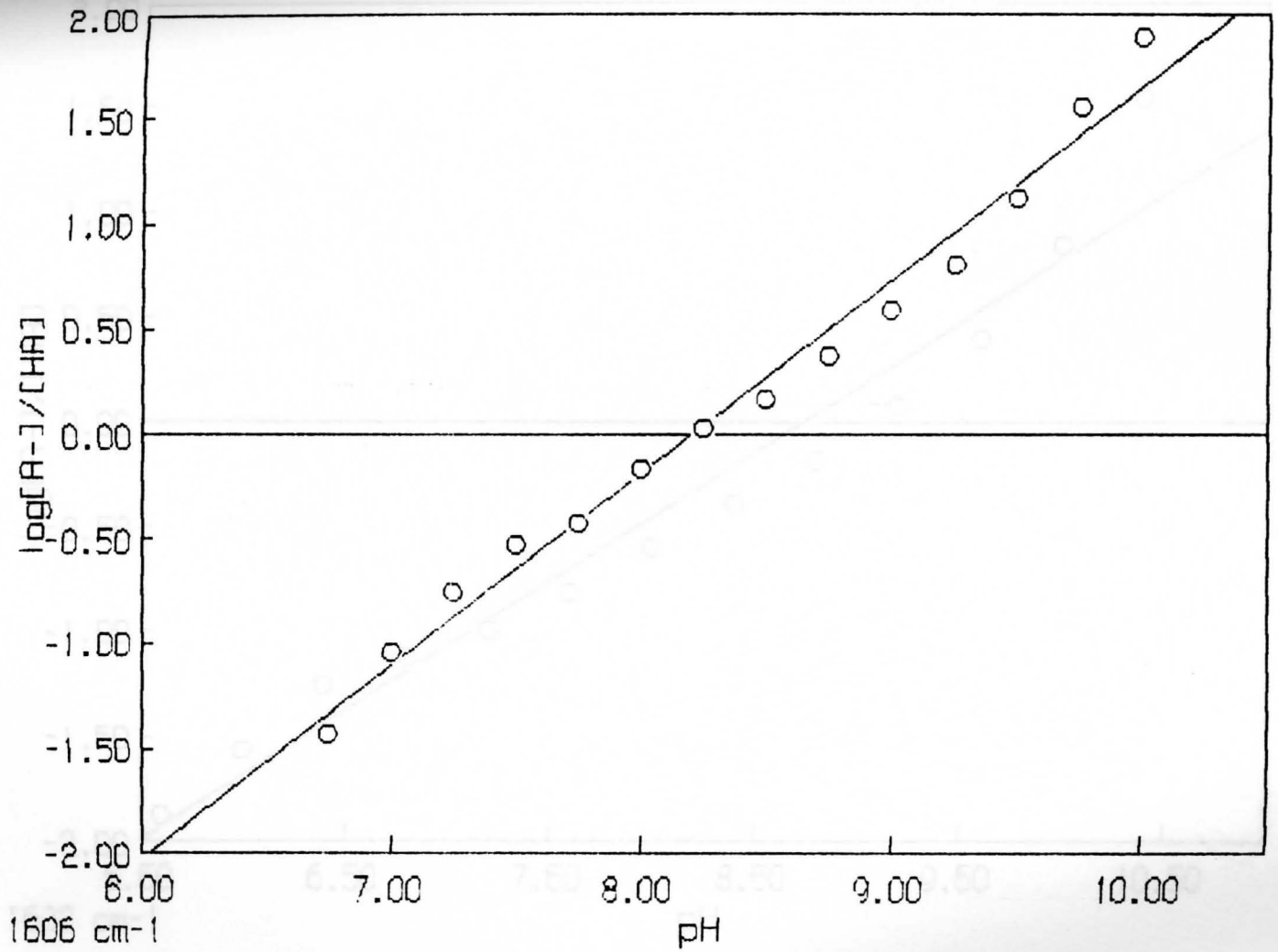

Figure 38. Log [A-]/[HA] vs pH for Peak X of Procaine in 50% Acetonitrile

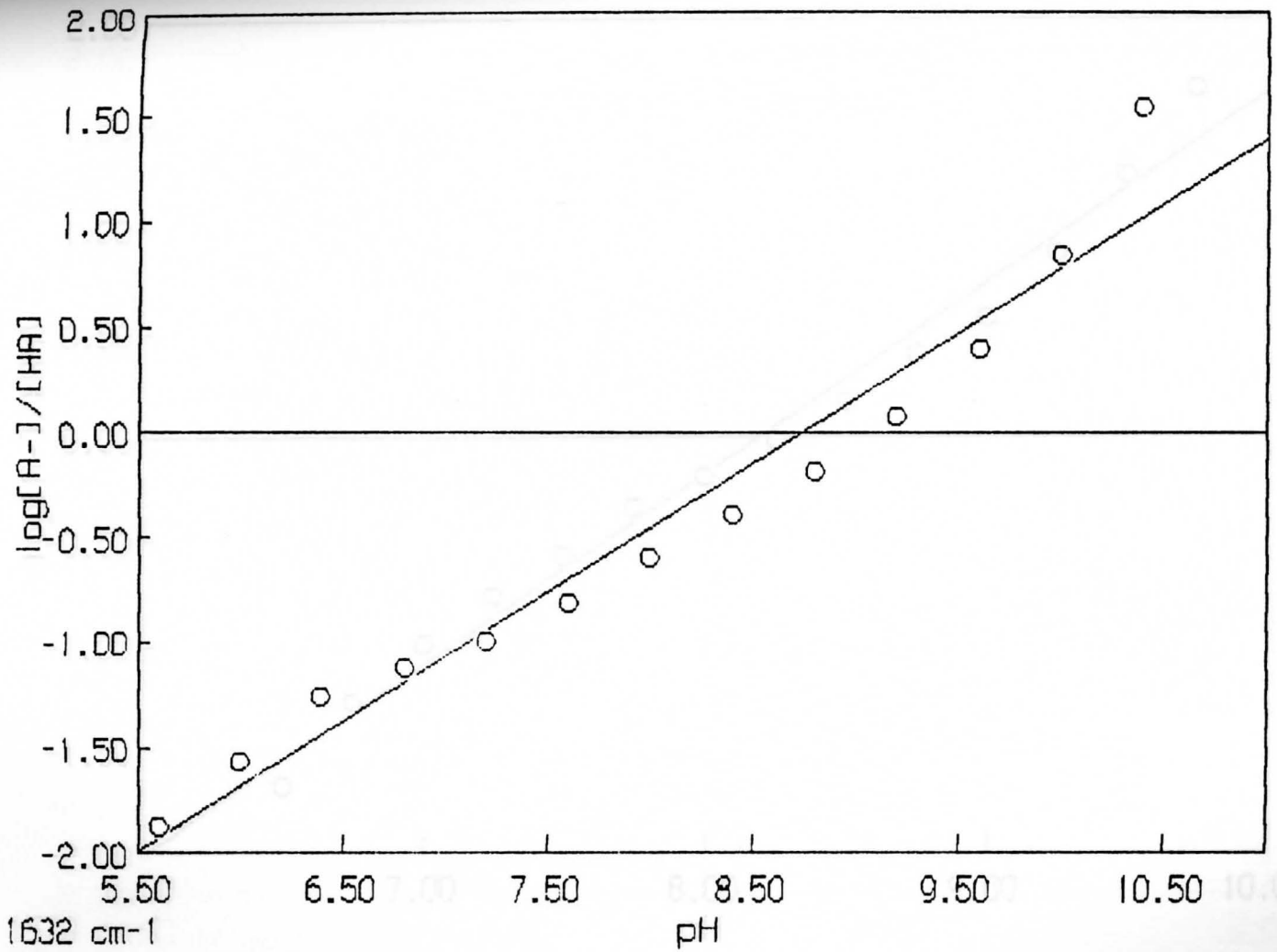

Figure 39. Log [A-]/[HA] vs pH for Peak X of Procaine in 75% Acetonitrile

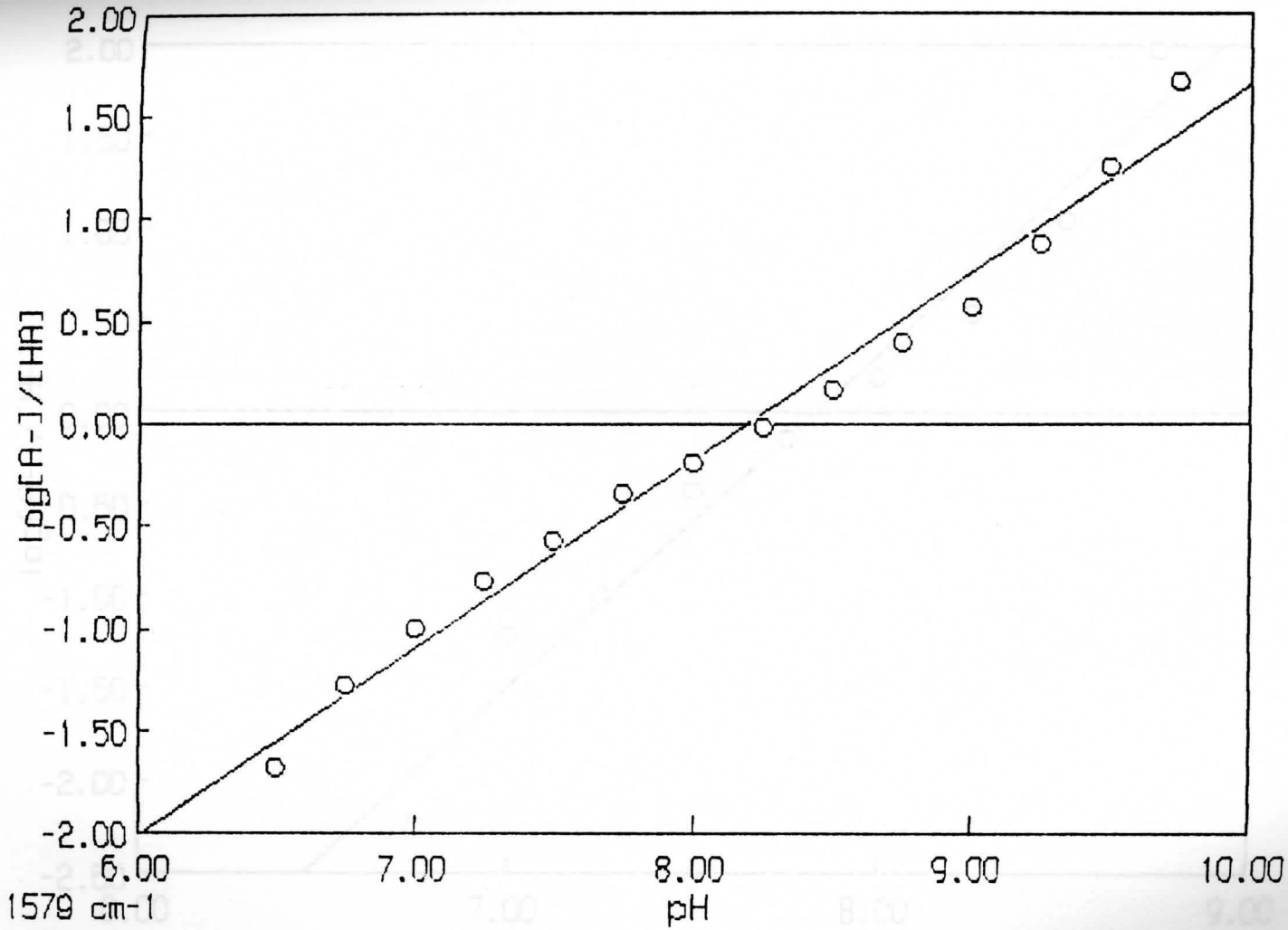

Figure 40. Log [A-]/[HA] vs pH for Peak X of Dibucaine in Water

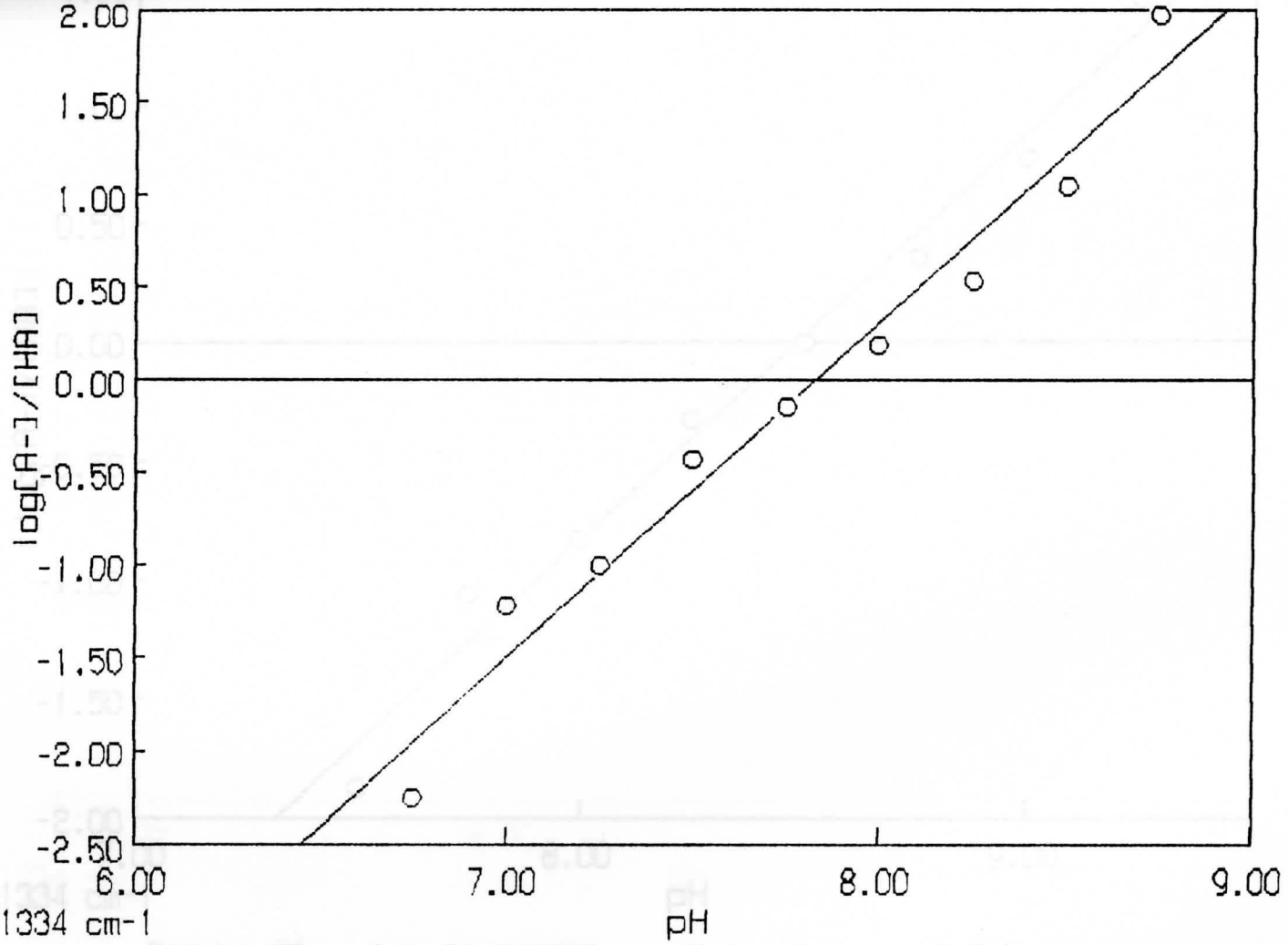

Figure 41. Log [A-]/[HA] vs pH for Peak X of Dibucaine in 25% Acetonitrile

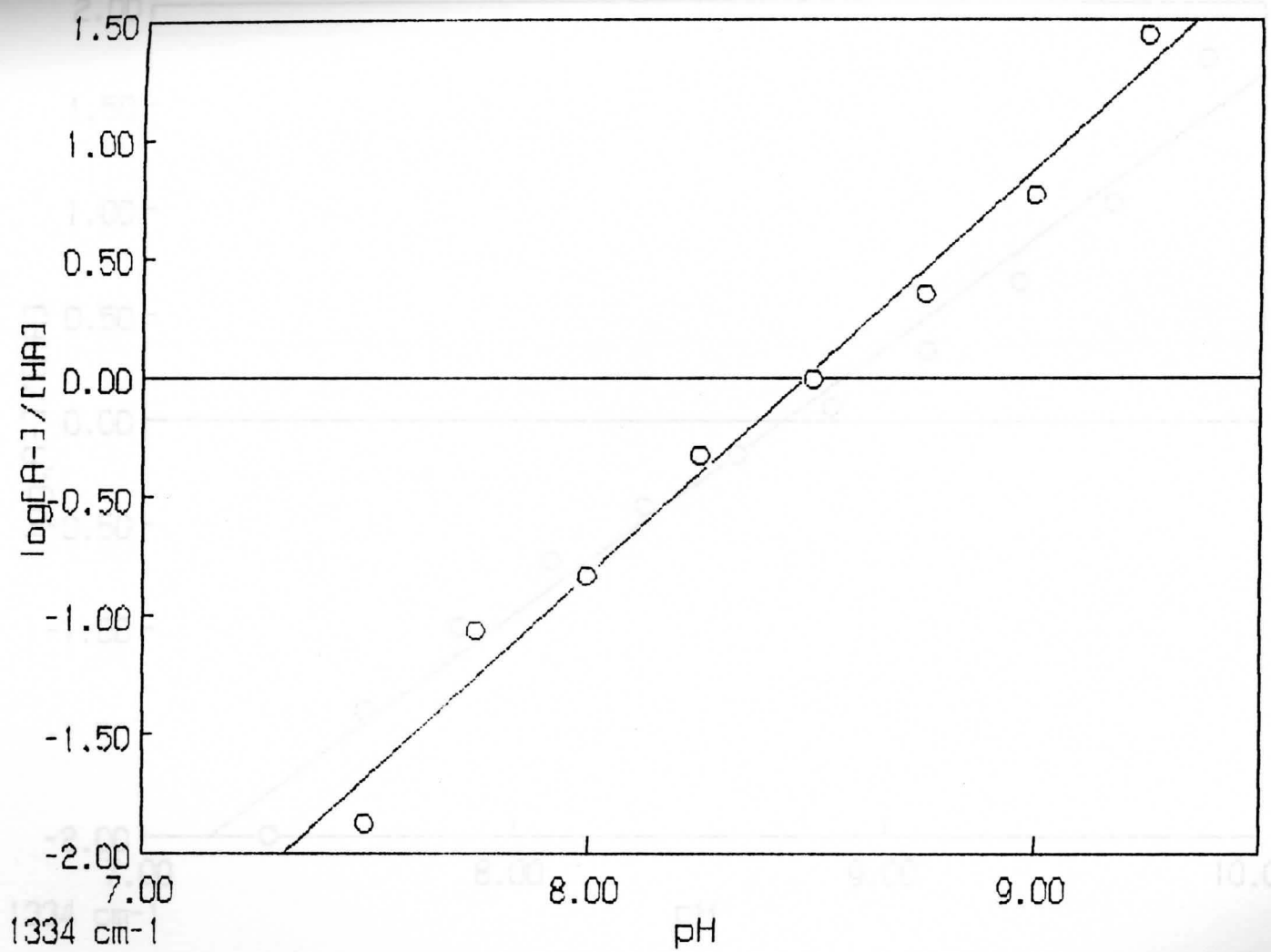

Figure 42. Log [A-]/[HA] vs pH for Peak X of Dibucaine in 50% Acetonitrile

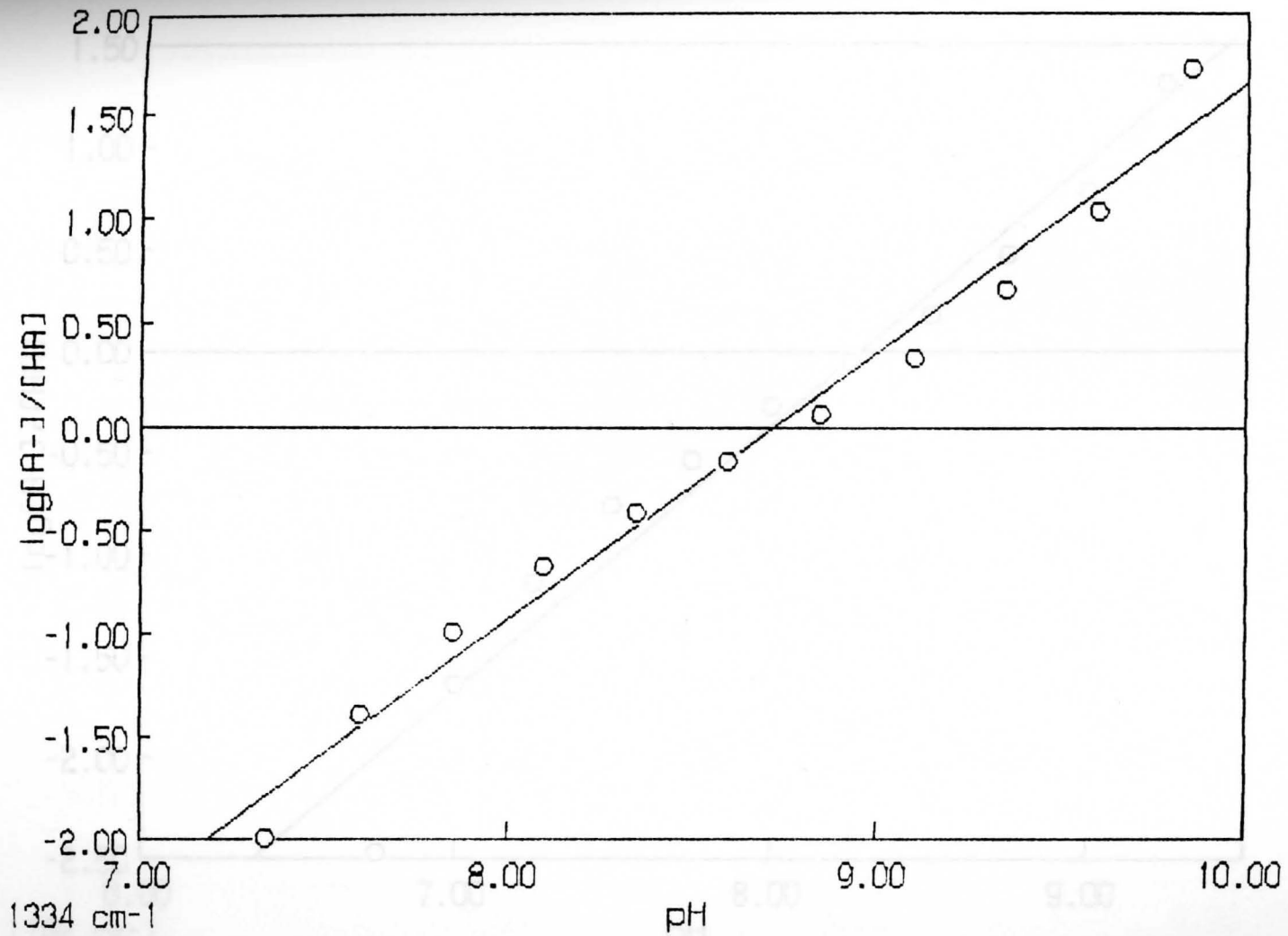

Figure 43. Log [A-]/[HA] vs pH for Peak X of Dibucaine in 75% Acetonitrile

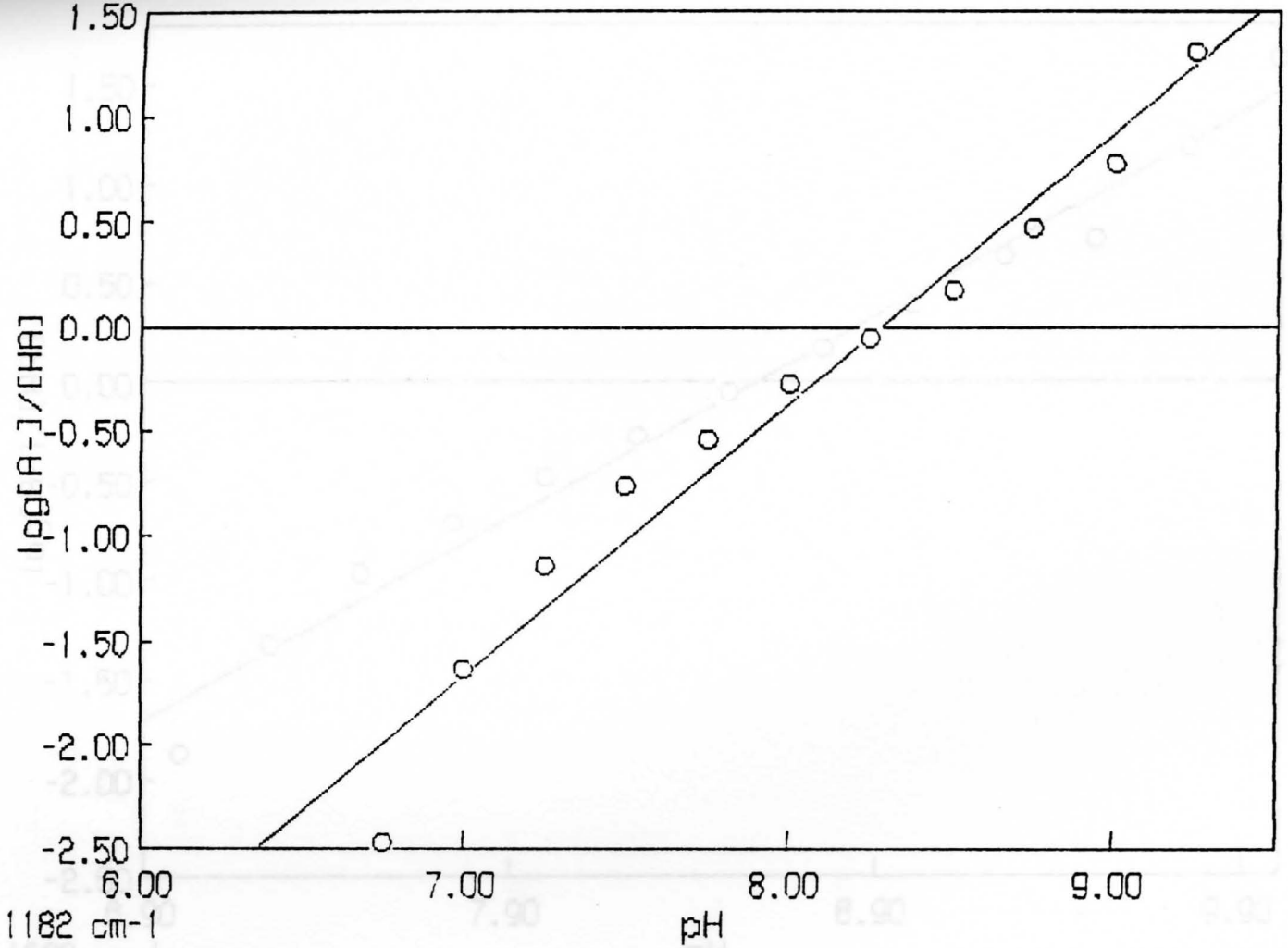

Figure 44. Log [A-]/[HA] vs pH for Peak X of Dyclonine in Water

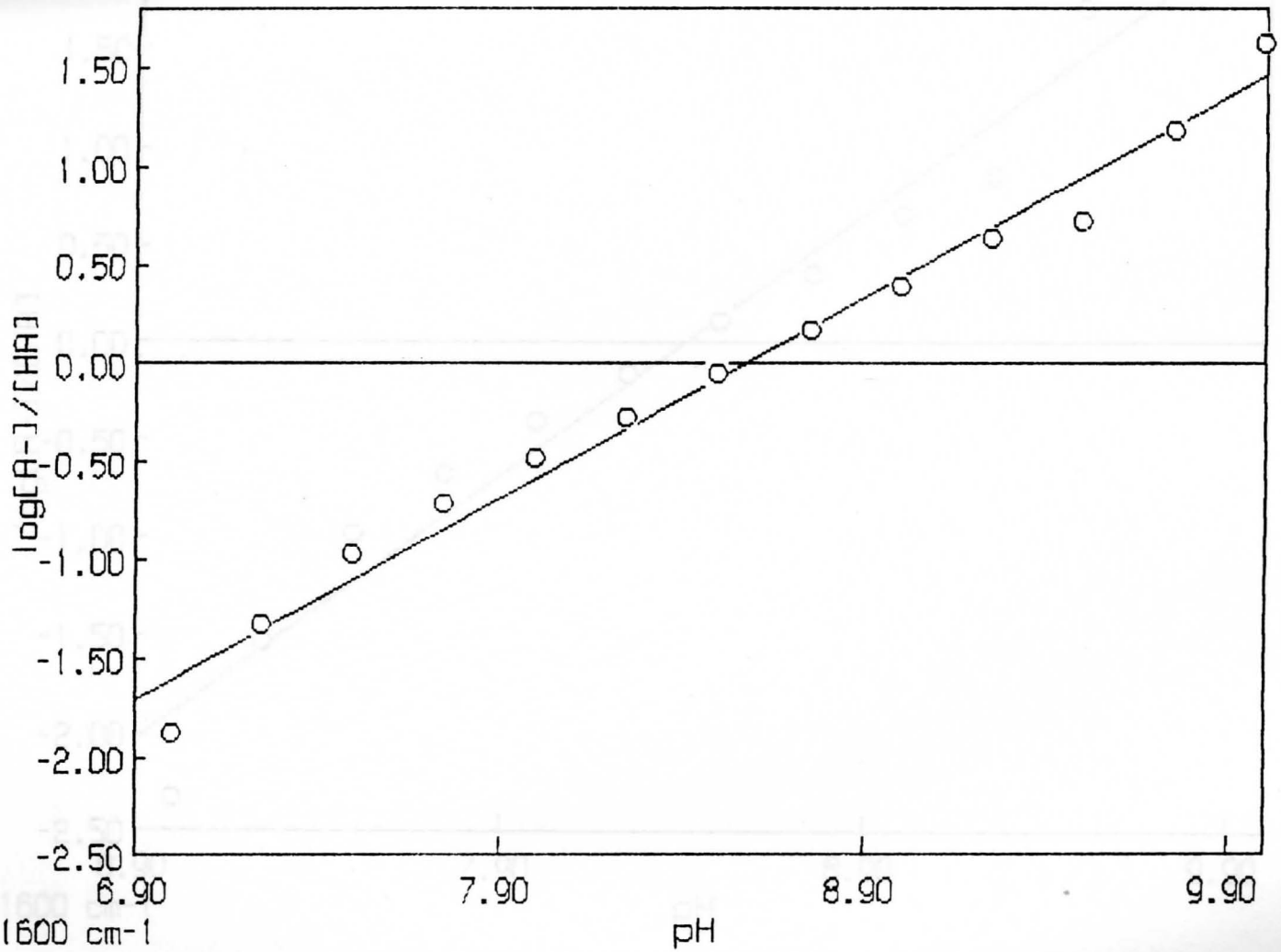

Figure 45. Log [A-]/[HA] vs pH for Peak X of Dyclonine in 25% Acetonitrile

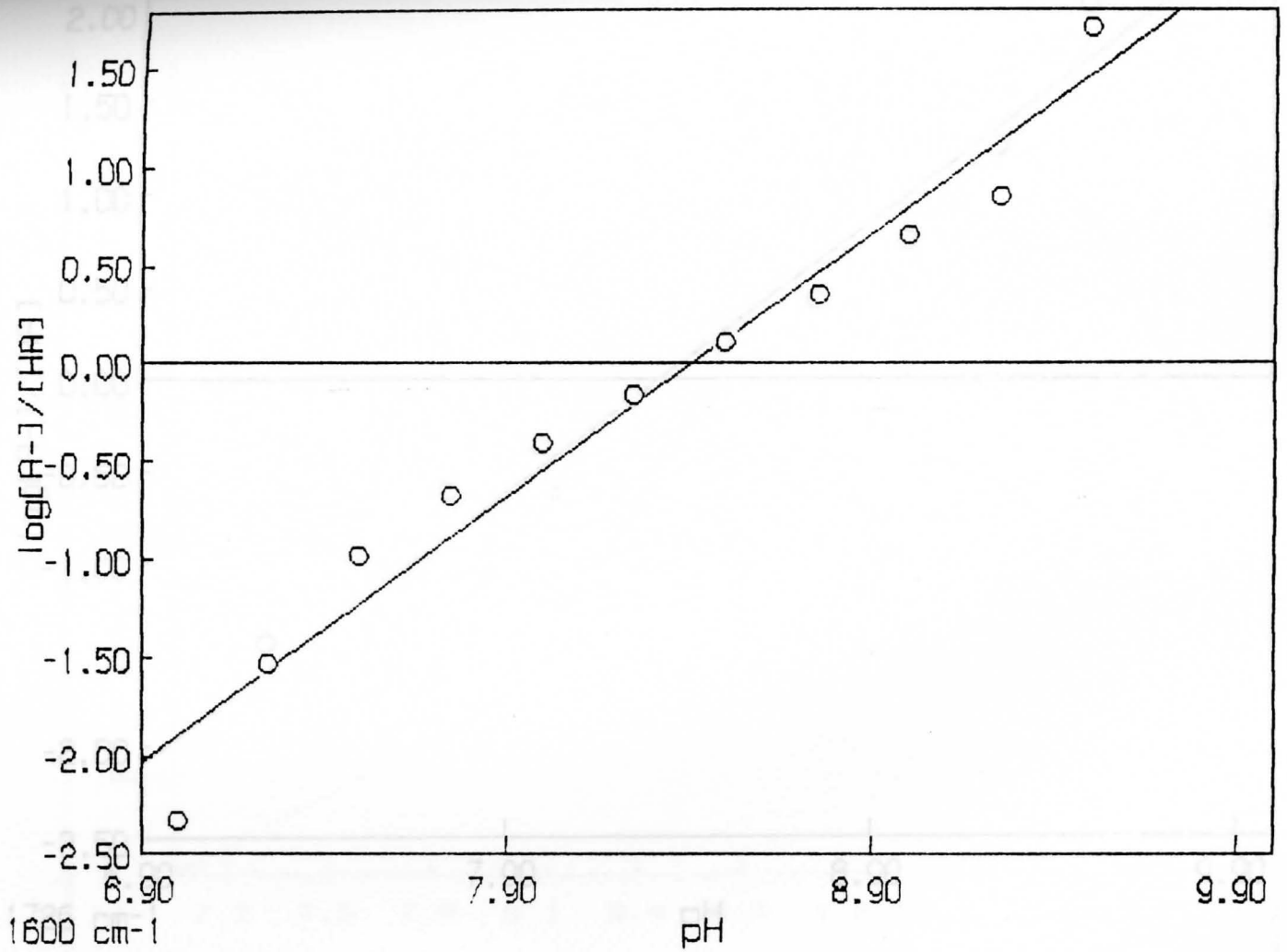

Figure 46. Log [A-]/[HA] vs pH for Peak X of Dyclonine in 50% Acetonitrile

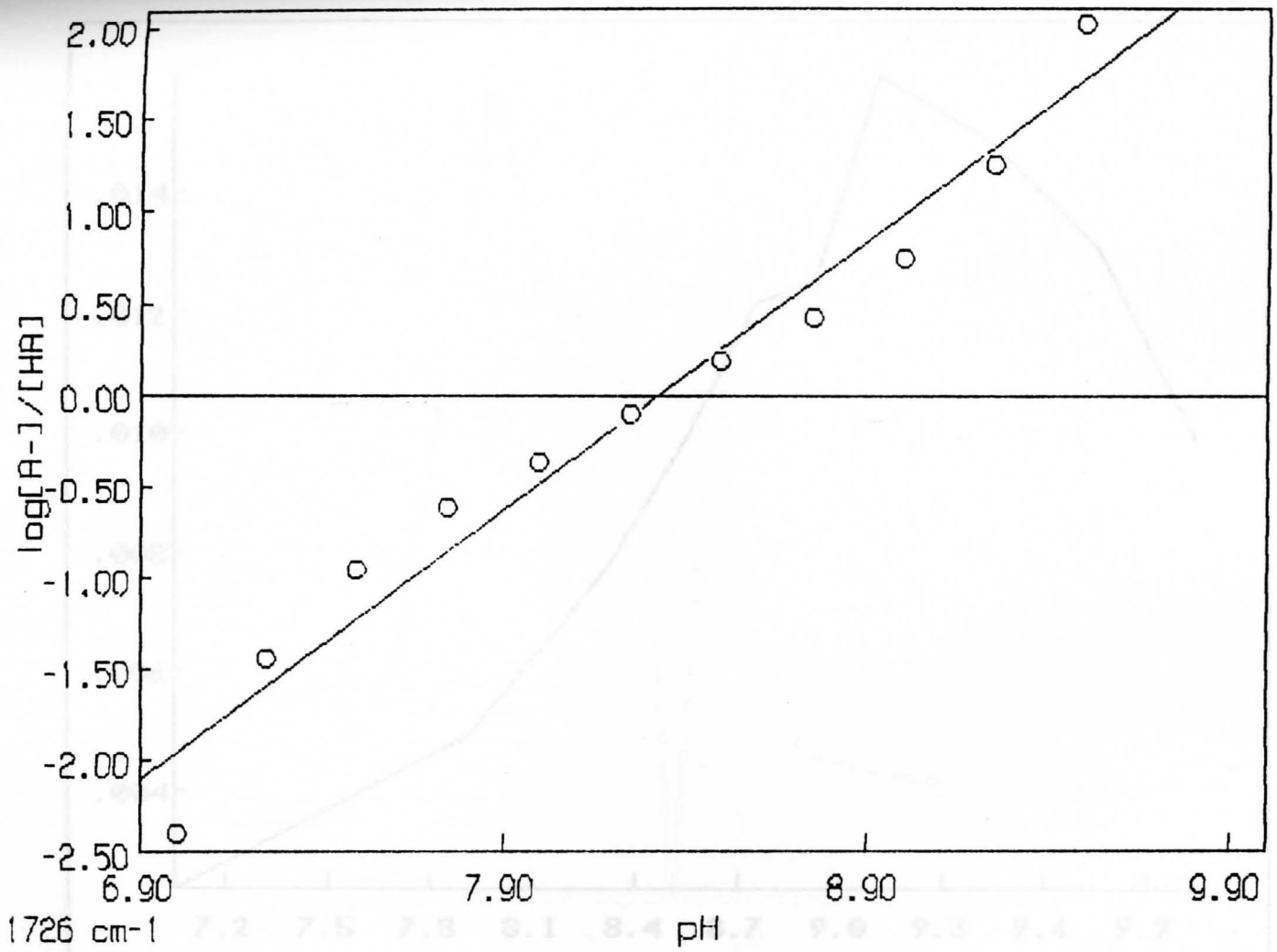

Figure 47. Log [A-]/[HA] vs pH for Peak X of Dyclonine in 75% Acetonitrile

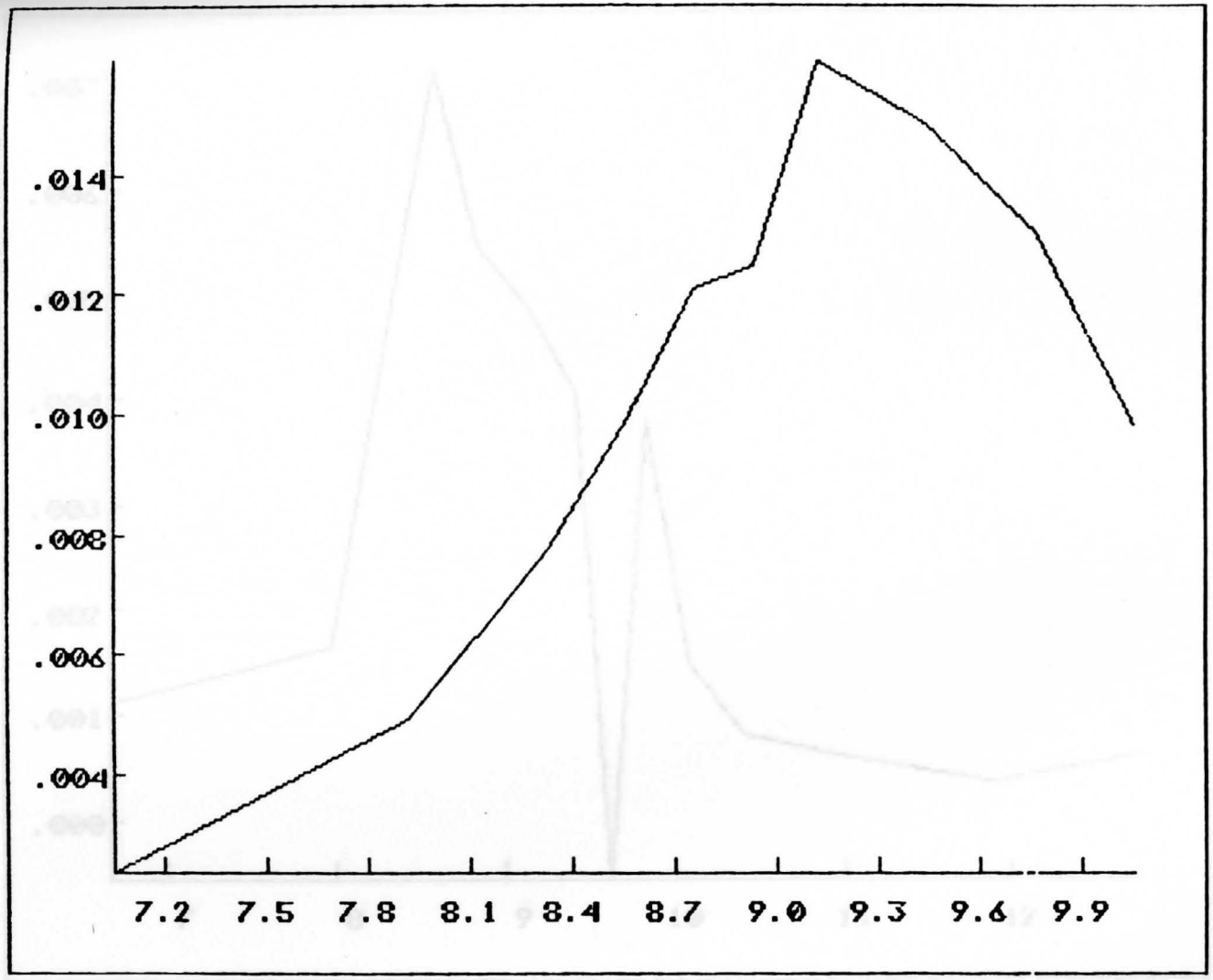

Figure 48. Hyperplot of Procaine in water

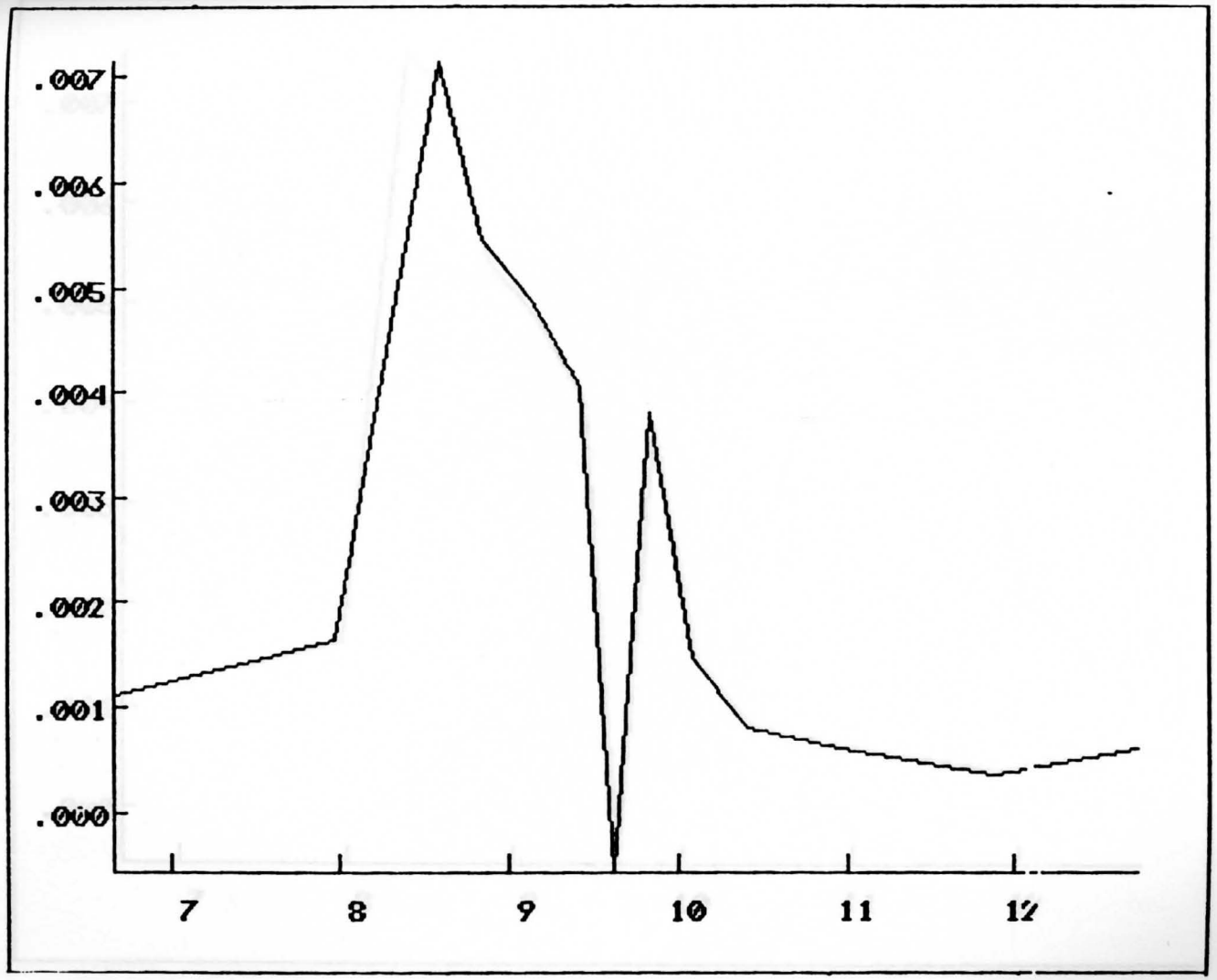

Figure 49. Hyperplot of Procaine in 25% Acetonitrile

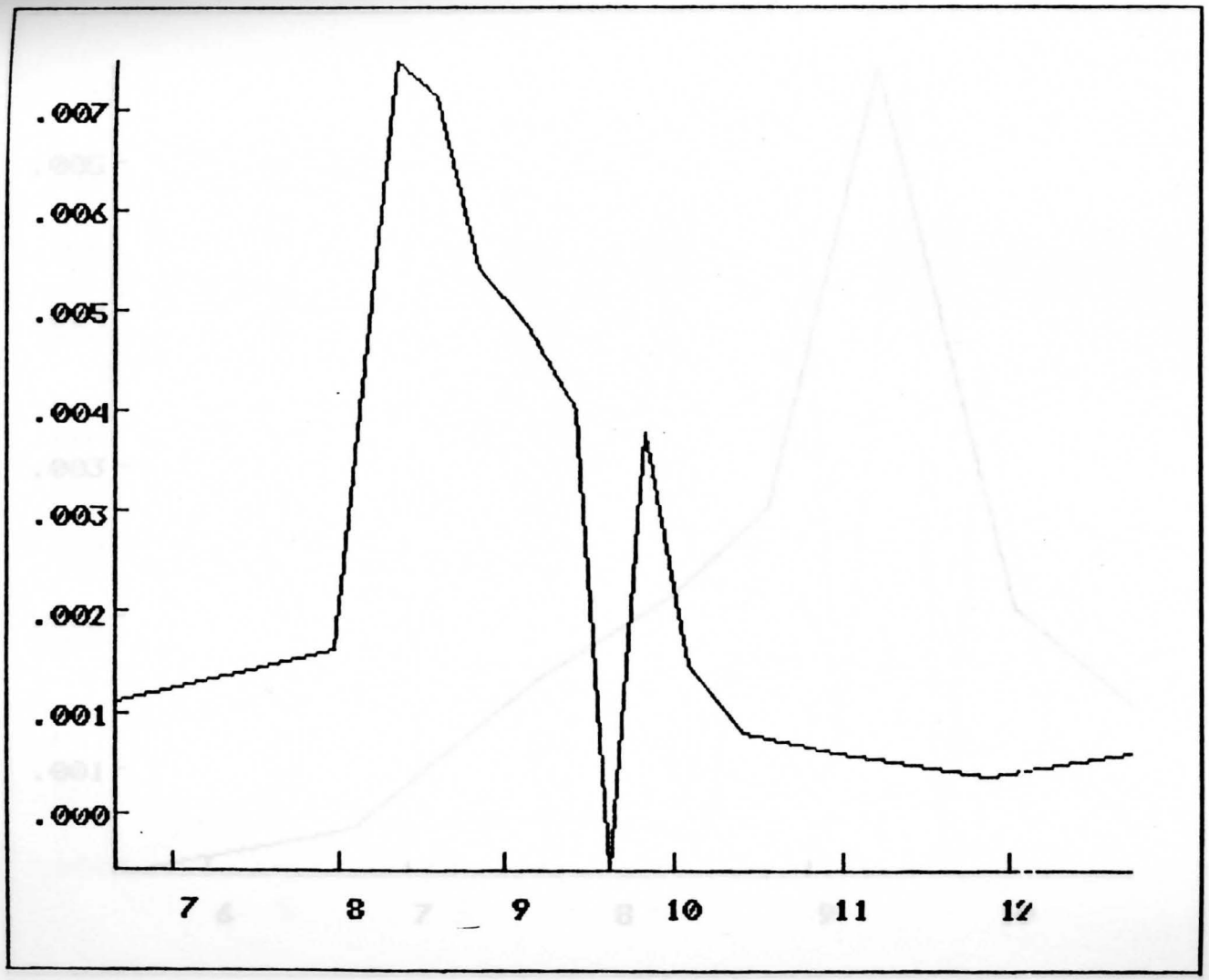

Figure 50. Hyperplot of Procaine in 50% Acetonitrile

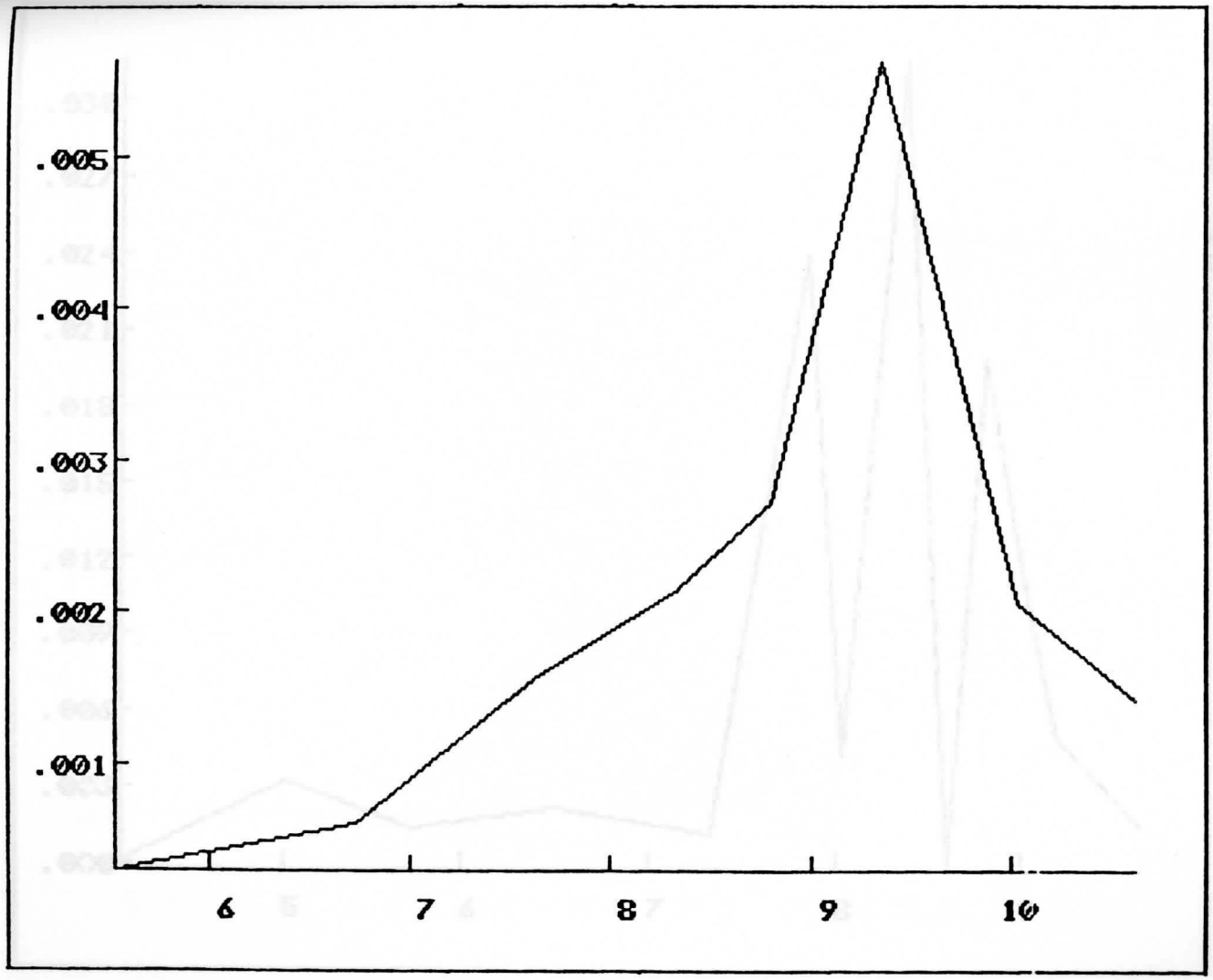

Figure 51. Hyperplot of Procaine in 75% Acetonitrile

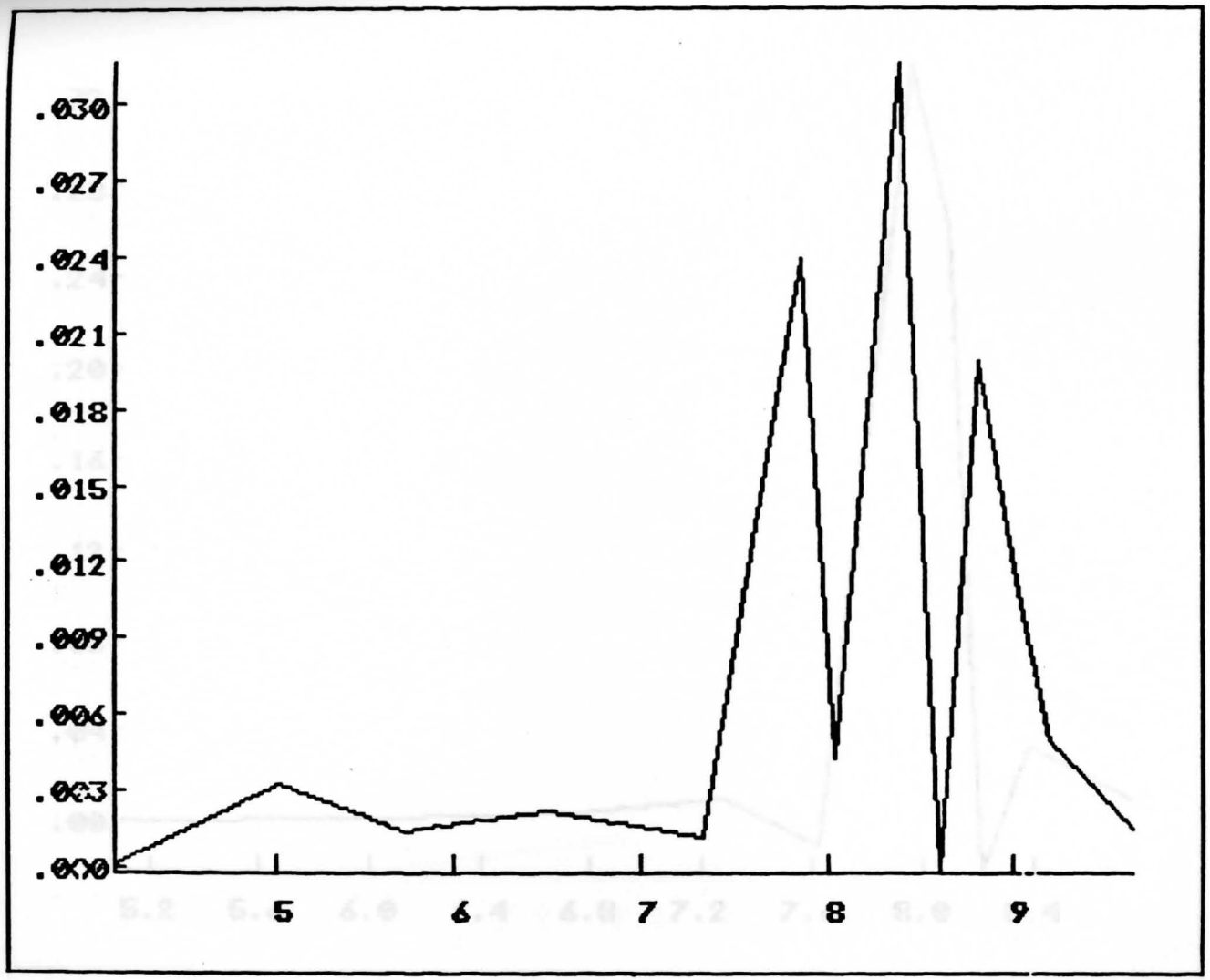

Figure 52. Hyperplot of Dibucaine in water

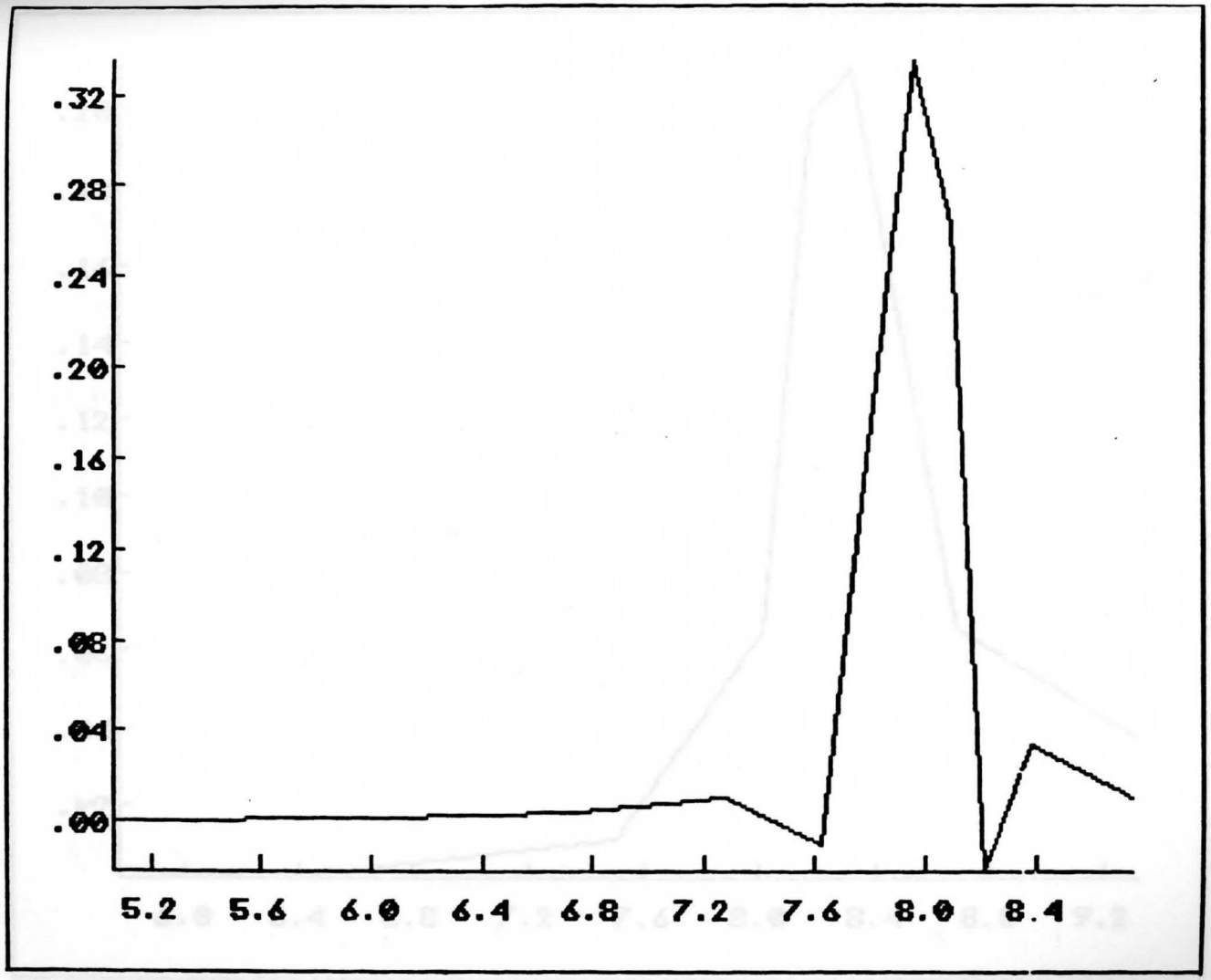

Figure 53. Hyperplot of Dibucaine in 25% Acetonitrile

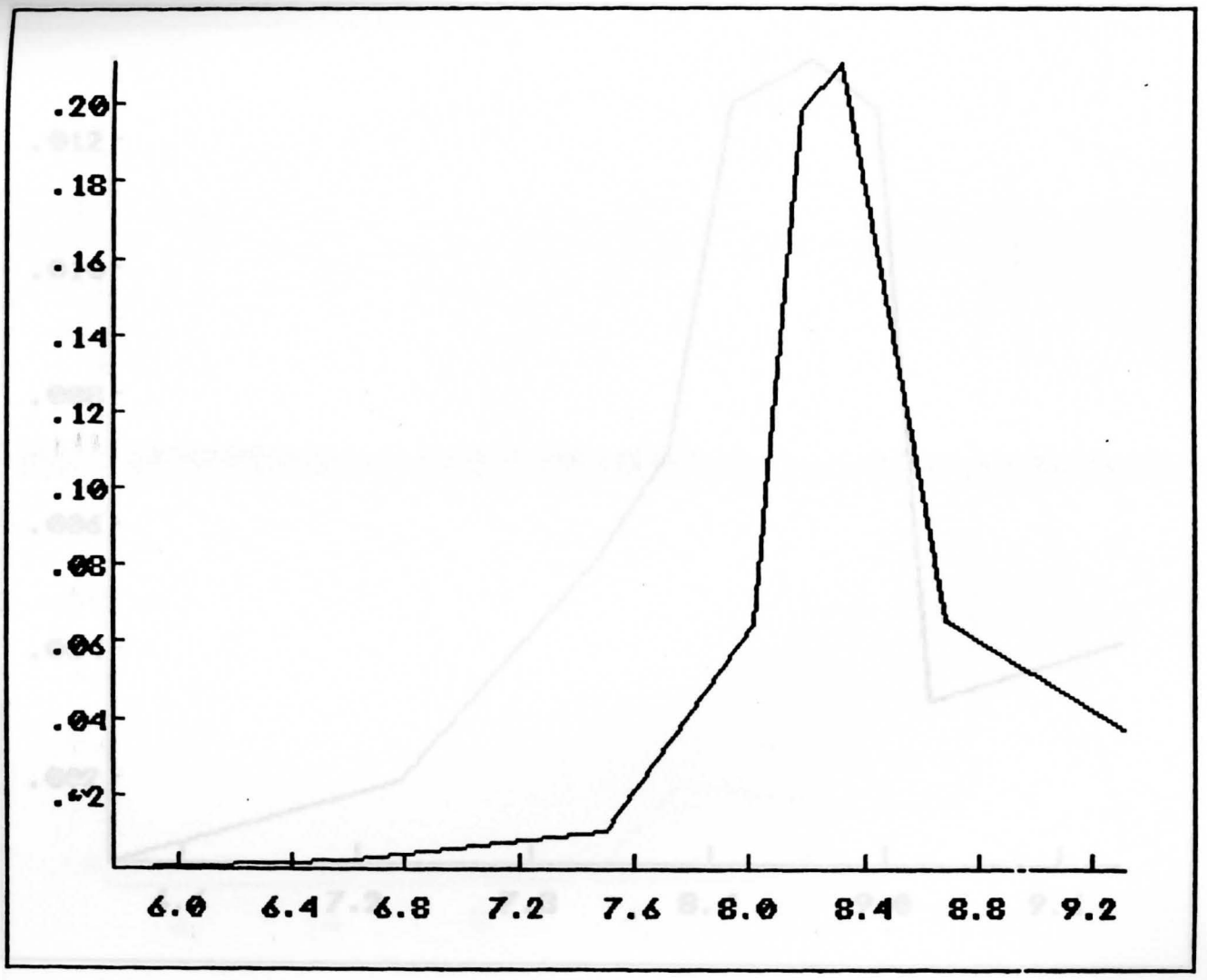

Figure 54. Hyperplot of Dibucaine in 50% Acetonitrile

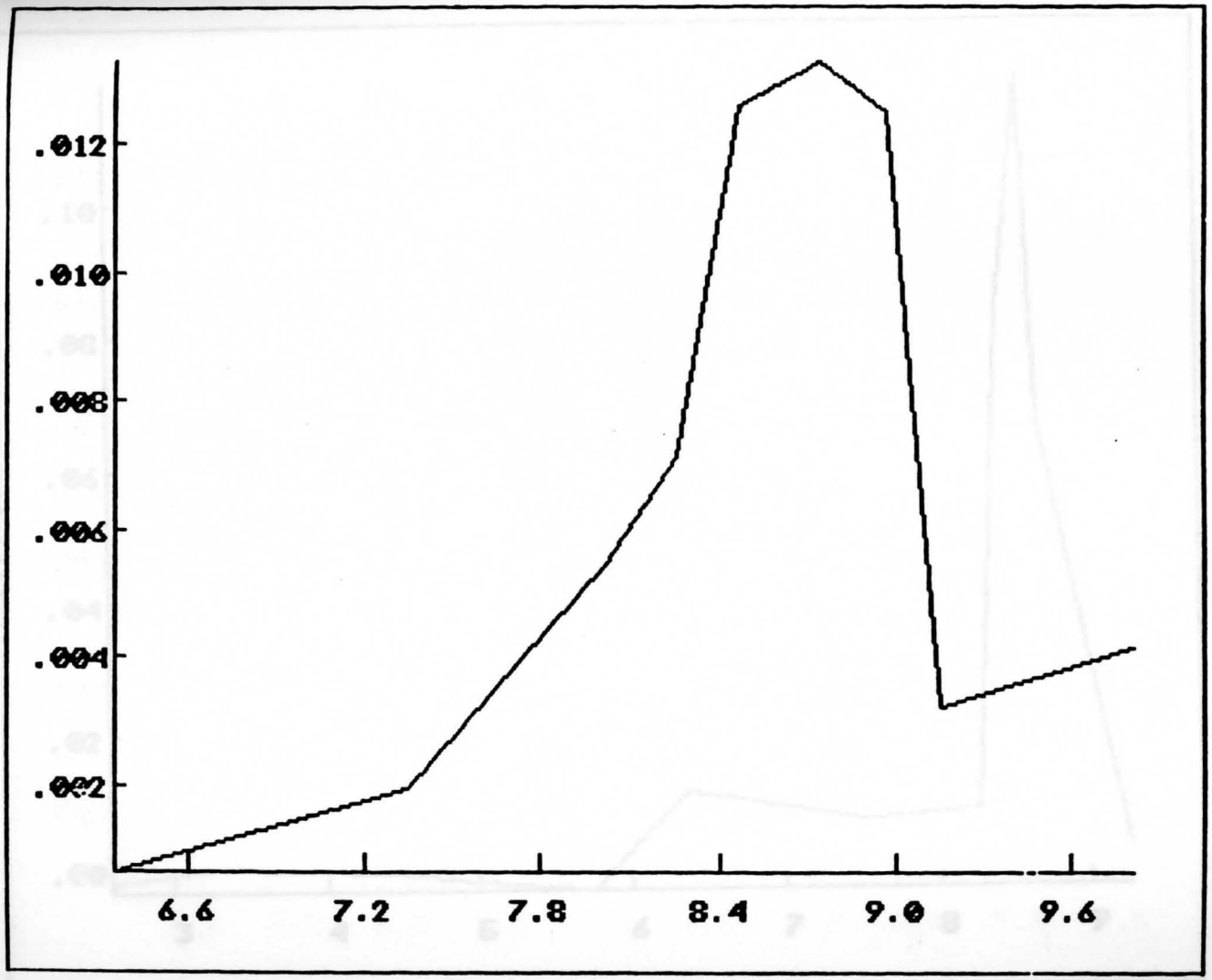

Figure 55. Hyperplot of Dibucaine in 75% Acetonitrile

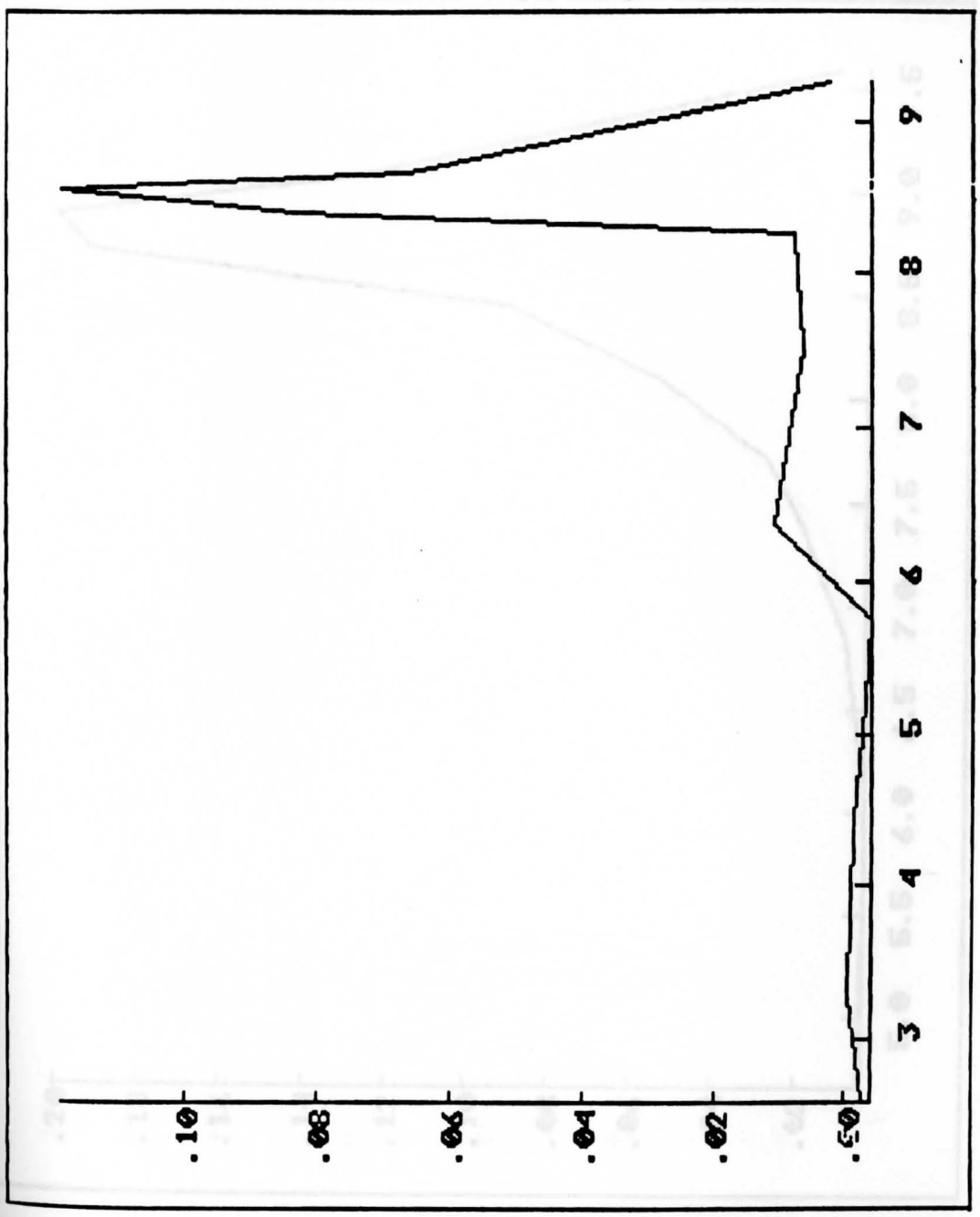

Figure 56. Hyperplot of Cyclonine in water

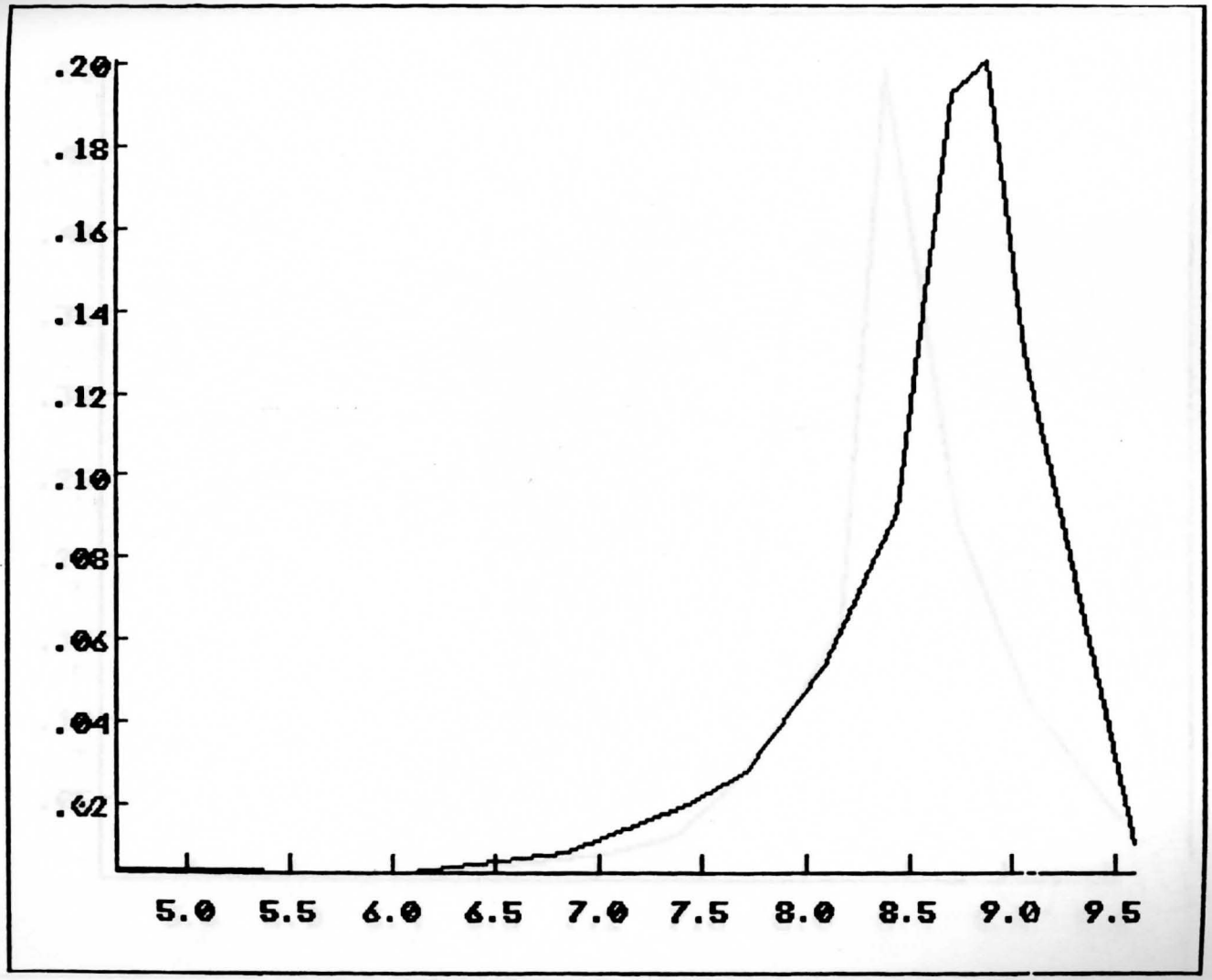

Figure 57. Hyperplot of Dyclonine in 25% Acetonitrile

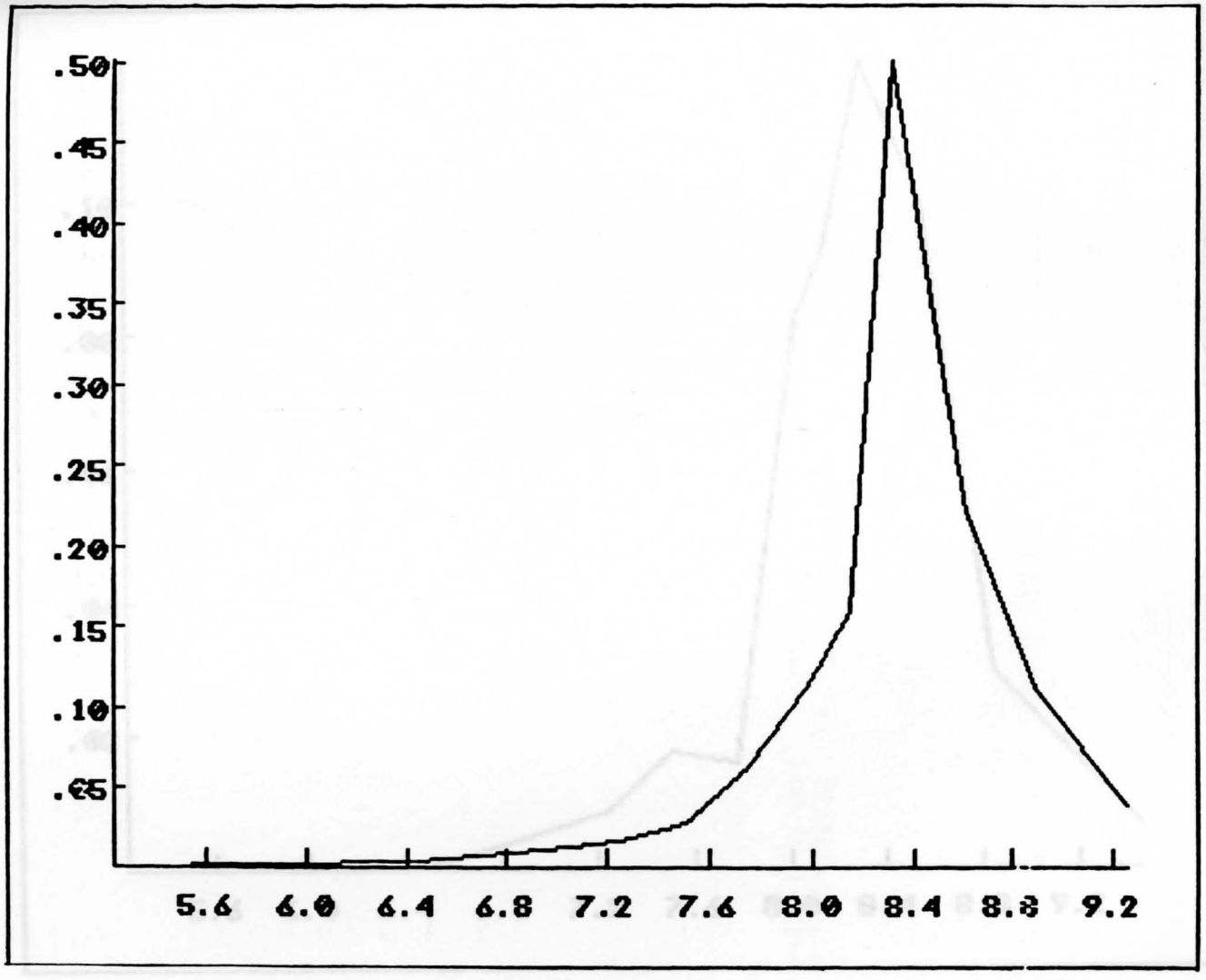

Figure 58. Hyperplot of Dyclonine in 50% Acetonitrile

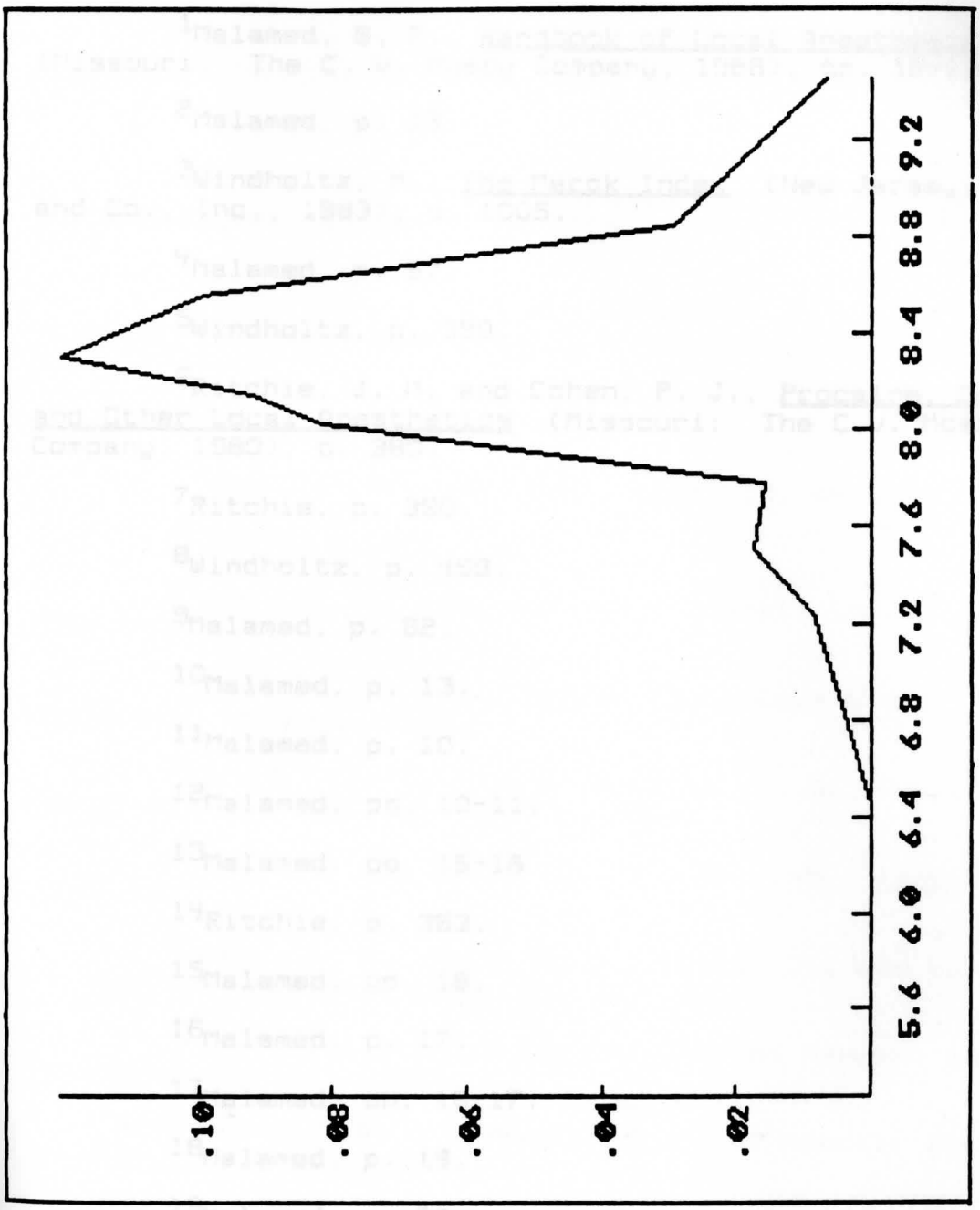

Figure 59. Hyperplot of Dyclonine in 75% Acetonitrile

BIBLIOGRAPHY

[1]Malamed, S. F., Handbook of Local Anesthesia (Missouri: The C. V. Mosby Company, 1986), pp. 12-13.

[2]Malamed, p. 13.

[3]Windholtz, M., The Merck Index (New Jersey: Merck and Co., Inc., 1983), p. 1005.

[4]Malamed, p. 57.

[5]Windholtz, p. 399.

[6]Ritchie, J. M. and Cohen, P. J., Procaine, Cocaine, and Other Local Anesthetics (Missouri: The C.V. Mosby Company, 1980), p. 380.

[7]Ritchie, p. 390.

[8]Windholtz, p. 459.

[9]Malamed, p. 62.

[10]Malamed, p. 13.

[11]Malamed, p. 10.

[12]Malamed, pp. 10-11.

[13]Malamed, pp. 15-16

[14]Ritchie, p. 383.

[15]Malamed, pp. 16.

[16]Malamed, p. 17.

[17]Malamed, pp. 16-17.

[18]Malamed, p. 19.

[19]Malamed, p. 20.

[20]Ritchie, p. 384.

[21]Ritchie, p. 386-387.

[22]Ritchie. p. 385.

[23]Adams, R., Johnson, J. R., and Wilcox, Jr. C. F. Laboratory Experiments in Organic Chemistry (New York: Macmillan Publishing Co., Inc., 1979), p. 485.

[24]Ewing, G. W., Instrumental Methods of Chemical Analysis (New York: McGraw-Hill Inc., 1985), p. 87.

[25]Ewing, pp. 84-88.

[26]Griffiths, P. R., Chemical Infrared Fourier Transform Spectroscopy. New York: John Wiley and Sons, 1975.

[27]Griffiths, P. R., and deHaseth, J. A., Fourier Transform Infrared Spectrometry. New York: John Wiley and Sons, 1986.

[28]Ewing, p. 89.

[29]Bartick, Dr., Am. Lab., 1984, 16, 56-62.

[30]Ewing, p. 90.

[31]Horlick, G. and Yuen, W. K., Anal. Chem., 1975, 47, 775A-780A.

[32]Baca, R.T., M.S. Thesis, Youngstown State University, August, 1986.

[33]Braue, Jr. E. H. and Pannella, M. G., Applied Spectroscopy., 1987, 41, 1057 - 1066.

[34]Rein, A. and Wilks Jr., P., Am. Lab., 1982, 14, 152 - 155.

[35]Wang, J. S., Rein, A. J., Wilks, D., and Wilks, J. P., Applied Spectro., 1984, 38, 32 - 35.

[36]3200 Data Station Getting Started Manual, Bio-Rad Laboratories, Inc., 1988.

[37]FTS-60/FTS-40 Hardware Technical Manual, Bio-Rad Laboratories, Inc., 1988.

[38]The Circle-Cylindrical Internal Reflection Accessory Instruction Manual, IBM Instruments, Inc., 1984.

[39]Orion Model SA 520 pH Meter Instruction Manual, Orion Research Inc., 1986.

[40]Orion Electrode Pamphlet, Orion Research Inc., 1986.

[41]Sigma Chemical Company, Biochemical and Organic Compounds for Research and Diagnostic Clinical Reagents. Missouri: Sigma Chemical Company, 1976.

[42]Eross, K. K., Comprehensive Analytical Chemistry. Amsterdam: Elsevier Scientific Publishing Company, 1976.

[43]Day, R. A. and Underwood, A. L., Quantitative Analysis. Philadelphia: Prentice-Hall, 1986.

[44]Hyperplot Instruction Manual, JHM International, Inc., 1986.

[45]"The Effect of Solvent Hydrophobicity on the Acid-Base Chemistry and Activity of Two Anti-Herpetic Drugs," Northeastern Ohio Universities College of Medicine, Ann F. Stankewicz and Ken S. Rosenthal.

[46]Mui, K. and McBryde, W. A. E., Can. J. Chem., 1974, 52, 1821 - 1833.

[47]Cohen, S. and Burns, R. G., Pathways of the Pulp. Missouri: The C. V. Mosby Company, 1984.

[48]Martucci, J. D. and Schulman, S. G., Anal. Chim. Acta, 1975, 77, 317.